Universitat de Girona

EMISSIONS REDUCTION POTENTIAL BY COUPLING A THERMOELECTRIC GENERATOR TO AN EXHAUST HEATER IN HEAVY DUTY VEHICLES

Joan Ximinis Tarrés

Universitat de Girona

DOCTORAL THESIS

Emissions reduction potential by coupling a thermoelectric generator to an exhaust heater in Heavy Duty Vehicles

Joan Ximinis Tarrés

2022

Universitat de Girona

DOCTORAL THESIS

Emissions reduction potential by coupling a thermoelectric generator to an exhaust heater in Heavy Duty Vehicles

Joan Ximinis Tarrés

2022

DOCTORAL PROGRAMME IN TECHNOLOGY

Directed by: Dr. Albert Massaguer Colomer and Dr. Eduard Massaguer Colomer

Tutorized by: Dr. Toni Pujol Sagaró

Document submitted to apply for the Doctorate degree from the University of Girona

Compendium of publications

This PhD thesis has been presented as a compendium of scientific publications according to the present regulation of the University of Girona (Text refós de la Normativa acadèmica dels estudis de doctorat de la Universitat de Girona, aprovada pel Consell de Govern en la sessió 3/2017 de 31 de març i finalment modificada en la sessió 4/2021 de 23 de juny). This thesis includes two published articles and one submitted article with pending publication.

The complete references of papers comprising this thesis, its impact factors, quartile, and category of the journals according to the present Journal Citation Report are specified below.

J. Ximinis, A. Massaguer, T. Pujol, E. Massaguer. NO_x emissions reduction analysis in a diesel Euro VI Heavy Duty vehicle using a thermoelectric generator and an exhaust heater. *Fuel*, Volume 301, 2021,121029. ISSN 0016-2361. (Impact factor: 6,609; Journal 20 of 143; 1st quartile; Engineering).

https://doi.org/10.1016/j.fuel.2021.121029

J. Ximinis, A. Massaguer, E. Massaguer. NO_x Emissions below the Prospective EURO VII Limit on a Retrofitted Heavy-Duty Vehicle. *Applied Sciences*. 2022; 12(3):1189. ISSN: 2076-3417. (Impact factor 3.021; 2nd quartile; Engineering).

https://doi.org/10.3390/app12031189

J. Ximinis, A. Massaguer, E. Massaguer. Towards compliance with the prospective EURO VII NO_x emissions limit using a thermoelectric aftertreatment heater. Submitted to *Applied Thermal Engineering*. ISSN 13594311. (Impact factor: 5.295; Journal 14 of 133; 1st quartile; Engineering).

Certificate

To whom it may concern.

Dr. Albert Massaguer Colomer from the University of Girona,

And

Dr. Eduard Massaguer Colomer from the University of Girona,

DECLARE:

That the thesis entitled *Emissions reduction potential by coupling a thermoelectric generator to an exhaust heater in Heavy Duty Vehicles* presented by Joan Ximinis Tarrés, has been developed under our direction. It meets the requirements to obtain the Doctoral degree from the University of Girona.

For all necessary purposes we hereby sign the present document.

Dr. Albert Massaguer Colomer Dr. Eduard Massaguer Colomer

Girona, March 2022

Acknowledgement

In first term I would like to thank my parents for their unconditional help and effort to transmit core values and inspiring me during life tough times. For their true love and comprehension despite not approving some of my decisions, for their patience and support all along my lifetime.

Special thanks to my two children for being patient with me in their own way. I owe hours of shared playtime with you. Thank you for being a capital reason to endure on my path and finish with this important milestone.

To my real love for being an important lighthouse in times of doubt, a trustful friend and an infinite source of optimistic kindness. I have learnt a lot at your side.

Finally, I would like to thank all members of Grefema group and specially my tutor and thesis directors. Thank you for your professionality, your help and your patience with my limitations in time, space and knowledge. A true and sincere acknowledgement to Albert and Eduard for their trust in my capabilities and our shared time in Nabla Thermoelectrics. It was a pleasure working at your side.

We would like to thank Fundación Repsol and EVARM INNOVACION SL for their support.

Nomenclature

α	Seebeck coefficient (mV/K)
λ	Thermal conductivity (W/mK)
η	Efficiency (%)
$\dot{m}$	Exhaust mass flow rate (kg/h)
Δp_{ATEG}	ATEG backpressure
Δp_{EGH}	EGH backpressure
ΔT	Increment of temperature (K)
CO	Carbon monoxide
HC	Hydrocarbons
H_2O	Water
N_2	Diatomic nitrogen
NOx	Oxides of nitrogen
SO_2	Sulfur dioxide
C_P	Specific heat at constant pressure
I_{EGH}	Intensity from EGH
NOx_{EGH_ON}	Nitrogen oxides when EGH is enabled
NOx_{EGH_OFF}	Nitrogen oxides when EGH is enabled
Q_{ATEG}	Exhaust volumetric flow rate through ATEG
Q_{EGH}	Exhaust volumetric flow rate through EGH
P_{ATEG}	ATEG power generated (W)
P_{EGH}	EGH power consumed (W)

R^2	Coefficient
R_T	Thermal resistance (K/W)
R_i	Electrical resistance (Ω)
r_{SUB}	Suburban time respect total mission time (%)
T	Temperature (K)
t	Time (s)
T_{AVG}	Thermoelectric average temperature (°C)
T_{A_EGH}	Temperature after EGH (°C)
T_{B_EGH}	Temperature before EGH (°C)
T_H / T_{HOT}	TEM hot side temperature (°C)
T_C / T_{COLD}	TEM cold side temperature (°C)
T_{IN_SCR}	SCR inlet temperature (°C)
T_{OUT_SCR}	SCR outlet temperature (°C)
t_{HIGH}	Time spent in highway conditions (s)
t_{INT}	Time spent in interurban conditions (s)
t_{SUB}	Time spent in suburban conditions (s)
V_{EGH}	Voltage from EGH (V)

Abbreviations

ATEG	Automotive thermoelectric generator
ATS	Aftertreatment system
BP	Backpressure
CAE	Computer aided engineering

CRT	Continuous regenerating trap
DEF	Diesel exhaust fluid
DOC	Diesel oxidation catalyst
DPF	Diesel particulate filter
ECU	Electronic control unit
EGH	Exhaust gas heater
EGR	Exhaust gas recirculation
EU	European Union
FS	Full scale
FTIR	Fourier transform infrared
FTPP	Full throttle pedal position
HDV	Heavy-duty vehicle
HEV	Hybrid electric vehicle
ISC	In-service conformity
LDV	Light duty vehicle
LTEH	Longitudinal thermoelectric energy harvester
MAW	Moving averaging window
MPPT	Maximum power point tracking
NEDC	New European driving cycle
OCE	Off-cycle emissions
OF	Organic fraction
ORC	Organic Rankine cycle
PCM	Phase change material

PCU	Power converter unit
PEMS	Portable emissions measurement system
SCR	Selective catalytic reduction
TATH	Thermoelectric aftertreatment heater
TEG	Thermoelectric generator
TEM	Thermoelectric module
WHSC	World harmonized stationary cycle
WHTC	World harmonized transient cycle
WLTP	Worldwide harmonized light vehicles test procedure
WNTE	Work no to exceed

Content

List of Figures

List of Tables

Resum

A la Unió Europea, prop del 70% de les emissions contaminants provenen del transport per carretera. Aquest fet és la principal causa de la contaminació de l'aire a les zones urbanes, mentre que els governs d'arreu del món estan centrant els seus esforços per millorar la qualitat de l'aire establint zones de baixes emissions. Aquestes polítiques poden millorar la qualitat de l'aire en algunes capitals o ciutats molt poblades, però en termes globals, el transport comercial està lluny de substituir els motors de combustió interna (ICE) com el principal sistema de propulsió, especialment per als vehicles pesats (HDV).

Els motors de combustió produeixen grans quantitats d'energia tèrmica durant el seu procés de treball. Al voltant de dos terços d'aquesta energia tèrmica es perden en forma de calor residual, el 40% d'aquesta pèrdua es transforma en gasos d'escapament emesos a l'atmosfera. A banda de contribuir a l'escalfament global, aquesta calor residual es podria transformar en una energia més aprofitable mitjançant un principi termoelèctric.

Les aplicacions termoelèctriques són diverses i especialitzades en molts camps de la ciència com la refrigeració en estat sòlid (Efecte Peltier) i la conversió d'energia tèrmica a elèctrica (Efecte Seebeck). L'aplicació de mòduls termoelèctrics (TEM) és especialment interessant pel que fa a la recuperació d'energia malbaratada. Aquest treball és un exemple aplicat d'energia tèrmica malgastada recuperada i utilitzada després per augmentar l'eficiència d'un sistema de posttractament (ATS) estàndard.

El nostre modest punt de vista i contribució per reduir l'impacte ambiental està relacionat amb la validació d'un sistema tancat energèticament per garantir un millor rendiment de l'ATS estàndard en un vehicle de càrrega pesada (HDV) EURO VI amb motor dièsel que circulen actualment per les nostres carreteres i autopistes. Actualment, els sistemes de reducció catalítica selectiva (SCR) comencen a funcionar amb temperatures de fums d'escapament superiors a 180 °C. La nostra recerca se centra en escurçar el temps d'inactivitat del sistema estàndard per tal de millorar les emissions contaminants principalment en rutes de baix règim de motor i condicions d'arrencada en fred.

La primera part d'aquesta investigació se centra a validar la viabilitat de l'escalfador de fums d'escapament (EGH) per reduir les emissions de NOx sense efectes negatius en un circuit estàndard de fums d'escapament. L'experimentació es va dur a terme amb un vehicle HDV Euro VI en un banc rodant certificat. Els resultats són encoratjadors, però el sistema s'ha d'adaptar i optimitzar adequadament. Estem buscant un equilibri entre la reducció de NOx i l'energia tèrmica malbaratada recollida per augmentar la temperatura dels gasos d'escapament.

La segona part d'aquest estudi explora la viabilitat del generador termoelèctric automotriu (ATEG) com a única font d'energia per alimentar l'EGH. Quantifica l'energia elèctrica produïda en tres règims de motor habituals (1000, 1250 i 1500 rpm). Mesura les variacions de producció afectades per diferents posicions del pedal en acceleració total (FTPP) al llarg dels règims exposats.

Aquest estudi presenta un escalfador de posttractament termoelèctric (TATH) com a solució acoblada a la configuració estàndard del vehicle. També determina la ubicació ideal tant de l'EGH com de l'ATEG per optimitzar el seu rendiment i mantenir l'ATS estàndard amb variacions mínimes. L'ús d'aquest sistema es divideix en dues fases diferents, fase d'escalfament i fase de recuperació. L'etapa d'escalfament és quan l'EGH consumeix electricitat per augmentar la temperatura dels fums d'escapament. D'altra banda, l'etapa de recuperació s'aplica quan les temperatures d'aquests fums són prou elevades per permetre que l'ATEG recuperi l'energia malbaratada. S'han tingut en compte paràmetres com la contrapressió i el pes afegit per tal de proporcionar un balanç energètic just a la comparativa. En aquest sentit, s'ha quantificat el consum extra de combustible del vehicle pesant testat.

La tercera part de la nostra investigació explora les diferents rutines HDV i les seves particularitats per tal de determinar en quines d'elles el TATH pot aportar una millora important de NOx emès. Els efectes d'aquest sistema s'exploren en una rutina de transport real d'un viatge de llarg recorregut. El sistema presentat està reduint les emissions contaminants en circumstàncies de règim de motor baix, principalment en zones urbanes poblades. L'etapa de recuperació del sistema es quantifica dins d'aquesta rutina específica. Posteriorment, es quantifica l'energia necessària per a l'etapa d'escalfament pel que fa als requisits de la missió.

Finalment, els resultats experimentals demostren que un HDV certificat EURO VI pot produir emissions de NOx 5 vegades per sobre del valor límit estàndard en circumstàncies específiques (règims de baixa velocitat). El compliment de l'actual EURO VI i la futura EURO VII s'ha analitzat tenint en compte els beneficis del sistema TATH proposat en comparació amb l'ATS homologat estàndard d'aquest vehicle en particular. Els resultats demostren una reducció de NOx de fins a un 97,2% utilitzant el sistema proposat en aquest perfil de missió concret. A banda d'això, també està demostrat que l'ATEG pot produir l'energia requerida per l'EGH en un perfil de missió de llarg recorregut. Tanmateix, s'espera que el pes afegit i la contrapressió provocada pel TATH augmentin el consum de combustible del vehicle en un 0,35%.

Resumen

En la Unión Europea, cerca del 70% de las emisiones contaminantes proceden del transporte por carretera. Este hecho es la principal causa de la contaminación del aire en las zonas urbanas, mientras que los gobiernos de todo el mundo están centrando sus esfuerzos por mejorar la calidad del aire estableciendo zonas de bajas emisiones. Estas políticas pueden mejorar la calidad del aire en algunas capitales o ciudades muy pobladas, pero en términos globales, el transporte comercial está lejos de sustituir a los motores de combustión interna (ICE) como principal sistema de propulsión, especialmente para los vehículos pesados (HDV).

Los motores de combustión producen grandes cantidades de energía térmica durante su proceso de trabajo. Alrededor de dos tercios de esta energía térmica se pierden en forma de calor residual, el 40% de esta pérdida se transforma en gases de escape emitidos en la atmósfera. Aparte de contribuir al calentamiento global, este calor residual podría transformarse en una energía más aprovechable mediante un principio termoeléctrico.

Las aplicaciones termoeléctricas son diversas y especializadas en muchos campos de la ciencia como la refrigeración en estado sólido (Efecto Peltier) y la conversión de energía térmica a eléctrica (Efecto Seebeck). La aplicación de módulos termoeléctricos (TEM) es especialmente interesante en cuanto a la recuperación de energía desperdiciada. Este trabajo es un ejemplo aplicado de energía térmica desperdiciada y después recuperada utilizandola para aumentar la eficiencia de un sistema de postratamiento (ATS) estándar.

Nuestro modesto punto de vista y contribución para reducir el impacto ambiental está relacionado con la validación de un sistema cerrado energéticamente para garantizar un mejor rendimiento del ATS estándar en un vehículo de carga pesada (HDV) EURO VI con motor diésel que puede circular en estos momentos por nuestras carreteras y autopistas. Actualmente, los sistemas de reducción catalítica selectiva (SCR) comienzan a funcionar con temperaturas de humos de escape superiores a 180 °C. Nuestra investigación se centra en acortar el tiempo de inactividad del sistema estándar para mejorar las emisiones contaminantes principalmente en rutas de bajo régimen de motor y condiciones de arranque en frío.

La primera parte de esta investigación se centra en validar la viabilidad del calentador de humos de escape (EGH) para reducir las emisiones de NOx sin efectos negativos en un circuito estándar de humos de escape. La experimentación se llevó a cabo con un vehículo HDV Euro VI en un banco rodante certificado. Los resultados son alentadores, pero el sistema debe adaptarse y optimizarse adecuadamente. Estamos buscando un equilibrio entre la reducción de NOx y la energía térmica sobrante almacenada para aumentar la temperatura de los gases de escape.

La segunda parte de este estudio explora la viabilidad del generador termoeléctrico automotriz (ATEG) como única fuente de energía para alimentar al EGH. Cuantifica la energía eléctrica producida en tres regímenes de motor habituales (1000, 1250 y 1500 rpm). Mide las variaciones de producción afectadas por distintas posiciones del pedal en aceleración total (FTPP) a lo largo de los regímenes expuestos.

Este estudio presenta un calentador de postratamiento termoeléctrico (TATH) como solución acoplada a la configuración estándar del vehículo. También determina la ubicación ideal tanto del EGH como del ATEG para optimizar su rendimiento y mantener el ATS estándar con variaciones mínimas. El uso de este sistema se divide en dos fases distintas, fase de calentamiento y fase de recuperación. La etapa de calentamiento es cuando el EGH consume electricidad para aumentar la temperatura de los humos de escape. Por otra parte, la etapa de recuperación se aplica cuando las temperaturas de estos humos son suficientemente elevadas para permitir que el ATEG recupere la energía desperdiciada. Se han tenido en cuenta parámetros como la contrapresión y el peso añadido para proporcionar un balance energético justo en la comparativa. En este sentido, se ha cuantificado el consumo extra de combustible del vehículo pesado testado.

La tercera parte de nuestra investigación explora las diferentes rutinas HDV y sus particularidades para determinar en cuáles de ellas el TATH puede aportar una importante mejora de NOx emitido. Los efectos de este sistema se exploran en una rutina de transporte real de un viaje de largo recorrido. El sistema presentado reduce las emisiones contaminantes en circunstancias de régimen de motor bajo, principalmente en zonas urbanas pobladas. La etapa de recuperación del sistema se cuantifica dentro de esa rutina específica.

Posteriormente, se cuantifica la energía necesaria para la etapa de calentamiento en lo que respecta a los requisitos de la misión.

Por último, los resultados experimentales demuestran que un HDV certificado EURO VI puede producir emisiones de NOx 5 veces por encima del valor límite estándar en circunstancias específicas (regímenes de baja velocidad). El cumplimiento del actual EURO VI y la futura EURO VII se ha analizado teniendo en cuenta los beneficios del sistema TATH propuesto en comparación con el ATS homologado estándar de este vehículo en particular. Los resultados demuestran una reducción de NOx de hasta un 97,2% utilizando el sistema propuesto en ese perfil de misión concreto. Aparte de esto, también está demostrado que el ATEG puede producir la energía requerida por el EGH en un perfil de misión de largo recorrido. Asimismo, se espera que el peso añadido y la contrapresión provocada por el TATH aumenten el consumo de combustible del vehículo en un 0,35%.

Abstract

In the European Union, about 70% of pollution emissions come from road transportation. This fact is the main cause of air pollution within urban areas while Governments around the world are focusing their efforts to improve air quality stablishing low emission zones. These policies can improve air quality in some capitals or cities highly populated but in global terms, commercial transportation is far from substituting Internal Combustion Engines (ICE) as the main propulsion system, specially for Heavy-Duty Vehicles (HDV).

Combustion engines produce great quantities of heat energy during their working process. Around two thirds of this thermal energy is lost as residual heat, with 40% of this loss transformed in exhaust gases emitted to the atmosphere. Apart from being a contributor to global warming, this residual heat could be transformed in a more usable energy by a thermoelectric principle.

Thermoelectric applications are diverse and specialized in many science fields such as refrigeration in solid state (Peltier effect) and energy conversion from thermal to electric (Seebeck Effect). The application of Thermoelectric modules (TEM) is specially interesting in terms of wasted energy recovery. This work is an applied example of thermal wasted energy recovered and used afterwards to increase the efficiency of a standard Aftertreatment System (ATS).

Our modest point of view and contribution to reduce environmental impact is related to a validation of an energetically closed system to ensure a better performance of the standard ATS in a diesel-powered EURO VI Heavy duty vehicles (HDV) currently circulating in our roads and highways. Nowadays Selective Catalytic Reduction systems (SCR) starts performing with exhaust gas temperatures higher than 180°C. Our research is focused on shortening the inactive time of the standard system in order to improve pollutant emissions mainly in low engine regime routes and cold start conditions.

First part of this research is focused in validating the Exhaust Gas Heater (EGH) viability in reducing NO_x emissions without negative effects in a standard exhaust gas circuit. Experimentation was held using a HDV Euro VI vehicle in a certified rolling bench. Results are encouraging but the system has to be properly adapted and optimized. We are seeking a balance between NO_x abatement and thermal wasted energy harvested for increasing exhaust gas temperature.

Second part of this study explores the Automotive Thermoelectric Generator (ATEG) viability as the only source of energy to power the EGH. It quantifies the electrical energy produced in three common engine regimes (1000, 1250 and 1500 rpm). It measures production variations affected by different Full Throttle Pedal Positions (FTPP) all along the exposed regimes.

This study presents a Thermoelectric Aftertreatment Heater (TATH) as a solution coupled to the vehicle standard configuration. It also determines the ideal location of both EGH and ATEG to optimize its performance and keep the standard ATS with minimal variations. The use of this system is divided into two different phases, heating stage and recovery stage. Heating stage is when EGH consumes electricity to rise exhaust gas temperature. On the other hand, recovery stage is applied when exhaust gas temperatures are high enough to allow ATEG recover wasted energy. Parameters such as backpressure and added weight has been taken into account in order to provide a fair energy balance to the comparison. In this regard, extra fuel consumption of the HDV has been quantified.

Third part of our research explores the different HDV routines and its particularities in order to determine in which ones the TATH can provide a major NO_x improvement. The effects of this system are explored in a real transportation routine of a long-haul journey. The presented system is reducing polluting emissions in low engine regime circumstances, mainly in urban areas that are populated. Recovery stage of the system is quantified within this specific routine. Afterwards, the amount of energy required for heating stage is quantified concerning routine requirements.

Finally, experimental results demonstrate that a certified EURO VI HDV can produce NO_x emissions 5 times above the standard limit value under specific circumstances (low-speed

regimes). The accomplishment of current EURO VI and prospective EURO VII has been analyzed taking into account the benefits of this proposed TATH compared to the standard homologated ATS of this particular vehicle. Results demonstrate a NO_x reduction up to 97.2% using the system proposed into this particular mission profile. Apart from that, it is also demonstrated that the ATEG can produce the energy required by the EGH in a long-haul mission profile. However, the added weight and the back pressure caused by the TATH is expected to increase the fuel consumption of the vehicle in 0.35%.

Chapter 1

General introduction

1.1 Research justification

Nowadays transportation is a relevant pollutant contributor all around the globe. Within European countries, road transportation is the main source of NOx emissions. According to European Environment Agency (EEA), in 2017 road transportation was directly responsible of emitting 28.3% of total NOx emissions, followed by international shipping (14.74%). Furthermore, this agency also advices the flattening trend on NOx emissions from 2013 onwards. This fact reflects an increasing difficulty for manufacturers to achieve a relevant impact in NOx abatement, specially for HDV.

Main thesis motivation is to provide tangible results in improving NOx reduction of modern HDV that are homologated according to Euro VI antipollution standard. The real problem with this transportation vehicle typology is related to cold start conditions and urban routines. This thesis demonstrates that standard ATS are capable of only partially cope with emissions problem (mostly after threshold DEF temperature). In particular, standard SCR efficiency is directly related to this target temperature to improve its working capabilities.

First hypothesis of our research aims to demonstrate that HDV can improve SCR efficiency by heating exhaust gas temperature. Our approach is focused specifically in an Euro VI HDV and its standard system. This genuine research combines different methodologies explained in Chapter 3 (Methodology). Results demonstrate that NOx reduction can improve more than 80% in low engine regimes (1000rpm and 1250rpm). However, a need to rationalize energy required for the heating stage is detected in this approach. An EGH with a maximum power of 5 kW is suitable for this vehicle and application.

A second hypothesis is related to energy balance. Our research demonstrates that using thermoelectricity it is possible to recover wasted heat from the system to be used afterwards to warm up the standard ATS. Heating stage in cold conditions is defined as well as recovery stage when wasted heat is transformed in electrical energy and stored. Results quantify the EGH power required to achieve maximum SCR efficiency (95%). In this regard, experimental SCR efficiency curve versus theoretical curve are presented as function of catalytic temperature.

NOx emissions (g/kWh) are compared by using EGH or not (as standard ATS). This study also quantifies backpressure and extra weight effects on fuel consumption (0.35%).

Finally, a third hypothesis is defined to explore the feasibility of this coupled system in order to fulfill Euro VI-VII in real transportation routines. This study demonstrates that operating in suburban conditions (the most demanding scenario), NOx emissions results are improved and maintained below regulation limits. Besides, it also demonstrates that an ATEG can provide enough power during a long-haul transportation routine for suburban requirements. To guarantee the energetic autonomy of the proposed TATH a correlation of time in different road conditions is calculated. If recovery stage is exclusive of suburban conditions, HDV must not exceed 3.1% of its all transportation routine in suburban scenario to accomplish standards. On the other hand, it can spend 4.9% of its routine in suburban conditions if recovery stage takes place during highway scenario.

Overall, this thesis presents a deeper research in thermoelectricity applied to recover energy in transportation vehicles. Research evolution provides detailed quantification of energy required to accomplish our hypothesis. It also provides a clear view of the system potential for prospective antipollution standards fulfillment and also its limitations of transportation routines typology. Finally, global results present the system boundaries in real word conditions scenario and opens the gate for future research to design a full TATH system for HDV.

1.2 Technology state of the art

The majority of trucks and buses currently circulating on our roads use diesel engines [1], contributing to NOx emission into our environment [2]. Future regulations apparat, there already exist technical solutions to improve pollution figures for present vehicles. Aftertreatment devices can be retrofitted to a HDV or can be specifically implemented from factory. These solutions encompass NOx absorbers, lean NOx catalyst systems, EGR and SCR systems, being the las two the more extended ones for its efficiency.

NOx absorbers present Sulphur poisoning issues despite having a high operating temperature window. Lean NOx catalyst systems accuse poor thermal conductivity and narrow working temperature window. EGRs are an effective and reliable solution for NOx emissions with reductions of 50% in absolute numbers. SCRs are even more efficient compared to previous technologies with reported NOx reductions of more than 90% [3]. Indeed, both technologies can be operated simultaneously in modern vehicles to increase emissions reduction capabilities.

Catalyst control technologies are simple and do not require modifying the engine's set up since they are focused on reducing the light-off temperature of the catalytic conversion. It can be done using alternative catalytic materials and/or reducing the time to reach the light-off temperature. This realistic strategy is currently investigating several alternatives such as rising the heat transfer inside the catalyst using higher cell densities and thinner wall designs, insulating the exhaust manifold and assembling the SCR as close as possible to the engine's block minimizing heat loos. Finally, it also includes the addition of an electrical resistance to preheat the SCR. In conclusion, the simplicity of electrically preheated catalysts (EHCs) makes it the most cost-effective technology for solving NOx emissions [4,5].

This thesis has been particularly focused on SCR systems for its effectiveness and research background. Its operation and recent research improvements are extensively detailed in Chapter 4. However, it is important to remark that exhaust gas temperature is directly related to SCR performance, reaching its maximum efficiency over 230°C [6]. On the other hand, urea solution is not injected into the aftertreatment system until exhaust gases reach 180°C so SCR conventional systems do not cut NOx emissions effectively in low speed routines or initial hauls below this target temperature. Indeed, it has been proved that cold starts are responsible of more than 50% of exhaust gas emissions during a specific driving cycle [7].

Thermal management of SCR systems is fundamental to increase its performance. Development of highly efficient low temperature catalysts could be a solution if material poisoning is addressed [8,9]. Hence, current research is focused in achieving a suitable NOx conversion without damaging SCR by accumulation of sulfate deposits [10]. Another strategy consists on avoiding thermal losses of exhaust gases by insulating the exhaust pipe between the urea

solution injection point and the SCR [11]. However, this solution increases SCR efficiency by only 0.6%.

Active heating systems have been developed to reach SCR operating temperature in a shorter period of time. One strategy proposed the direct heating of urea solution using glow plugs [12]. This research obtained a 60% conversion of NOx at 160°C into a conventional SCR unit. This system obtained efficiency levels of 90%. Rink et al. [13,14] successfully developed and tested an specific SCR containing an electrical resistance for preheating the catalyst. However, these solutions are less effective than heating directly exhaust gases.

In this regard, Sharp et al. [15] compared several options to reduce NOx emissions on a 361 kW Volvo MD13TC. A 2 kW electrically heated catalyst, followed by a hydrolysis catalyst alone or in combination with a 5 kW additional heater placed before the DEF injection point and afterwards the DPF, was tested and compared to an adjustable-power (8-20 kW) mini-burner. These systems provided respectively a 45%, 70%, and 80% of potential NOx reduction.

Furthermore, another research [16] demonstrated the ability of an electric heater to raise exhaust gas temperature and overcome the effect of moisture and low exhaust temperature, allowing NOx conversion to begin sooner. Different electric heaters from 12 kW to 30 kW were used to heat the exhaust gases of a Cummins ISDe 6.7-liter engine. Results shown that it is possible to achieve high NOx conversion temperatures faster with robust heater technology that is specific for diesel applications.

After analyzing these previous results on the field of SCR combined with a preheated system it was a clear choice for its cost-efficient and improvement results in NOx emissions. However, in these studied solutions it is assumed that the energy consumed by electrical heaters come from the standard vehicle electrical system. In consequence, fuel consumption and overall vehicle efficiency worsen and must be carefully quantified.

In this direction, Massaguer et al. [17] analysed the use of an ATEG coupled to an EGH, reducing up to 97% the NOx emitted by a light duty vehicle during cold starts. The ATEG converted waste heat from exhaust gases, downstream of the aftertreatment system, into electricity. A battery

stored the electricity generated, which could be used by the EGH later to shorten the time that urea is injected and reduce NOx emissions. This EGH+ATEG system, also known as Thermoelectric Aftertreatment Heater (TATH), was created to be energetically autonomous, so there is no extra consumption of fuel. Energy can be balanced because ATEG produces electricity in the most part of the cycle while EGH consumes only when exhaust gas temperature is lower than the target. Note that ATEG backpressure and extra weight of the whole system would be factors that contribute to an increase in fuel consumption and they need to be taken into account for our case study.

Another important research field explored for this thesis setting up was the HDV emissions while performing different routines. In this regard, targeting potential real word situations for applying the presented technology was a major goal that led us to understand in which situations HDV polluted over emission regulation limits and its causes. Time figures and energy balance situation for both stages (Heating and Recovery) are based on these scenarios.

Concerning low-speed operations mainly in urban driving, Posada et al. [18] observed that a significant amount of NO_x emissions. HDV circulating at speed lower than 40 km/h presented NOx emissions of more than five times the certification limit. Furthermore, a single line-haul truck emits the NOx equivalent of 100 cars for each mile driven in urban driving. Based on 160 tests with a Portable Emissions Measurement System (PEMS), this study also shows that these trucks, which are optimized for highway driving, spend on average 43% of their time and emit 40% of the total mass of NOx in urban-like operation, including idling and low-speed driving. Under these conditions is when EGH is needed, defining the Heating stage boundaries.

Some catalytic converter prototypes with an exhaust heater have been successfully tested to improve results under the New European Driving Cycle (NEDC) [5,19]. there are relevant results... These heat-integrated catalysts need a constant heating of 2.5 kW during 120 s for a 90% reduction of CH_4 emissions in comparison with non-preheated values. This 2.5 kW in 120 s is equivalent to a mean electrical power consumption of 254 W during the NEDC that must be generated by the alternator and, hence, by the engine. This technical solution contributes to a vehicle extra fuel consumption and could be improved by an energetically closed solution.

1.3 Thesis background

In order to fully understand this research purpose, it is relevant to introduce some aspects of our nowadays living context. In most countries, there is a growing environmental protection consciousness manifested with new challenging regulations. Scarcity in raw materials, specially semiconductors, is a persistent global fact affecting manufactured products including all transportation vehicles. Our work is a result of applying thermoelectric technology to minimize NO_x emissions. This demonstrates that current EURO VI HDV can accomplish restrictive antipollution standards (EURO VII/7) with a retrofitted equipment. Thus, the antipollution system presented is a proven technology for LDV and now for HDV thanks to its modularity and previous research from our team.

The thermoelectric principle in charge of this application is the Seebeck Effect. An electromotive force or voltage is created as a result of a difference in temperature for two semiconductors. Thermoelectric generators also known as Peltier Modules or Thermoelectric modules (TEM), are specially designed to maximize the Seebeck Effect. The commercial TEMs used in our research experiments are Marlow Industries TG12-8-01LS. This model presents a working surface temperature that fits with our exhaust system application (continuous maximum temperature of 200°C and temperature peaks of 230°C). Figure 1.1 shows its composition (left) and presents how the Seebeck Effect works (right). Further information on how are distributed forming different arrays and connections is exposed on Chapter 4.

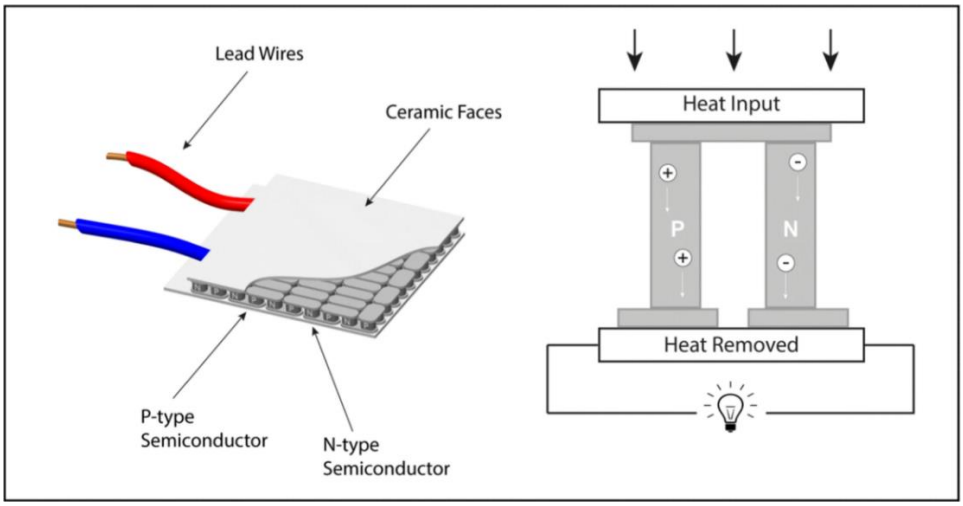

Figure 1.1. Marlow Industries TEM parts (left) and schematic of the Seebeck Effect (right) [20].

Previous research determined key parameters to optimize TEM performance to increase energy recovery. This determines the configuration and assembly of the different components exposed in Figure 1.2. As stated before, surface contact is crucial to guarantee heat transfer. Fasteners provide a solid and permanent contact between TEM surfaces and cooling plate (cold surface) or inner hot side of this device (hot surface). Focusing on cooling plate, this part present different manufacturing techniques to increase its cooling capabilities. CNC machining of billet aluminum faces provides a circuit that afterwards is externally welded to guarantee free leakage of the cooling liquid. Finally, two standard connectors are threated to one extreme of the plate as inlet and outlet of the circuit.

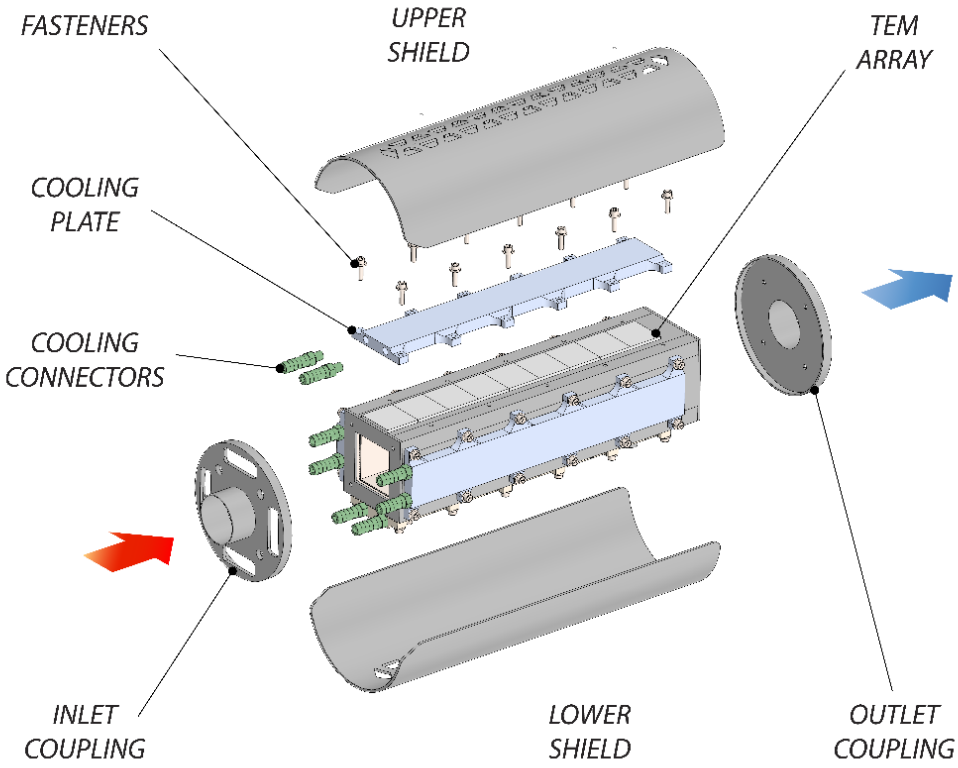

Figure 1.2. Single ATEG exploded view with its components.

As explained in Chapter 4, a strong point of this ATEG design is its modular possibilities as an adaptation to maximize heat recovery in different vehicles. Figure 1.3 shows an example of this modularity with a finished package of three ATEG units working together in parallel. This configuration presents triple holed coupling plates that are attached to the exhaust pipe using both inlet and outlet manifolds.

The main structure of this design is formed by the three ATEG units and the two aluminum lightweight beams attached to the coupling plates. Finally, there are two lightweight shields perforated to allow a minimum ventilation of the cold plates. This product design combines protection and weight saving while it can grow in both directions: length for TEM increase in series and height to add an entire new line of ATEGs to the final device.

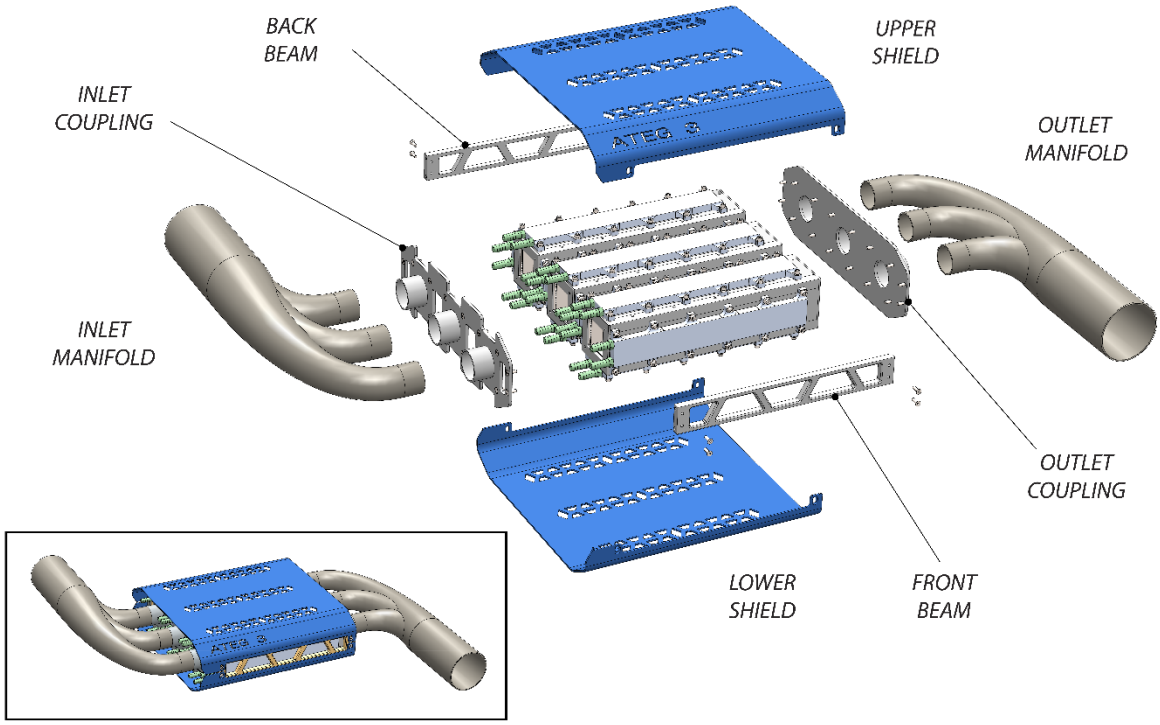

Figure 1.3. Three units ATEG configuration and its exploded view.

1.4 Thesis organization

This thesis research line and its internal cohesion developed in different chapters is exposed in this section. General objectives presented in Chapter 2 are divided into three groups according to its relation to each publication. Experimental set up is explained in Chapter 3 (Methodology) as it is an important part of research experimentation used to acquire data and develop the whole research. As a compendium of publications, the main core of this thesis is the transcription on three scientific articles that form Chapters 4-6. Results and discussion obtained are summarized afterwards in Chapter 7. Finally, in Chapter 8 there is a general conclusion of this research and future steps that follow the same research line of this team.

Journal publications of Chapters 4-6 are transcribed as published (i and ii) and as submitted (iii) papers:

(i) "NOx emissions reduction analysis in a diesel Euro VI Heavy Duty vehicle using a thermoelectric generator and an exhaust heater".

(ii) "NOx emissions below prospective EURO VII limit on a retrofitted Heavy-Duty Vehicle".

(iii) "Towards compliance with the prospective EURO VII NOx emissions limit using a thermoelectric aftertreatment heater".

This work has been organized according to different phases planned at the initial stage of this research. Milestones of this plan are the scientific publications that reflect the evolution and results achieved at each step. Summarizing, the thesis development has been organized as follows:

- Key parameters and data definition to explore future results (Chapter 4 - Article 1).
- Experimental set up with a real HDV (Chapter 4 - Article 1).
- Data gathering and its analysis (Chapter 4 - Article 1).
- EGH energetic needs (Chapter 4 - Article 1).
- ATEG capabilities and its boundaries (Chapter 4 - Article 1).
- HDV retrofitted and EURO VI-VII compliance (Chapter 5 - Article 2).
- HDV retrofitted and real routine conditions (Chapter 6 - Article 3).
- ATEG parameters definition for HDV (Chapter 6 – Article 3).

EGH study and its contribution to NOx abatement is studied in different engine regime conditions and presented in Chapter 4. ATEG energetic contribution was firstly validated as a simulation model with data gathered from the first experiment. Finally, its individual configuration was tested in real conditions with temperature and mass flow rate being extracted parameters from the real vehicle. These are exposed in Chapter 6 and are a fundamental step to establish the ATEG layout for HDV according to EGH requirements and vehicle exhaust system capabilities.

Applicability of the proposed TATH is also explained, concluding that it could be specially recommended for long-haul transportation routines. At the end of Chapter 6 there is recovery and heating stages time correlation that demonstrates its feasibility.

The final ATEG design is out of the scope of this thesis but previous models have been designed, manufactured and tested with success. These prototypes contributed to relevant information related to design geometry of the internal faces of any ATEG. In order to minimize backpressure and avoid major influences into mass flow rate behaviour, sharp edged must be minimized.

1.5 Research cohesion

This presented research is related to a huge amount of previous work made by students and professors of GREFEMA group and collaborators. This compendium of publications pretends to add some scientific information to the research field of thermoelectricity applied to recover energy. It makes sense to see it as a step forward to a knowledge path of applied science using TEM to increase efficiency and reduce pollution.

In 2016, Dr. Eduard Massaguer presented his thesis *Advances in the modelling of thermoelectric energy harvesters in waste heat recovery applications*, as member of GREFEMA research group. As its title suggests it includes relevant information related to Thermoelectric Generators (TEG) modeled and validated. TRNSYS environment was used as modelizer of this array with respect to the fluid direction, i.e. exhaust gases. Finally, MATLAB was chosen to effectively calculate electrical interconnections of the TEG array. An experimental model presented a TEM configuration that was successfully tested as energy harvester. This same basic configuration has been successfully proven for a HDV ATEG in this present research.

In 2018, Dr. Albert Massaguer presented his thesis *Electrically tunable thermal conductivity and exhaust heat recovery applications of thermoelectric materials*, also as a member of this group. In this particular work, relevant information was gathered relative to the use of an ATEG coupled to a gasoline engine exhaust system. Tests were carried under steady state and transient driving cycles. One relevant contribution was that thermal contact resistant has a

significant influence in power results. Thus, the use of adequate materials and optimized design of the system has been fundamental.

In 2019, another GREFEMA member, Dr. Martí Comamala presented his thesis *Development and characterization of thermoelectric generators for thermal energy recovery from reciprocating internal combustion engines*. In this thesis a radial ATEG was developed and tested to compare a simulated result using ANSYS-CFX and its equivalent experiment. Furthermore, this research explored the consequences of coupling an ATEG to a real Sport Utility Vehicle (SUV) exhaust system. Knowledge acquired in GT-SUITE and fuel economy is now used to precisely calculate in this present work the real impact of using a TATH in a Euro VI HDV.

This present thesis is a step forward in exploring ATEG real capabilities in HDV transportation routines. Experimental legacy and acquired knowledge from previous works are being reflected in different areas of this research, as exposed before. However, there is also a strong and tangible cohesion between articles published that form the main core of this thesis. As stated before, thesis organization is designed as a plan and the publications are milestones linked to different steps of this plan.

The scope in each step was achieving more precision as different variables were being analyzed and evaluated. The first article proves that EGH contribution to a standard ATS is significantly improving SCR efficiency. Afterwards, energy balance quantification was stablished validating the possibility to incorporate an ATEG to provide an energetically closed system. The second article explores the conditions where an ATEG is suitable for HDV, defining routines were improvement is relevant and comparing results with standard EURO VI and EURO VII maximum limitations. The third article analyzes a long-haul transportation routine with the same tested vehicle and defines conditions and boundaries where the proposed system contributes to meet antipollution EURO VI-VII standards.

Chapter 2

Objectives

This research is focused on exploring the NOx emissions improvement of a HDV using thermoelectricity. As publications presented suggest, it has been a gradual study that has included analysis, viability, and boundaries definition.

The analysis of the NOx emissions in a particular EURO VI vehicle has been the first step in order to compare via experimentation the capabilities of the ATEG+EGH system to abate emissions. After gathering the different parameters of vehicle and system, it has been demonstrated a great improvement. The following chapter gives a clear vision of the methodology used in experimentation. Next step is related to explore the viability to work as an energetically closed system using only heat recovered from the exhaust system as power source for the heater. EGH power consumption to improve SCR efficiency (up to 95%) has been the demonstration of when and how long this system can provide energy for the heating stage.

Afterwards, the recovery stage has been quantified using data extracted from the experimentation. This allowed to define a simulated ATEG that provided time figures for the recovery stage. All time figures are within maximum driving time allowed of 4 hours. Furthermore, the viability of implementing this system is reinforced by a group of three tests and different engine regimes (1000, 1250 and 1500 rpm) to determine if exhaust gas temperature is enough to provide power at recovery stage in a daily drive routine of a HDV.

Finally, our efforts are focused to determine which transportation routines are suitable to cope with this system characteristics. In this regard, long haul vehicles seem to be an ideal choice for its long time in highway conditions and low millage within urban boundaries. The goal is to quantify NOx emissions using the system proposed. It also explores the compliance of EURO VI and EURO VII antipollution standards for HDV.

Objectives can be summarized and distributed into the three publications that form this thesis as follows:

General objectives summarized:

- NOx reduction analysis comparing standard ATS with EGH retrofitted.
- EGH power consumption vs SCR efficiency.
- Recovery stage viability though ATEG use.

- Establish potential regimes for ATEG viability.
- Real transportation routines emissions.
- Antipollution standards compliance and improvement.
- ATEG for HDV usability and its boundaries.

Objectives from article 1 – Chapter 4:

- Analysis of NOx reduction with EGH coupled enabled and disabled. In each FTPP there is temperature data (before and after EGH), power consumed by EGH and NOx emitted in ppm for both conditions.
- Correlation of EGH power consumption vs SCR efficiency. This quantifies the maximum power (kW) needed to achieve SCR maximum efficiency (95%) for different engine regimes.
- ATEG simulation in GT-Suite to demonstrate theoretical viability in order to provide enough power to supply the EGH. ATEG dimensions viability is also explored.
- SCR improvement at 1000 rpm with power supplied at 1500 rpm. Time recovering wasted energy form exhaust system is viable (less than 4h) to provide enough energy to maximize SCR performance when engine is cold.

Objectives from article 2 – Chapter 5:

- Experiment with 3 transient tests presented (1000, 1250 and 1500 rpm) ranging from 260 s up to 340 s.
- Analysis of Euro VI standard compliance trough NOx emissions (g/kWh) compared while using EGH or not. Temperatures and power supplied to EGH are also included as time function. Brief exploration of Euro VII boundaries.
- Experimental SCR efficiency curve vs theoretical curve as function of catalyst temperature. SCR performance comparison with EGH enabled and disabled.
- Comparative theoretical power consumption within the tests to achieve target urea solution injection (stablished at 220°C).
- Study of EGH power required to achieve 95% SCR efficiency during a real speed profile of a long-haul HDV.
- Extra weight and backpressure parameters study and quantification as a fuel increasing factor.

Objectives from article 3 – Chapter 6:

- EURO VI HDV vehicle emissions at low engine regimes and its compliance within limits.
- Heating stage and Recovery stage of the proposed system within long haul routine specifications.
- EGH experiment with NO_x emission results related to EURO VI-VII boundaries.
- EGH power demand to specifically meet standards demand under worst scenario.
- ATEG layout taking into account backpressure and added mass parameters.
- Definition of ATEG usable limits within real working routines.
- Analysis of system weight as fuel consumption factor.

Chapter 3

Methodology

As exposed in Chapter 1 this present work has been planned before making any test set up. The methodology used to carry out this research combines experimentation of real vehicles with simulation models and finally experimentation with prototypes in real conditions. This variety of procedures must be planned carefully and explained properly.

First part of this research was focused on acquiring relevant parameters from a real HDV. Important parameters of the vehicle are summarized in Table 4.1 inside Chapter 4.3. After securing the vehicle on the rolling bench and testing its cinematics, the team proceeded to retrofit the current ATS with the addition of an EGH, a 12 kW Watlow ECOTEG unit. As seen in Figure 3.1 (upper right side), the EGH power was supplied by a three-phase circuit with a specific controlled regulation system. This same figure shows other data controlling and monitoring devices extensively explained in Chapter 4.3. In this regard, ECU parameters were monitored and calibrated by our team members. The sequence for setting one test was the following:

1- Temperatures check (engine T< 90°C).
2- EGH circuit check (only for half of the tests).
3- NOx sensor check.
4- Engine regime and gear selection set.
5- Rolling bench parameters stabilized.
6- FTPP was regulated and stabilized.
7- Time synchronization for all acquisitions.
8- Simultaneously record for future data processing.

In order to perform this sequence properly we needed a team of 4 people. As it can be guest in Figure 3.1 one person was into the cabin and was in charge of calibrating the pedal according to ECU parameters monitored in real time. Another person was monitoring these parameters and validating the FTPP calibration. Meanwhile, another member of the team checked EGH parameters (if it was necessary) and temperature acquired from the thermocouples located inlet and outlet of the EGH. Finally, the fourth member that previously checked the rolling bench parameters, was in charge or recording NO_x emissions only when ECU parameters where correct. Synchronization time was noted for afterwards data adjustment and processing.

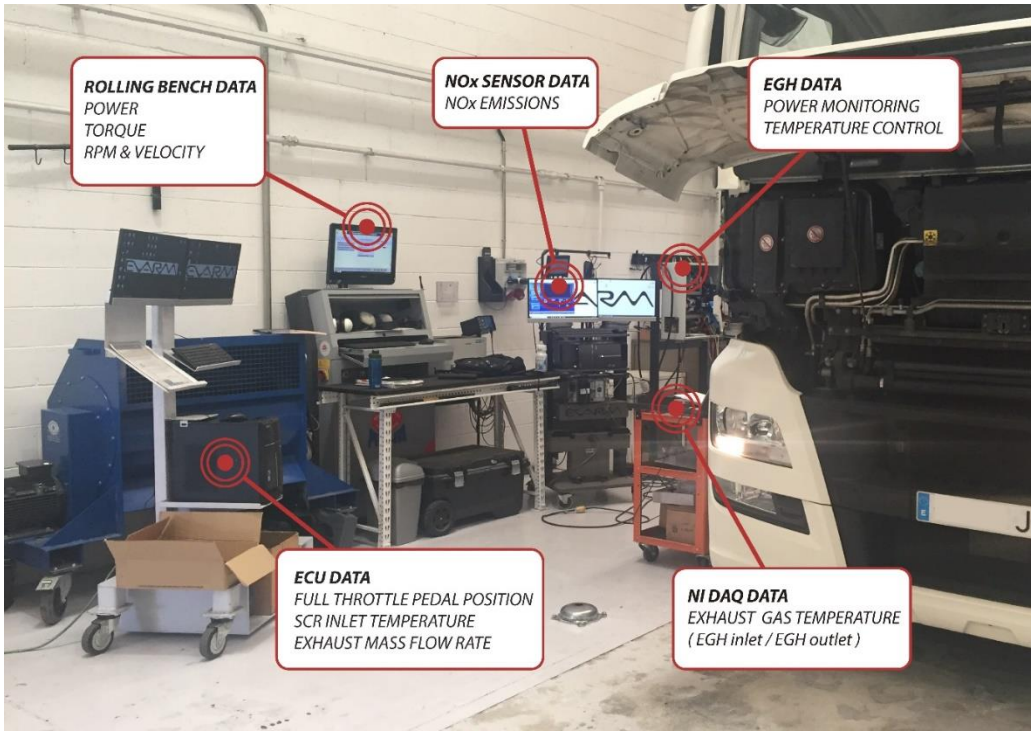

Figure 3.1. NO_x emissions experiment set up including HDV and rolling bench.

After acquiring and processing key parameters from the mentioned experiment, results demonstrated a relevant EGH effect on NOx ppm numbers. Afterwards, EGH energy parameters were analyzed and then a simulation of an ATEG was done using GT-SUITE software. Mass flow rate and exhaust gas temperature (SCR outlet temperature being inlet ATEG temperature) were introduced to the predefined model as they depend on each specific engine regime and FTPP. This methodology allowed to simulate an array of TEM (see Figure 3.2) with previously tested real conditions. For further information please check Chapter 4.5.

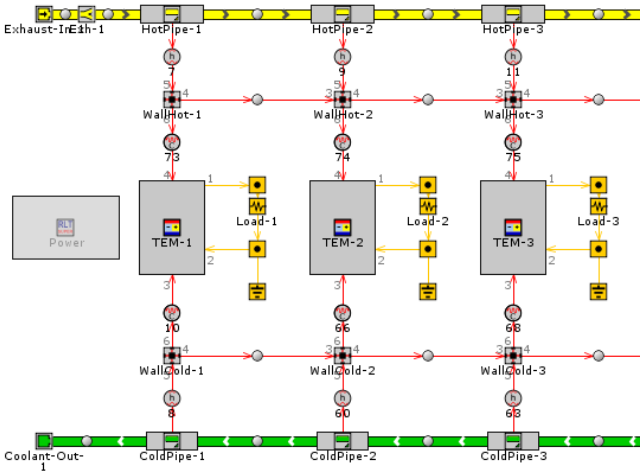

Figure 3.2. Part of the ATEG simulated model using GT-SUITE software.

Another group of tests were designed using the same configuration presented on Figure 3.1. The research goal was to study the viability of the proposed TATH in real transportation routines and then define its capacities to meet EURO VI and prospective EURO VII NO_x limits. Transient tests were defined to establish a correlation of time vs power supplied to EGH and exhaust gas temperatures. Afterwards, a long-haul transportation routine was analyzed and EGH power quantified to achieve 95% of SCR efficiency. For further details, please read Chapters 5.2 and 5.3.

A step forward for this research was the study of a single unit ATEG (ATEG_su). An experimental bench was assembled (see Figure 3.3) in order to test this prototype with simulated real parameters acquired from previous tests using the cited HDV. These parameters were provided by the air flow bench and the EGH. A chiller reproduced real conditions cooling for TEMs cold sides in all four arrays of the prototype. ATEG_su data was acquired by backpressure differential sensor, a pair of thermocouple sensors, and a DAQ unit. Energy output was regulated and maximized by a DC/DC converter and stored in a battery (both of them out of this figure scene). All elements used in this experiment can be seen in the scheme of Figure 6.9. A detailed description of this experiment can be consulted in Chapter 6.4.1.

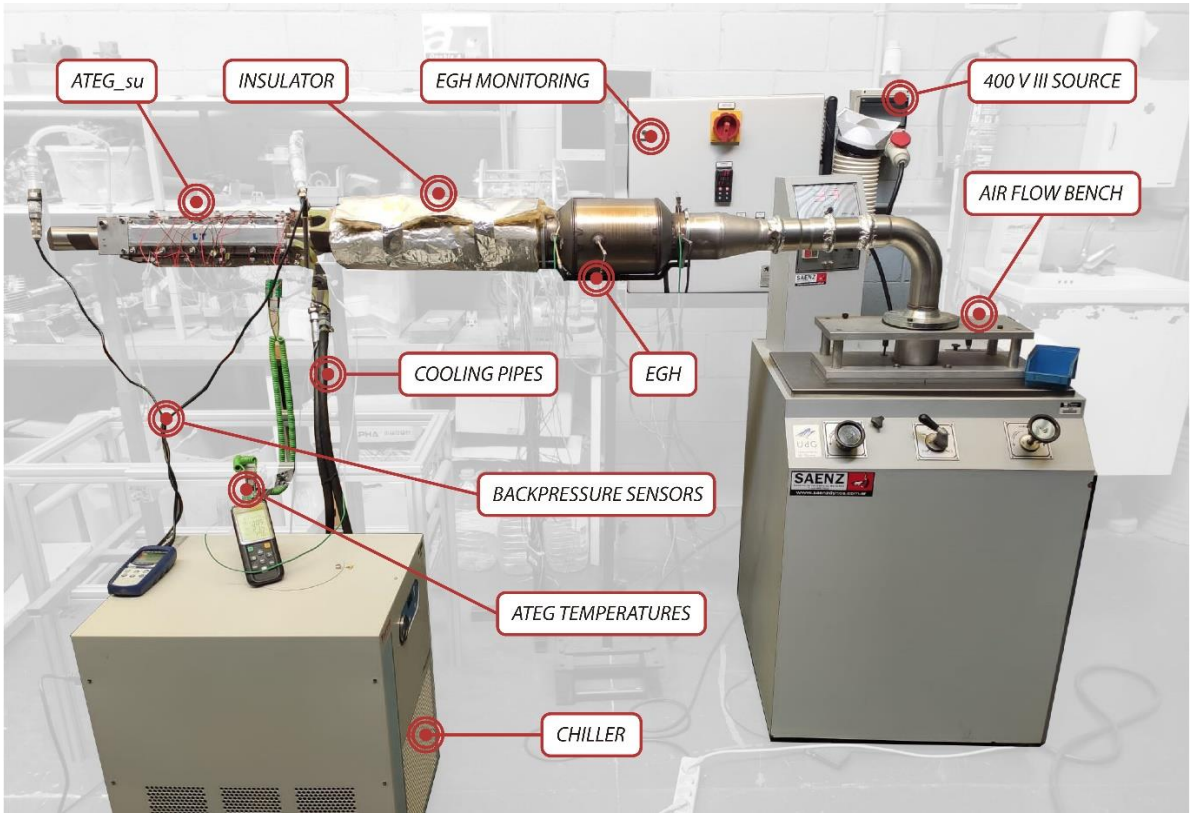

Figure 3.3. ATEG_su experiment set up with chiller and air flow bench.

The methodology used to calculate absolute uncertainty values depends on the equipment accuracy. NOx and temperature standard uncertainties have been obtained by using the measurement accuracy provided into the manufacturer's datasheet (see Chapter 4.3). Voltage and current (used to calculate EGH power consumption) are separately obtained and its uncertainties also calculated using the same method.

Taking into account that EGH power is an indirect parameter, its uncertainty is the result of both electrical magnitudes as it depends on these parameters [21]. Then, the measurement uncertainty of EGH power was calculated combining the uncertainties in measured parameters to arrive at an uncertainty value for an experimental result that depends on these parameters [22,23].

Indeed, results presented in Chapter 4.4 and 5.4 present data error bars of less than 5% for all cases. This low value makes it impossible to represent the error bars properly into the different graphs presented. Its small size may be even lower than the graphic symbology.

Chapter 4

NOx emissions reduction analysis in a diesel Euro VI Heavy Duty Vehicle using a thermoelectric generator and an exhaust heater

---

This section is a full content transcription of the following paper (a copy of the published version can be found in Appendix A):

J. Ximinis, A. Massaguer, T. Pujol, E. Massaguer. NO_x emissions reduction analysis in a diesel Euro VI Heavy Duty vehicle using a thermoelectric generator and an exhaust heater. *Fuel*, Volume 301, 2021,121029. ISSN 0016-2361. (Impact factor: 6,609; Journal 20 of 143; 1st quartile; Engineering).

https://doi.org/10.1016/j.fuel.2021.121029

Abstract

Selective Catalytic Reduction systems (SCR) are very efficient on reducing NOx. However, they only perform properly when exhaust gas temperature is higher than 180°C. This means that for low engine regimes combined with cold engine temperatures, SCR systems remains inactive.

This study presents a new approach to minimize the amount of NOx emitted by diesel engines of Heavy-Duty Vehicles during low engine regimes and low exhaust gases temperature conditions. We propose the addition of an Automotive Thermoelectric Generator (ATEG) coupled to an electric Exhaust Gas Heater (EGH) to make the SCR system inject the urea solution at low engine regimes. This EGH-ATEG system, which can be retrofitted in any existing vehicle, is designed to be energetically closed, so there is no extra consumption of fuel. Experimental results show that NOx emissions can be reduced up to 80% when an EGH is added to a standard diesel-powered Euro VI Heavy Duty truck configuration. Apart from that, the use of an ATEG installed downstream of the aftertreatment system can produce the energy required by the EGH, which means that the EGH-ATEG system can work energetically autonomous and independent from the vehicle's electric system. This system can improve SCR efficiency up to 55% during low engine regimes.

4.1 Introduction

A large proportion of buses and trucks operating in the EU's urban areas are still diesel-powered. In addition, many of them are not yet close to the end of their life [1]. They suffer from generation of gas pollutants, particularly oxides of nitrogen (NOx) [2], which are facing increasingly severe emission regulations.

However, these vehicles may be retrofitted with efficient exhaust aftertreatment devices. Several systems allow high NOx reduction such as EGR (Exhaust Gas Recirculation), NOx absorbers, lean NOx catalyst systems and SCRs (Selective Catalytic Reduction).

NOx absorbers have a high operating temperature window, being highly sensitive to Sulphur poisoning. On the other hand, lean NOx catalyst systems are not suitable for mobile vehicles due to their poor thermal conductivity and narrow temperature window. EGRs are used nowadays in vehicles after demonstrating to be a reliable and effective system. NOx emission can be reduced by 50% in absolute numbers using this technology. SCR systems compared with technologies mentioned before, achieve more than 90% of NOx emissions reduction [3].

SCR works as an advanced active emissions control that converts nitrogen oxides (NOx) into diatomic nitrogen (N_2) and water (H_2O) with the aid of a catalyst. A reducing agent, a solution of urea (32.5%) and distilled water commonly known as AdBlue, is needed to achieve this conversion reaction. This urea solution is decomposed into water vapor and ammonia that is adsorbed on the catalyst substrate as it is injected before SCR. Finally, adsorbed ammonia reacts with NOx and is reduced into harmless water vapor and nitrogen.

Concerning urea solution evaporative process, some studies report that catalyst reaction is mainly affected by temperature and the spatial droplet size [24]. Different operating conditions and modified solution injector designs can cause a variation in the reaction rate of this process. Recent researches have remarked that this process strongly depends on temperature [25,26]. Ammonia process reaction generally starts from 180°C, reaching its maximum reaction rate around 350°C [27]. When exhaust gas temperature is lower than 180°C, urea decomposition

reaction can generate derivatives such as cyanuric acid, biuret, melamine, ammelide and ammeline as deposits on pipe wall [28], which are highly undesired for impeding the regular flow of gases. In order to avoid by-products, urea injection generally starts when exhaust gas temperature is higher than 180°C.

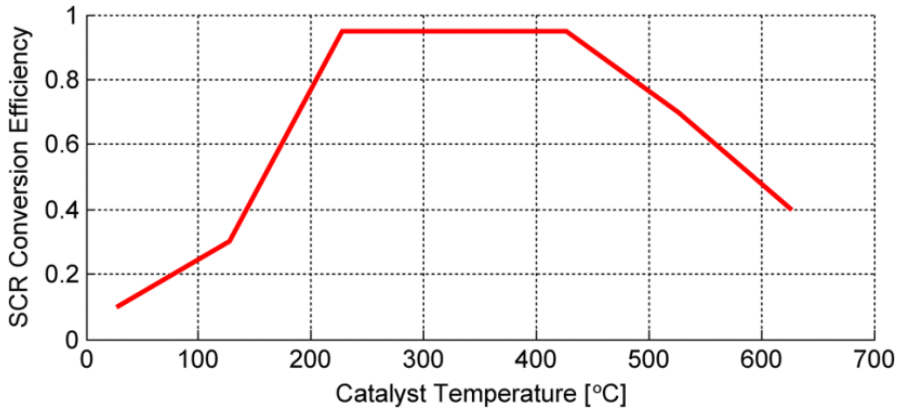

Figure 4.1. SCR conversion efficiency as a function of catalyst temperature [6].

Figure 4.1 is a static map of SCR efficiency. In order to achieve maximum de-NOx efficiency (around 0.95) the catalyst requires temperatures over 230°C. This paper is focused on the first step of this heating process, reducing the time to achieve the proper target temperature when the urea solution is injected into the conversion system. This low temperature range (up to 130°C) can be found at engine starts, during interurban routes or in vehicle operation modes with minor engine loads. SCR efficiency is also affected by ammonia storage and injection control of urea solution, both out of our scope.

Heavy Duty Vehicles (HDVs) for local freight transport, municipal vehicles and delivery vans are often driven for only short distances or through frequently interrupted routes. Under these driving conditions, these engines may not achieve the minimum exhaust gas temperature required to cut nitrogen oxide emissions effectively with conventional SCR systems. Gao et al. [7] demonstrated that more than 50% of exhaust gas emissions, in a given driving cycle, are emitted during cold starts.

Hybrid Electrical Vehicles (HEVs) also face the challenge of high NOx emissions, as its internal combustion engine are commonly switched off at low speed and wheel torque, when the brake specific fuel consumption is especially high. Hybrid diesel buses present higher NOx values

compared to full diesel buses. The poor SCR efficiency in HEVs is a consequence of low exhaust gas temperatures [29,30]. Recent studies demonstrated that NOx emissions can increase around 30% for hybrid powertrains in urban real-life cycles [31]. Therefore, the thermal management of the catalyst is fundamental for both HEVs and conventional vehicles.

In this regard, many strategies have been applied to develop highly efficient low temperature catalysts[8,9]. However, these catalytic materials present some drawbacks such as catalyst poisoning by H_2O or/and SO_2. Hence, active investigation is being held in order to achieve a suitable NOx conversion without compromising feasibility for this SCR catalysts [10].

Avoiding heat leakage of exhaust gases is another strategy to mitigate the low temperature problem. A double-wall insulation system can be mounted over the exhaust pipe between the urea solution injector and the SCR element [11]. However, this method only represents a 0.6% improvement of SCR efficiency.

Jiang et al. [32] and Hamedi et al. [33] proposed the use of a Phase Change Material (PCM) in order to store excess thermal energy from exhaust gases. This energy can be released in a controllable way in order to maintain relatively stable exhaust gas temperatures. The systems proposed combine exhaust gas temperature control and an SCR that can improve NOx emission conversion up to 38%.

Finally, some active heating systems have been developed to shorten the time in which the SCR unit is not operative.

Okada et al. [12] suggested a method that consists in directly heating the urea using glow plugs as heat source. In this research, they considered improving the ammonia generation efficiency by urea reforming. This system allowed to achieve a 60% conversion of NOx at 160°C on a conventional SCR system. The system was able to generate ammonia with an efficiency of more than 90%.

Rink et al. developed a catalytic converter that incorporate an internal electrical resistance for preheating the catalyst and have been tested with relevant results [13,14].

Sharp et al. [15] compared several options to achieve ultra-low NOx emissions on a 361 kW Volvo MD13TC engine with a fixed geometry turbocharger. Among others, a 2 kW electrically heated catalyst, followed by a hydrolysis catalyst alone or in combination with a 5 kW additional heater placed downstream the DPF and before the DEF injection point, was investigated and compared to an adjustable-power mini-burner going from 8 kW to 20 kW. These systems can bring, respectively, a 45%, 70%, and 80% potential reduction in the overall tailpipe NOx emissions at the expense of increased energy consumption that has to be carefully quantified.

Culbertson et al. [16] studied the ability of an electric heater to effectively raise the temperature of the exhaust and overcome the effect of moisture and low exhaust temperature, allowing NOx conversion to begin sooner. Different electric heaters from 12 kW to 30 kW were used to heat the exhaust gases of a Cummins ISDe 6.7-liter engine. Results shown that it is possible to achieve high NOx conversion temperatures quickly with robust heater technology that is suited for diesel applications.

However, the energy consumed by electrical heaters tested in these studies assumed that they were powered by the vehicle's electrical system. Therefore, to proceed to an overall evaluation, the impact of such systems on fuel consumption and overall vehicle efficiency must be addressed.

Recently, a theoretical study [17] demonstrates that the use of an Exhaust Gas Heater (EGH) coupled to an Automotive Thermoelectric Generator (ATEG) can improve the aftertreatment's efficiency of a light-duty vehicle (LDV) in cold-starts without the need of using extra energy. On one hand the EGH is used to raise exhaust temperatures before the catalyst. On the other side, the ATEG is used to convert waste exhaust heat, downstream of the aftertreatment system, into electricity. This energy is stored into a specific battery, which is used lately by the EGH when exhaust gases are cold.

On the basis of [17], the main objective of this study is to experimentally demonstrate that this system, an EGH-ATEG, can work energetically closed and can reduce NOx emissions in diesel-

powered HDVs during low demanding regimes. Unlike [17], in this study the EGH is used to heat the exhaust gases upstream of the SCR during low-speed regimes. This will shorten the time required to reach the SCR light-off temperature where AdBlue is injected and will improve NOx emissions reduction. Additionally, a secondary objective is proposed: demonstrate that this system can work energetically autonomous and independent from the vehicle's electrical system.

To carry out this study, (i) an EGH has been installed to the most suitable position of the exhaust gas system, before the aftertreatment unit. The EGH behaviour has been tested experimentally under steady state driving conditions using a MAN TGX EURO VI on a dynamometer roller bench. (ii) The gathered information from the experiments has been used to analyse the viability of the proposed EGH under different heating power set points. Furthermore, (iii) the obtained data is introduced in a theoretical ATEG simulation software to prove its viability as an exclusive power source for the EGH during low engine regimes.

4.2 EGH-ATEG system

As stated before, the proposed system to reduce NOx emissions consists in a combination of the standard vehicle parts and specific added components such as an EGH. In this first approach, we will focus particularly on each part assembled downstream the exhaust pipe. There is a detailed description for the standard components of the HDV tested in Section 3. This system is designed to work in two different stages illustrated in Figure 4.2.

Heating stage (1): this first step consists in rising the exhaust gas temperatures using the EGH. This device, an electrical resistance, consumes power from a dedicated electrical battery. The goal of this phase is to increase the exhaust gas temperature at SCR inlet. The beginning of this stage is when the engine starts as exhaust gases are on its lowest temperature level. The duration of this stage is determined by the target temperature (= 180°C), being around 12 minutes at idling in this tested vehicle using its standard exhaust system. Reaching this target temperature (=180°C) is crucial because at this point urea solution is dosed into the system and its catalyst reaction is made properly, obtaining a faster and more efficient NOx reduction.

Recovery stage (2): this second step is related to ATEG conversion of thermal energy from exhaust gases into electricity. This electrical power is managed by the electronic control that stores it into the dedicated battery. This step starts when the engine is turned on and it can last up to 240 minutes (by assuming a maximum continuous driving time limited to 4 hours). The objective of this second phase is to maximize the amount of electrical energy stored for its later use by the EGH under low engine regime conditions. Note that the power generated by the ATEG (P_{ATEG}) increase with the engine regime [34,35]. At high engine regimes, exhaust temperatures are higher, increasing the temperature difference between the hot side and the cold side of each thermoelectric module (TEM), $\Delta T = T_{HOT} - T_{COLD}$. Considering that $P_{ATEG} \propto \Delta T^2$, it can be concluded that the higher the engine regime, the higher the power generated by the ATEG. Moreover, the longer the time spend at high engine regimes (e.g. >80km/h), the higher the energy recovered by the ATEG. Therefore, long-distance transport vehicles are the most suitable to incorporate the thermoelectric aftertreatment heater (TATH).

Regarding the exhaust gas flow, each component of the proposed system is specifically located in order to optimize its functionality. If we begin upstream the aftertreatment system, and after the turbocharger, we find the EGH. This component is located just before the standard SCR and DPF (Diesel Particle Filter) package of the vehicle. This standard lot of components includes the urea dosing system, not represented in Figure 4.2, and they are explained in the following section. The specific location of the EGH is important as it will maximize its impact into the standard NOx reduction system by providing a rise in temperature with minimal thermal loss. On the outlet side of the standard SCR-DPF package there is a bypass represented by a bifurcation of the exhaust pipe. Its function is to avoid high exhaust gas temperatures that damage the ATEG thermoelectric modules. Figure 4.2 represents an external solution that uses electrical valves to modulate the gas flow. However, Massaguer et al. have also developed an internal solution proven to succeed in its aim [17]. The ATEG is located at the end of the exhaust system. It is important to be downstream of SCR as ATEG reduces the temperature of the exhaust gases and SCR needs a high temperature in order to perform efficiently. Furthermore, ATEG thermal loss will be reduced as post SCR catalytic converters rise exhaust gas temperature when performing.

The objective of obtaining emissions reduction without adding extra fuel consumption requires a compromise between energy consumed and produced. This system operates in two stages, as explained before. Heating stage (1) and recovery stage (2) are represented in Figure 4.2 by its energy flow respectively. In the first stage, the control unit feeds the EGH with the energy stored in the battery. In the second stage, the control unit feeds the battery with the energy recovered by the ATEG. ATEG requires a cold focus, then the thermal scheme is complemented with a cooling circuit composed by a low temperature heat exchanger and a water pump (not represented in Figure 4.2).

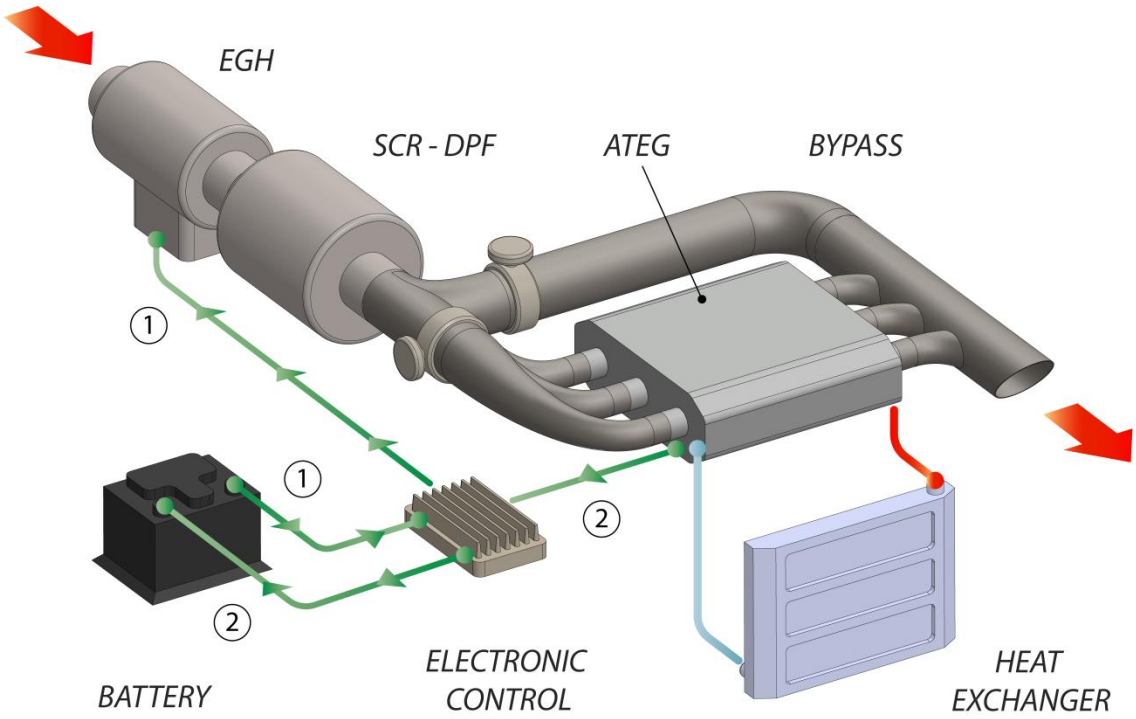

Figure 4.2. Proposed EGH-ATEG solution with electrical energy flows: heating stage (1) and recovery stage (2).

Note that the inclusion of the EGH and the ATEG may cause a backpressure (BP) increase in the exhaust pipe. Massaguer et al. [36,37] analysed this effect in a light duty vehicle (engine power < 100 kW) and demonstrated that if the BP increase stays below 40 mbar, the vehicle's fuel consumption is not affected. In [34], authors tested an ATEG in a light-duty vehicle with a maximum power production of 200 W, a weight of 8kg and a maximum backpressure of 10 mbar. They observed that the BP caused in the exhaust pipe did not adversely affect engine performance. A part form that, according to the fuel economy assessment method of ref. [37], the additional weight of the ATEG (i.e. generator and cooling system) only suppose an increase

of 0.08% in fuel consumption. Considering that the ATEG used in this study is based on the model developed in [34], both the backpressure and the additional weight added by the ATEG has been neglected.

Finally, the EGH was tested in a hot air flow bank under the maximum exhaust conditions: 1700 rpm and 358 kW to analyse its backpressure. The results from this test showed a maximum pressure loss of 1.8 mbar at 416 g/s. With this information it can be concluded that the inclusion of the EGH into the exhaust system will not adversely affect the engine performance.

4.3 Experimental set up

The active and most demanding antipollution standard for HDV in the European Union is the Euro VI standard (Euro VII is planned for fourth quarter 2021). This current regulation is a great challenge, especially for Heavy Duty Vehicle manufacturers. The most common system adopted for manufacturers consists on the combination of sophisticated ECU (Electronic Control Unit) software, together with a catalytic chemical reaction, to obtain NOx ppm values below antipollution regulation limits. In this study, a Heavy Duty Vehicle Euro VI TGX 18.480 Efficient Line 2 from MAN is used to carry out the tests. Figure 4.3 shows this vehicle disposition and the main data acquisition that include the ECU and the rolling bench controls.

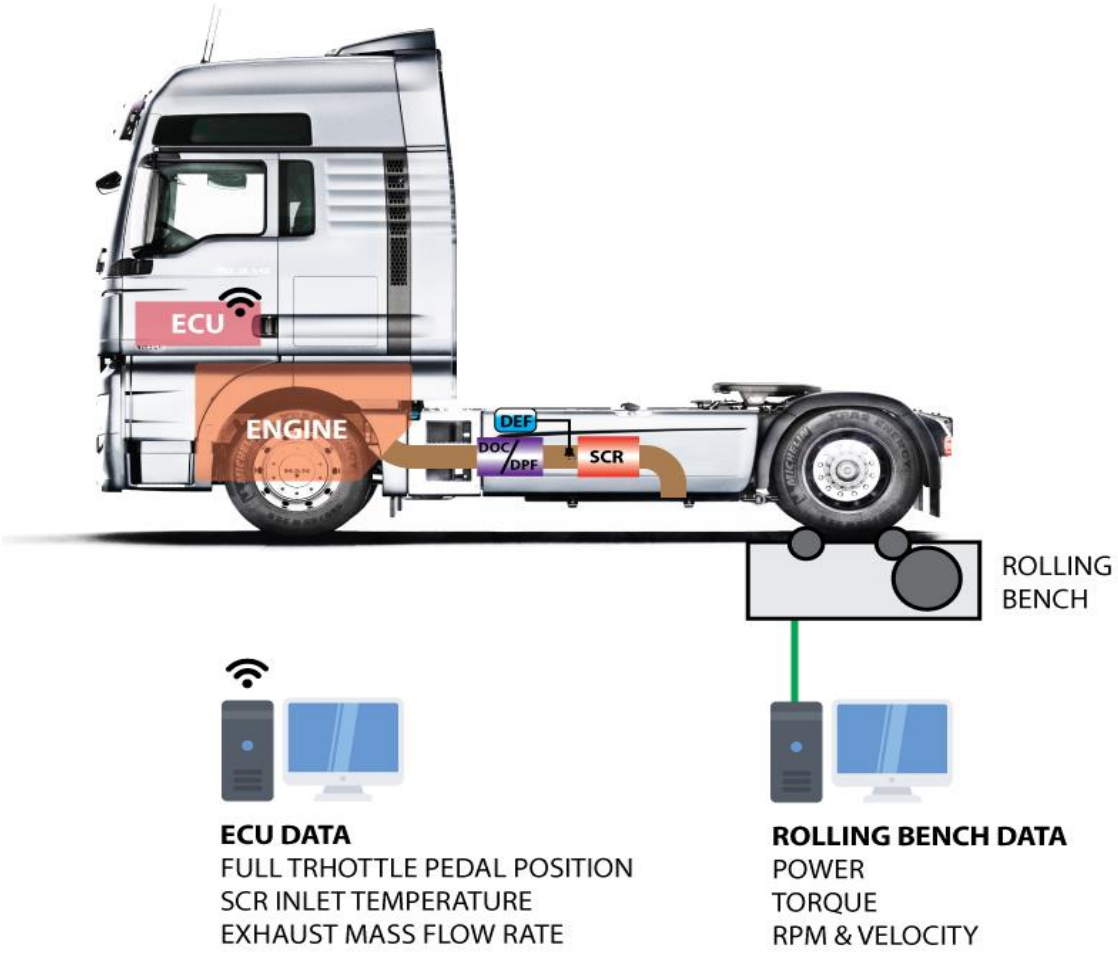

Figure 4.3. Scheme of data acquisition obtained from ECU and rolling bench.

The system used consisted of an EGH located upstream of the standard aftertreatment system, see Figure 4.4. The EGH is a Watlow ECOTEG unit with 12 kW of power. This device contains an electric heating coil controlled by a temperature regulation system designed specifically for this application. In order to simplify the test, a three-phase circuit externally powered the EGH. The regulation was done through a specific control unit that adjusted the power injected to the EGH according to the temperature set point. A discussion about which are the most suitable heating power values according to the vehicle's electric capacity will be presented in section 5. The whole system was laid out as seen in Figure 4.5. Selected key parameters such as temperatures, ppm NOx or engine regime, are synchronized, monitored, and registered to guarantee future correlations while the heater was in use along all the tests.

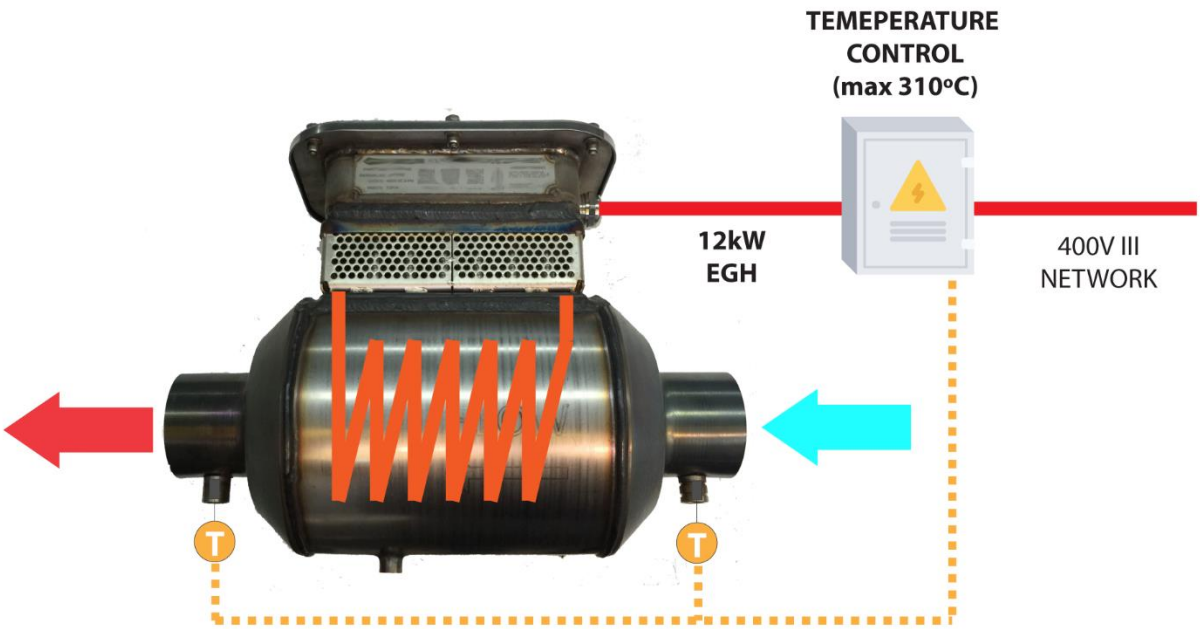

Figure 4.4. Function scheme of the used EGH.

In second place of exhaust gases circuit, we find a unit composed by a Diesel Oxidation Catalyst (DOC) and a DPF. The first one is in charge of oxidation of carbon monoxide (CO) and unburned hydrocarbons (HC). In addition, it allows a continuous regeneration of the DPF. This second one is very important to capture as many organic fraction (OF) of diesel particles as possible. Soot is the main component trapped in the filter walls, being burned when the DPF reaches a maximum backpressure. The manufacturer fixes this threshold value and when reached, a forced regeneration starts by injecting more fuel to rise exhaust gases temperature and burn the particles.

Downwards, we find a set of devices related to Diesel Exhaust Fluid (DEF) composed by the tank, the supply module and the dosing module. This particular vehicle uses a commercial urea solution as fluid, all this set is controlled by ECU parameters and this solution is not injected into the system until the exhaust gases reach 180°C. The dosing module uses temperature and NOx sensors (one located before the DOC and another after the SCR) to adjust in real time the exact dose of urea solution required to meet a particular standard (i.e. Euro VI). Finally, this solution mixed with exhaust gases enter into the SCR (Selective Catalytic Reduction) unit. Inside this device a catalytic reaction is produced to convert NOx into diatomic nitrogen (N_2), and water (H_2O).

The parameters acquired from the ECU and the rolling bench are listed in Figure 4.3. These data are crucial, as Full Throttle Pedal Position (FTPP), engine regime and the SCR inlet temperature are required to carry out the tests. The other data, such as EGH inlet and outlet temperatures (T_{B_EGH} and T_{A_EGH} respectively), the electrical power consumption of the heater ($P_{EGH} = \sqrt{3} \cdot V_{EGH} \cdot I_{EGH} \cdot cos\,\varphi$ being V_{EGH} the voltage and I_{EGH} the current) and NOx emissions (NOx_{EGH}) are obtained from external equipment. A scheme of these data acquisition can be seen in Figure 4.5.

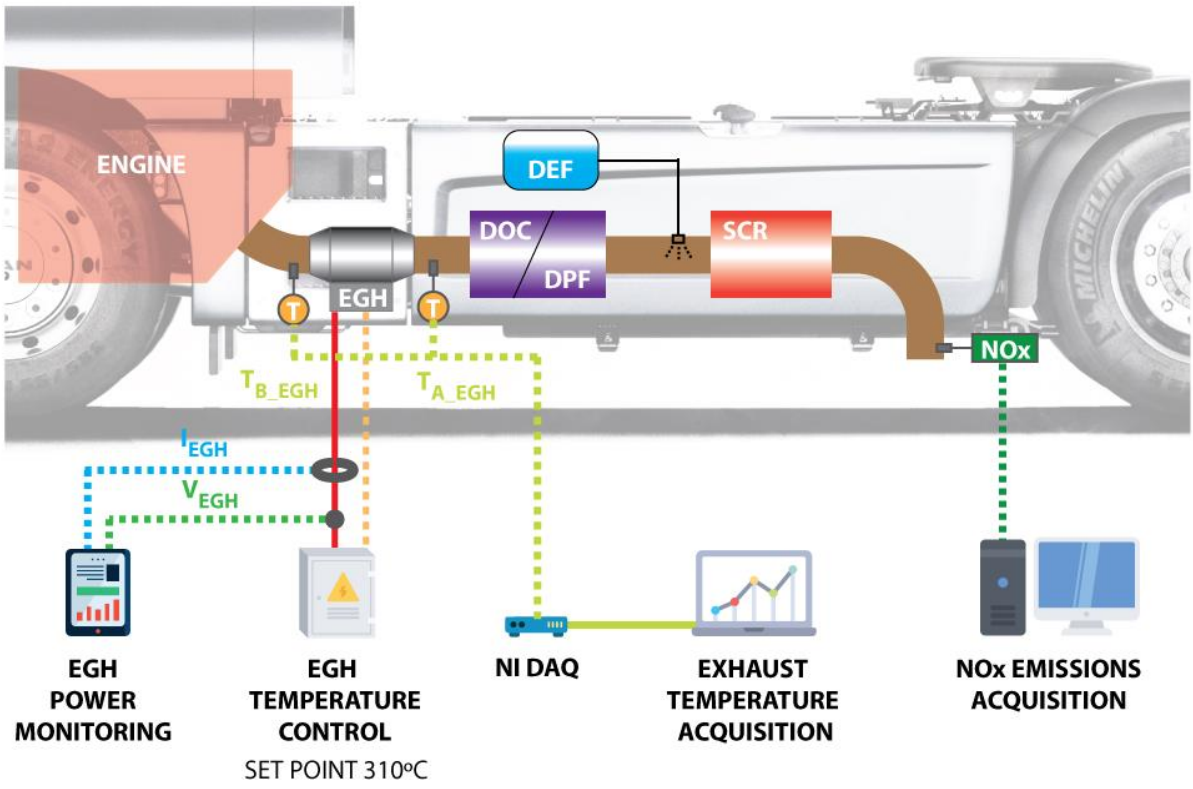

Figure 4.5. Scheme of emissions reduction system in tested vehicle.

With this particular distribution of the components, it is presumable that a rise in exhaust gases temperature can increase the efficiency of the catalytic reaction into the SCR during cold start conditions and low demanding routes with frequent stops. Furthermore, this temperature rise represents a good effect for the DPF regeneration. This system could contribute to a more efficient fuel consumption, as extra doses of fuel may not be needed for burning particles inside the DPF. The most suitable place for the addition of an ATEG to harvest thermal energy is at the

end of the standard SCR system, thus alterations of both flow and exhaust gas temperatures are minimized.

The location of the EGH during the test can be seen in Figure 4.6, with minimal deviation of the original exhaust pipe in order to maintain the original vehicle design and to avoid gas flow alterations. Thermocouple sensors shown in Figure 4.5 can be seen at inlet and outlet of the heating device. Temperatures before EGH (T_{B_EGH}) and after the EGH (T_{A_EGH}) are fundamental in order to analyse the performance of the proposed system.

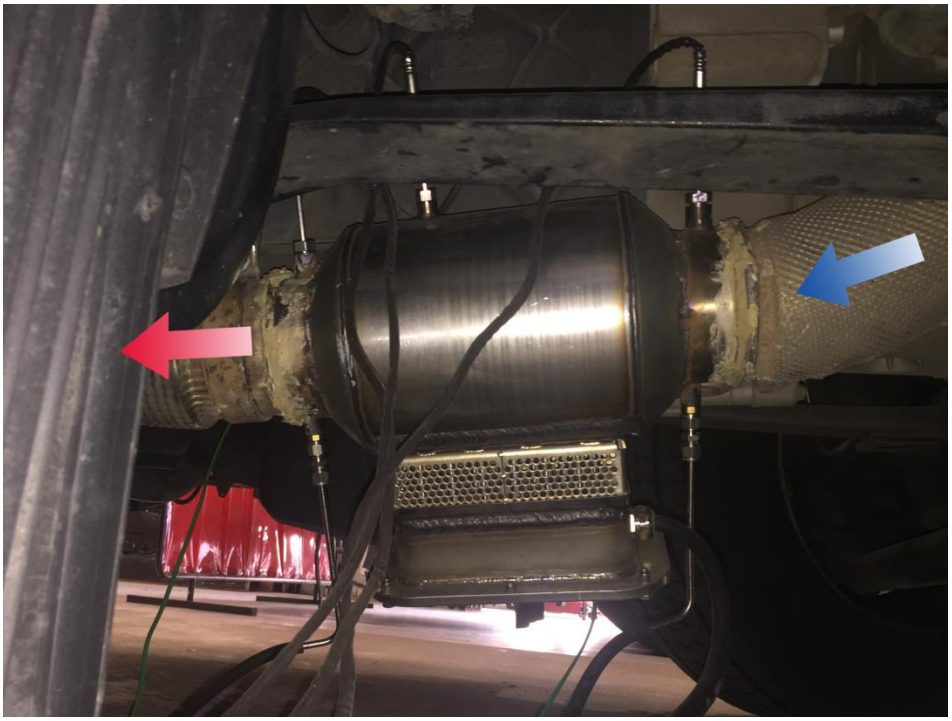

Figure 4.6. EGH installation upstream of the aftertreatment system and gas flow direction.

A certified test bench for HDV (Maha Powerdyno R200/1) is used to simulate a real vehicle in specific use conditions. This equipment is also used to capture the FTPP from the ECU. Unfortunately, it was impossible to get the specifications of the on board acquisition system, so the accuracy of FTPP measure is not available. A MIAC G4.0 was used to measure NOx emissions at the end of the exhaust pipe. This device presents a measure range from 0 to +5000ppm, an accuracy of ±5% of mv (+100 to +2000ppm) and ±5ppm (0 to +99.9 ppm) with a resolution of 0.1ppm (0 to +500ppm). The equipment used to measure the EGH power consumption was a Dranetz Power Explorer PX5 power meter with the following specifications:

voltage measuring range from 1-600Vrms with 0.1% rdg (reading) + 0.05% FS (full scale), 256 samples/cycle, 16 bit ADC; current measuring range from 1-6000Arms with 0.1% rdg + CTs (4), 256 samples/cycle, 16 bit ADC. Exhaust temperatures were recorded with a National Instruments DAQ with one NI 9211 acquisition module. This device presents a maximum measure error of 2.2°C (0-400°C) with a measurement sensitivity <0.07°C. All temperature probes used were type K thermocouples.

The vehicle selected as an experimental unit was a MAN TGX 18.480. Its specifications are summarized in Table 4.1.

Table 4.1. Main specifications of tested vehicle.

Parameter	**Value**
Maker	MAN
Model	TGX 18.480 Efficient Line 2
Gearbox	Automatic (12 gears)
Max. rated power	353 kW (at 1800 rpm)
Max. rated torque	1500 Nm (at 930-1400 rpm)
Emission standard	Euro VI

The rolling bench was configured with enough load to prevent rear tires from sliding while testing as seen in Figure 4.7. All tests were made using the same load. This load can be considered irrelevant for the conclusions of the present work.

Figure 4.7. Vehicle position on the rolling bench during the experiment.

Three different stationary points were selected to conduct the study. All of them presented low rpm values in order to analyse low demanding engine speed. The eleventh gear was selected to obtain all range of FTPP. Stationary regime was rapidly reached and stabilized in each particular test and only after this point data was registered. Engine temperature was always below 90°C in order to keep the same engine conditions during the tests, simulating a cold start condition. A short period was held to reduce the engine temperature between tests. All regimes selected for this experiment, shown in Table 4.2, can be found in a typical daily drive. NOx emissions were analysed under the following engine regimes and FTPPs.

Table 4.2. Stationary points selected for the tests.

Test	**Engine regime (rpm)**	**FTPP (%)**	**Vehicle speed (km/h)**
1	1000	30, 35, 40, 45, 50, 55, 60, 70, 80, 90	55
2	1250	30, 35, 40, 45, 50, 60, 70, 80, 90	68
3	1500	30, 35, 40, 45, 50, 60, 70, 80, 90	82

4.4 EGH experimental results

The first part of this section presents a comparative analysis of NOx emitted by a standard HDV, with and without the use of a 12kW EGH. As explained in Table 4.2, this comparative analysis was divided into three different categories according to each engine regime: 1000 rpm (55km/h), 1250 rpm (68km/h) and 1500 rpm (82km/h). In all regimes, the target temperature of the EGH was set to 300°C.

Considering that a power consumption of 12kW may be excessive for the electrical system of the vehicle, in the second part, a more realistic approach on EGH power consumption (P_{EGH}) is conducted. The objective is to determine the SCR efficiency improvement at different values of EGH power, from 0.5 to 5kW [5]. These values will be useful to carry out the theoretical study of Chapter 4.5, where the viability of using a thermoelectric waste heat recovery system to supply the energy required by the EGH is studied.

4.4.1 NOx reduction analysis under different engine regimes

As it can be seen in Figure 4.8, at 1000 rpm, the NOx ppm values are the highest of the three regimes (Figures 4.8 to 4.10). NOx emissions, considering that EGH was disabled NOx_{EGH_OFF} , achieved 578 ppm when the FTPP was at 60%. At the same conditions, NOx measured with the EGH enabled NOx_{EGH_ON} was about 87 ppm. This was the maximum reduction achieved in all tests. In absolute numbers, it represented a NOx reduction of 508 ppm. In relative terms, however, the greatest reduction was achieved at 50% FTPP with 97.2% of ppm reduction.

Detail analysis of Figure 4.8 reveals that inlet and outlet EGH temperatures, T_{B_EGH} and T_{A_EGH}, converged at high FTPP values. This can be explained by the higher exhaust gas temperatures generated by the combustion engine that made the EGH to turn off for temperatures higher than 300°C (note that the setpoint temperature of the EGH was set to 300°C). A dramatic decrease in NOx emissions was obtained at 60% FTPP when the EGH was disabled. As mentioned before, urea solution is dosed over 180°C. This means that a NOx reduction should have been registered at 50% FTPP and above. However, NOx emissions start to fall at 60% FTPP. This short delay (15 seconds in the experiment) can be related to ECU parameters that control

the exact moment of dosing. Note that EGH was not needed at maximum FTPP where the power demand by the EGH was effectively reduced below 3 kW. Contrarily, at low engine loads (i.e. FTPP < 80%), EGH consumed much more power to increase the exhaust gas temperature to the desired set point. Consider that the exhaust mass flow rate tends to increase with FTPP. That is the reason why the power consumed by the EGH at 80% FTPP is the similar to 60% FTPP, despite having different inlet temperatures. Peak power consumption P_{EGH} of 11.26 kW is reached at 45% FTPP obtaining a NOx reduction of 400 ppm. For medium range FTPP values, P_{EGH} is being slowly reduced as exhaust gas temperatures tend to stabilize around 300°C.

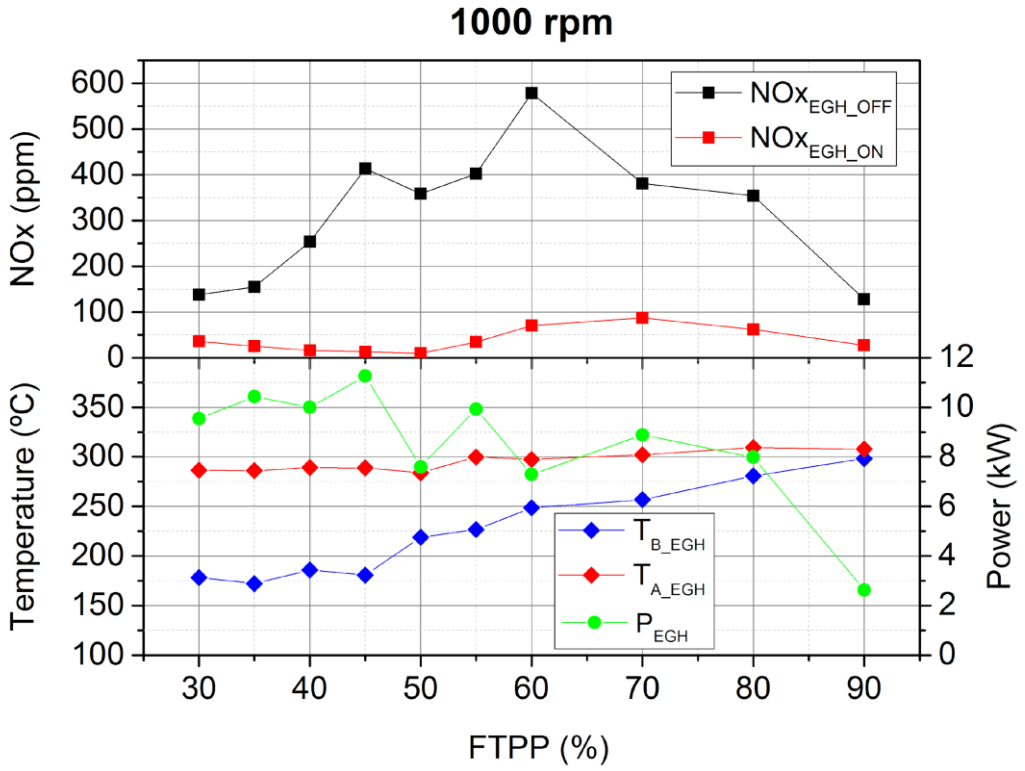

Figure 4.8. NOx emissions with EGH on and off (upper graph) and exhaust gas temperatures before and after EGH with power consumed by EGH at 1000 rpm (lower graph) as a function of the FTPP. Note that error bars are smaller than the size of symbols.

In Figure 4.9, at 1250 rpm, it can be observed that EGH also permitted a reduction of NOx emissions. However, in this case the NOx values with the EGH turned off (NOx_{EGH_OFF}) substantially decreased in comparison with the previous regime at 1000 rpm (Figure 4.8). This tendency is also observed at 1500 rpm although in a less pronounced way (see Figure 4.10). At 1250 rpm the NOx_{EGH_OFF} peak was reached at 70% FTPP with a value of 81 ppm. This

stationary point presented a NOx reduction of almost 100% after enabling the EGH. It represents the most relevant NOx reduction at 1250 rpm in absolute numbers. At this regime, an almost completely reduction of NOx started at 60% FTPP and it was maintained for higher FTPP values. On the other hand, the same behaviour as in 1000 rpm, regarding the temperature convergence at high FTPP values, was observed. Both EGH inlet and outlet gas temperature curves took the same tendency at the end of the test with a difference of just 18.5°C at 90% FTPP. It also can be appreciated a coincidence between the peak demand (9.66 kW) at 45% FTPP and the peak of T_{A_EGH} (314.33°C). After this value, power decreased and T_{A_EGH} was stabilized until 80% FTPP. The EGH power consumption was 7.95 kW at the major NOx reduction point found at 70% FTPP (81 ppm).

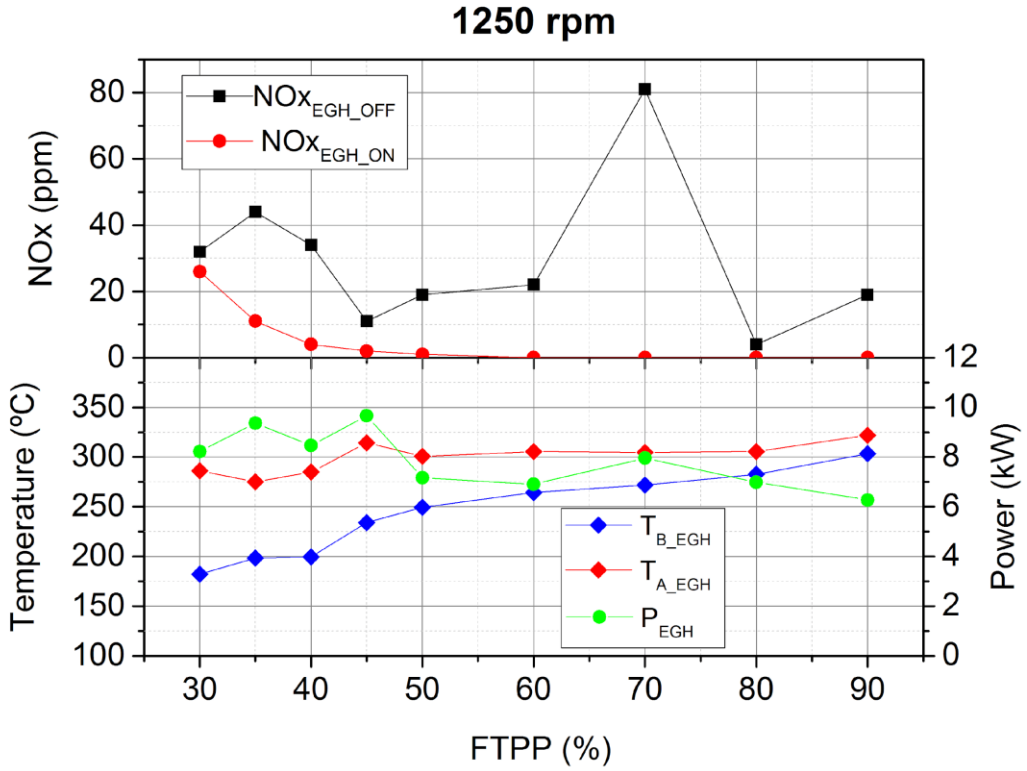

Figure 4.9. NOx emissions with EGH on and off (upper graph) and exhaust gas temperatures before and after EGH with power consumed by EGH at 1250 rpm (lower graph) as a function of the FTPP. Note that error bars are smaller than the size of symbols.

Figure 4.10 shows the stationary points at 1500 rpm. It can be observed that the contribution of the EGH was non-existent along the first FTPP points. Note that NOx emissions are higher when EGH is turned on than off. This can be explained by the EGR valve aperture at the 30%-45%

FTPP that cut NOx emissions through the reinjection of the exhaust gases into the admission port. ECU controls the valve opening angle and may be slightly different in the two tests. On the other hand, it was at FTPP values higher than 45% when the EGH contribution was relevant. A NOx_{EGH_OFF} peak point of 132ppm at 70% FTPP was observed. These NOx emissions NOx_{EGH_ON} were reduced up to 98.48% through the use of the EGH.

The major difference between T_{B_EGH} and T_{A_EGH} was achieved at the beginning of this test (30% FTPP). This initial heating led to very low NOx_{EGH_ON} values during the entire test, despite not being as low as NOx_{EGH_OFF} values until 45% FTPP. Overall, this test registered a total NOx reduction of 89.46% and this was achieved specially at middle FTPP range with a significant power consumption (6.5 kW - 8.5 kW). Regarding both EGH inlet and outlet temperature curves we can see a steady increase after 50% FTPP. This is because in mid-high demanding regimes, such as 1500 rpm, the engine produces great amounts of thermal energy that produces high exhaust gas temperatures. This particular regime is an example where EGH is less required because combustion engines produce enough heat to make the catalytic conversion highly efficient, see Figure 4.1. Notice the dramatic decrease of P_{EGH} at the last third of the test.

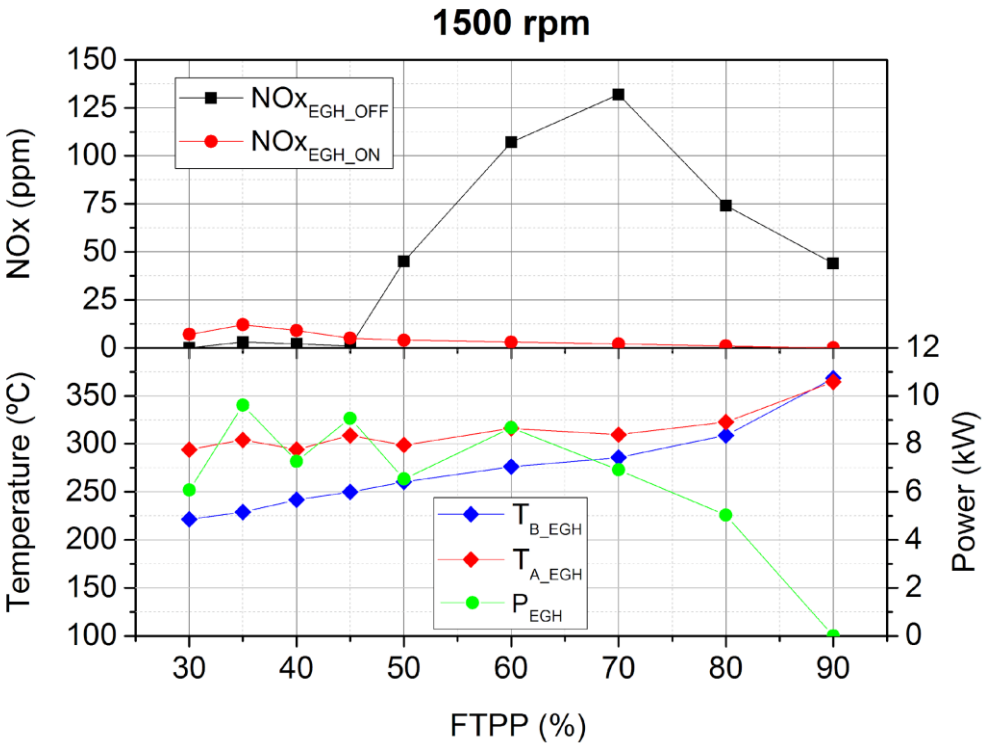

Figure 4.10. NOx emissions with EGH on and off (upper graph) and exhaust gas temperatures before and after EGH with power consumed by EGH at 1500 rpm (lower graph) as a function of the FTPP. Note that error bars are smaller than the size of symbols.

Regarding the power consumption of EGH, there was a tendency repeated in all three tests. There was a huge amount of energy required to rise temperatures in a short period, for the first half of stationary points studied. As FTPP increased for the same regime, temperatures of the exhaust gas also increased and EGH power demand decreased drastically at the end of each test. The lowest point of instant power demand was always at 90% FTPP.

A common pattern was detected through the three studied regimes. Without EGH, the NOx_{EGH_OFF} peak was reached between 60-70% FTPP. However, thanks to the inclusion of the EGH, the urea solution injection threshold was reached earlier. Consequently, the earlier catalytic conversion provided a dramatic descend of NOx_{EGH_ON}.

Results in Figure 4.8 to 4.10 include the absolute uncertainty values of measured data. NOx and temperature standard uncertainties have been calculated using the measurement accuracy obtained from the manufacturer's datasheet (see Chapter 4.3). Note that EGH power was indirectly obtained by the product of voltage and current, separately read with the power meter. Then, the measurement uncertainty of EGH power was calculated combining the uncertainties in measured parameters to arrive at an uncertainty value for an experimental result that depends on these parameters [22,23]. However, the error bars of data are less than 5% for all cases and may be even lower than the size of the symbol used in the graphs.

In Table 4.3, the overall results of NOx reduction are summarized. Achievements are remarkable in all cases being the less average reduction obtained in Test 3 (53.94%). This result is mainly due to the high exhaust gas temperatures produced by the engine at 1500 rpm. These high temperatures make the SCR conversion more efficient without the need of an EGH. We must take into account there was higher NOx emissions NOx_{EGH_OFF} at 1500 rpm compared with the 1250 rpm regime. On the other hand, if we sum comparative ppm values of all FTTP cases in each regime, we can observe that Test 1 gave the best result of total NOx reduction (2780 ppm). Furthermore, all tests presented results over 80% in total NOx reduction. This indicates the important role of the EGH to eliminate a significant quantity of NOx at low engine regimes.

Table 4.3. Comparative NOx reduction results in different tests.

TEST	Average NOx reduction (%)	Total NOx reduction (%)	Total NOx reduction (ppm)	Average EGH power consumption (kW)
1	86.35	87.97	2780	8.55
2	84.28	83.45	222	7.89
3	53.94	89.46	365	6.58

However, there is an issue that needs to be analysed in more detail. As seen in Table 4.3, power consumption is far beyond maximum capabilities of an EGH connected to an ATEG. The main goal of the following subsection is to establish a compromise between SCR efficiency at low temperatures and the power consumed by the EGH providing the energy demand requirements in order to design a suitable ATEG.

4.4.2 EGH power consumption vs SCR efficiency

Thermoelectric generators can reach efficiencies of 5%. These efficiencies can only be achieved when TEGs are subjected to its maximum temperature difference [38–41]. However, when TEGs are interconnected between them and located along the exhaust pipe, last modules are subjected to lower temperature differences than first modules, producing a decrease on the overall efficiency of the ATEG [42,43]. As seen in current research, ATEG systems can achieve effective efficiencies around 2,5% [34]. Thus, it is necessary to determine if an ATEG can supply the energy demanded by the EGH. In this section, a feasibility study on EGH power as well as energy consumption is conducted. It is possible to determine the SCR efficiency improvement for different P_{EGH} using the SCR conversion efficiency data from Figure 4.1, the experimental SCR inlet gas temperatures (T_{IN_SCR}) and exhaust mass flow rate ($\dot{m}$) obtained from the ECU.

Test 1 scenario will be used for this theoretical approach due to its low engine regime (1000 rpm) and its low gas temperatures that reflect a typical low speed route done by a HDV. Selected FTPP values are in the low range (30%-45%) because it is where the T_{B_SCR} are lower than the urea solution threshold (T<180°C). Data in Table 4.4 contains a SCR inlet gas temperature comparison between the standard system (EGH disabled), the same system with the EGH enabled, and a proposed EGH. This last group of gas temperatures is calculated using

the heat transfer equation $P_{EGH} = \dot{m}c_p(T_{A\_EGH} - T_{B\_EGH})$ by assuming that all electrical power supplied to the EGH is effectively transferred to the exhaust gases in terms of heat. In the previous equation, P_{EGH} is the proposed power of the EGH, $\dot{m}$ is the measured exhaust gas mass flow rate at a constant FTPP, c_p is the specific heat at constant pressure of the exhaust gases calculated using the temperature value registered for each FTPP, and T_{B_EGH} is the measured exhaust gas temperature before the EGH at a constant FTPP. As seen in Chapter 4.3, the SCR is installed downstream the EGH. For this reason, we consider $T_{A\_EGH} = T_{B\_SCR}$. Table 4.4 shows the SCR efficiency improvements under different values of P_{EGH}, ranging between 0.5 and 5kW.

Table 4.4. SCR efficiency for different EGH powers at 1000 rpm.

	SCR inlet temperature (T_{B_SCR})			**SCR conversion efficiency**		
FTPP (%)	**EGH disabled (°C)**	**Tested EGH enabled (°C)**	**Proposed EGH enabled (°C)**	**EGH disabled (%)**	**Tested EGH enabled (%)**	**Proposed EGH enabled (%)**
EGH proposed of 0.5 kW						
30	178.27	286.41	183.94	64%	95%	67%
35	172.15	286.1	177.63	60%	95%	63%
40	185.9	289.13	191.09	68%	95%	72%
45	180.7	288.82	185.58	65%	95%	68%
EGH proposed of 1 kW						
30	178.27	286.41	189.61	64%	95%	71%
35	172.15	286.1	183.11	60%	95%	67%
40	185.9	289.13	196.28	68%	95%	75%
45	180.7	288.82	190.46	65%	95%	71%
EGH proposed of 2 kW						
30	178.27	286.41	200.96	64%	95%	78%
35	172.15	286.1	194.07	60%	95%	74%

40	185.9	289.13	206.66	68%	95%	82%
45	180.7	288.82	200.21	65%	95%	78%
EGH proposed of 3 kW						
30	178.27	286.41	212.30	64%	95%	85%
35	172.15	286.1	205.04	60%	95%	81%
40	185.9	289.13	217.04	68%	95%	88%
45	180.7	288.82	209.97	65%	95%	84%
EGH proposed of 4 kW						
30	178.27	286.41	223.65	64%	95%	93%
35	172.15	286.1	216.00	60%	95%	88%
40	185.9	289.13	227.42	68%	95%	95%
45	180.7	288.82	219.72	65%	95%	90%
EGH proposed of 5 kW						
30	178.27	286.41	234.99	64%	95%	95%
35	172.15	286.1	226.96	60%	95%	95%
40	185.9	289.13	237.79	68%	95%	95%
45	180.7	288.82	229.48	65%	95%	95%

As seen in Table 4.4, low P_{EGH} provides a slightly increase in exhaust gas temperatures that leads to a moderate benefit in SCR conversion efficiency. P_{EGH} values below 2kW only contribute to increase the SCR efficiency about 3% to 7%. SCR efficiencies up to 80% can be found at 40 FTPP with a P_{EGH} of 2 kW. To conclude these comparative results, it is clear that 95% of SCR efficiency needs EGH consumption values between 4kW and 5kW.

These results demonstrate that the standard SCR performed at 60-68% of its efficiency. It is interesting to note that the lowest FTPP (30%) value is not the poorest in efficiency terms. In the same way, the highest FTPP (45%) is not the best performing regarding power consumption values. Maximum efficiency (95%) is reached firstly at 40% FTPP with 4kW consumed.

At this point it is important to remark that it is unnecessary to consume 12kW in an EGH to substantially reduce NOx emissions. Considering temperature of urea solution injection around 180°C, it is clear that the EGH device should only heat the exhaust gases up to reach this target

value. To provide an extra thermal power to the exhaust gases is useless and counter-productive. The SCR efficiency reaches its maximum in the worst FTPP scenario of low exhaust gas temperatures with a 5kW EGH.

In a conventional system, the power supplied as well as the energy consumed by the EGH must be extracted from the electrical system of the vehicle. The electrical power generated by the vehicle comes from the alternator, which converts part of the mechanical energy produced by the combustion engine into electricity. This means that a system with EGH to achieve an extra NOx reduction would demand more electrical energy. Hence, more time using the alternator would imply an increase on the vehicle's fuel consumption.

To avoid this emission increment, our research focuses on the viability of using the exhaust waste heat to produce the electricity needed for the EGH. The goal is to simulate and quantify an ATEG model to convert waste heat, downstream of the aftertreatment system, into electricity. This will avoid the need for the electric system to consume more fuel to produce the extra electrical energy. Many theoretical models [34,37,43–45] and experimental prototypes [35,46–49] have been developed which demonstrate the feasibility of automotive ATEGs. Other ways to produce this additional energy from exhaust gases may be the use of Organic Rankine Cycle (ORC) [50–52].

4.5 ATEG simulation model

In order to validate the previous exposed idea, a simulation model of an ATEG is launched with relevant data gathered during the experimental test described in Chapter 4.3. The idea is to explore the theoretical capabilities of commercial Thermoelectric Modules (TEM) disposed in a particular array that guarantees enough power to supply electrical energy to the EGH. Focusing on this goal, a 1500 rpm regime is chosen as it contains the highest tested exhaust gas temperatures without surpassing the TEM maximum working temperature (230°C). As explained in Section 4.4.2, EGH may not be needed with high exhaust gas temperatures at this regime. On the other hand, ATEG benefits from these conditions to convert thermal energy into electricity for a future use in a low regime (for example 1000 rpm).

GT-SUITE [53] is chosen as the simulation software due to its proven research in the automotive sector [42,47,54–57]. This multiphysics CAE simulation tool is a commonly used software for engine modelling, which also incorporates a TEG block in its library to model and size automotive thermoelectric generators for exhaust waste heat recovery. This software has been validated with experimental data in multiple references [47,54,55]. Despite our specific configuration proposed, exhaust systems of internal combustion engines have been successfully simulated and validated with this tool. For example, Massaguer et al. [42] compared and validated a longitudinal thermoelectric energy harvester (LTEH) by using a mathematical model and experimental data. Furthermore, Cózar et al. [55] successfully reproduced the performance curve of the same commercial TEM (Marlow TG12-8-01LS) used in our simulation model.

Exhaust gas temperature and its mass flow rate are both variables depending on a particular FTPP value. It is important to keep in mind the most suitable location for an ATEG into the exhaust system of this particular vehicle. During the thermoelectric energy conversion, the ATEG reduces the temperature of the exhaust gases, the opposite effect to what is sought inside the ATS. Having this in mind, the best location of the ATEG is downstream of the ATS. This location allows us to conclude that the exhaust inlet temperature parameter introduced into the simulation is going to be the SCR outlet temperature obtained from the ECU during the experimentation. On the other hand, there are constant parameters introduced such as coolant mass flow rate (0.12 kg/s) and coolant inlet temperature (25°C). This cooling circuit relies on a water pump and a heat exchanger that provides a constant flow along the cold face of every TEM. Ambient temperature registered from the day of the experiment (30°C) is introduced for the TEM initial temperature parameter. Table 4.5 provides a general overview of the different case studies of this ATEG simulation. Each case study represents a particular FTPP analysed with the HDV on real conditions. Notice that ATEG inlet temperatures correspond to data registered at the end of the standard exhaust system tested, as is the optimal position for coupling this ATEG component.

Table 4.5. Exhaust gas parameters in different FTPP values.

CASE STUDY	FTPP (%)	Exhaust mass flow rate (kg/h)	ATEG inlet temperature (°C)
1	30	313.2	242
2	35	474.7	223
3	40	513	201
4	45	541.7	186
5	50	636.5	186
6	60	789.2	196
7	70	1013.2	214
8	80	1315.7	249
9	90	1315.7	295

The thermoelectric module used in the simulation was the TG-12-08 from Marlow Industries. This module uses bismuth telluride as a thermoelectric material. It was chosen because it has shown a high correlation between manufacturer's data and experimental data [42]. Apart from that, its maximum working temperature is 230°C, which is very similar to the average engine exhaust temperatures. The TG-12-08 has the following dimensions 44.7x40.3x3.53mm (LxWxH). The external contact plates are made of aluminum oxide to electrically insulate the inner circuit.

To carry out the simulation, it is necessary to obtain the characteristic parameters of the thermoelectric module and enter them into the software. These are: the Seebeck coefficient, the thermal resistance and the electrical resistance of the TG-12-08 at different average temperatures T_{avg}. Thermoelectric average temperature T_{avg} is calculated in °C as follows: $T_{avg} = (T_H + T_C)/2$ where T_H is the hot side temperature and T_C is the cold side temperature of the module.

Using the manufacturer data, a regression line is obtained for each parameter, Eq. 1 to 3, which give a high coefficient of determination R^2>0.95. These linear equations are then used by the software to find new values.

Seebeck coefficient [mV/K]

$$\alpha = (-4.142 \cdot 10^{-2}) \cdot T_{avg} + 58.26 \ (R^2 = 0.95) \quad \text{(Eq.1)}$$

Thermal resistance [K/W]

$$R_t = (-1.3293 \cdot 10^{-3}) \cdot T_{avg} + 1.314 \ (R^2 = 0.98) \quad \text{(Eq.2)}$$

Electrical resistance [Ω]

$$R_i = (9.2738 \cdot 10^{-3}) \cdot T_{avg} + 1.4579 \ (R^2 = 0.99) \quad \text{(Eq.3)}$$

The above exposed calculations are considered close enough to experimental data regarding R^2 values (0.95-0.99). Thus, it is considered that TEM parameters are reliable and ATEG simulation can provide a theoretical model close to reality.

Finally, to simplify the model, the following parameters have been neglected:

- Contact resistance between elements.
- Convective and radiative heat losses in the TEG.
- Thomson effect. This effect has a very low impact in TEG performance, typically two times less than the Joule effect [58]. This work [59] rigorously demonstrates that the standard thermoelectric model, neglecting Thomson effect, produces the exact module output power and efficiency if an integral-averaged Seebeck coefficient is used.

TEMs form an electrical array as shown in Figure 4.11. Each cell is represented by a voltage source $V_{1,\dots,180}$ and an internal resistance $R_{1,\dots,180}$. To begin with, 15 TEMs are connected in series. Afterwards, this pattern is repeated in 12 parallel rows up to a total number of 180 thermoelectric units. The ATEG can operate under two system stages as exposed in Chapter 4.2. Heating stage (1) is activated when the system increases the exhaust gas temperatures by means of the EGH to improve the SCR efficiency. As represented, PCU controls the electrical energy delivery from the battery. Recovery stage (2) transforms waste heat into electrical energy and the PCU stores it into the battery for future uses. This ATEG electrical configuration

is designed to obtain a proper relationship between current and voltage to feed the PCU converter. In order to charge correctly the battery, voltage is stabilized at 12.8 V.

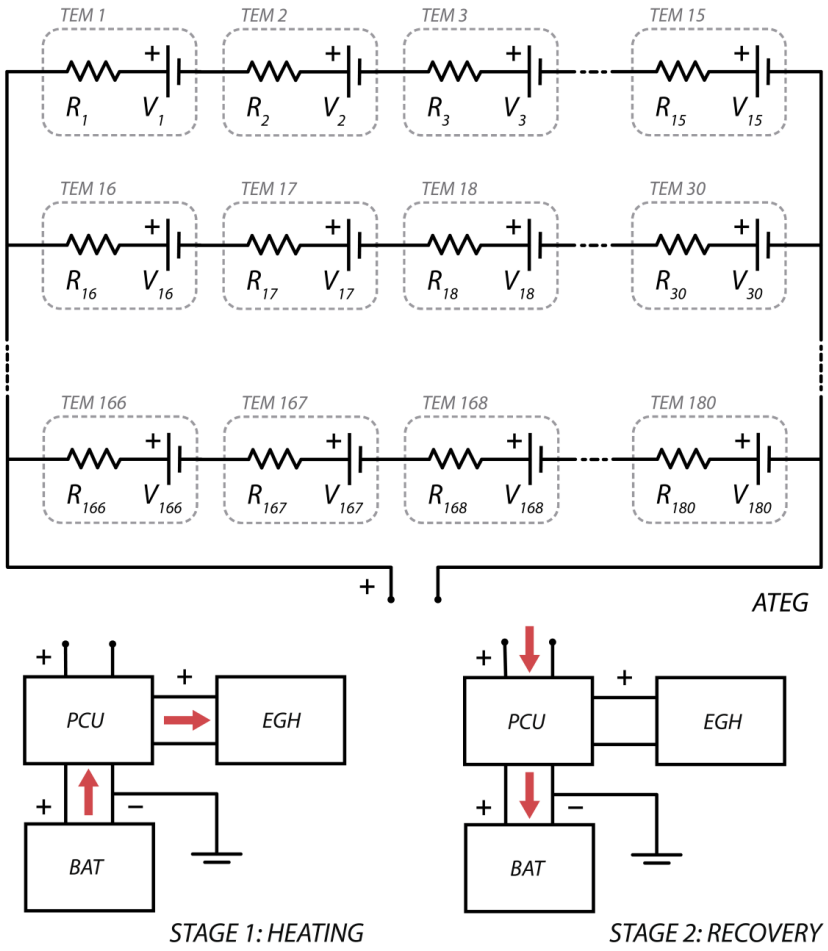

Figure 4.11. Simulated electrical scheme of system proposed. Includes ATEG with its TEM array, Heating stage (1) and Recovery stage (2) with its particular energy flow between battery, PCU, EGH and ATEG.

The distribution and assembly of the different TEMs is taken from a trusted model already tested in a car [17]. The full TEM assembly contained in the simulated ATEG appears in Figure 4.12. Its square shape is used to pack them in four rows of 15 TEM each. This composition is repeated in three subassemblies. Hot sides of TEMs are the interior ones where exhaust gas is canalized. Cold sides of TEMs are the exterior ones for its refrigeration using cold plates. Notice the counter-flow disposition between exhaust gas and coolant.

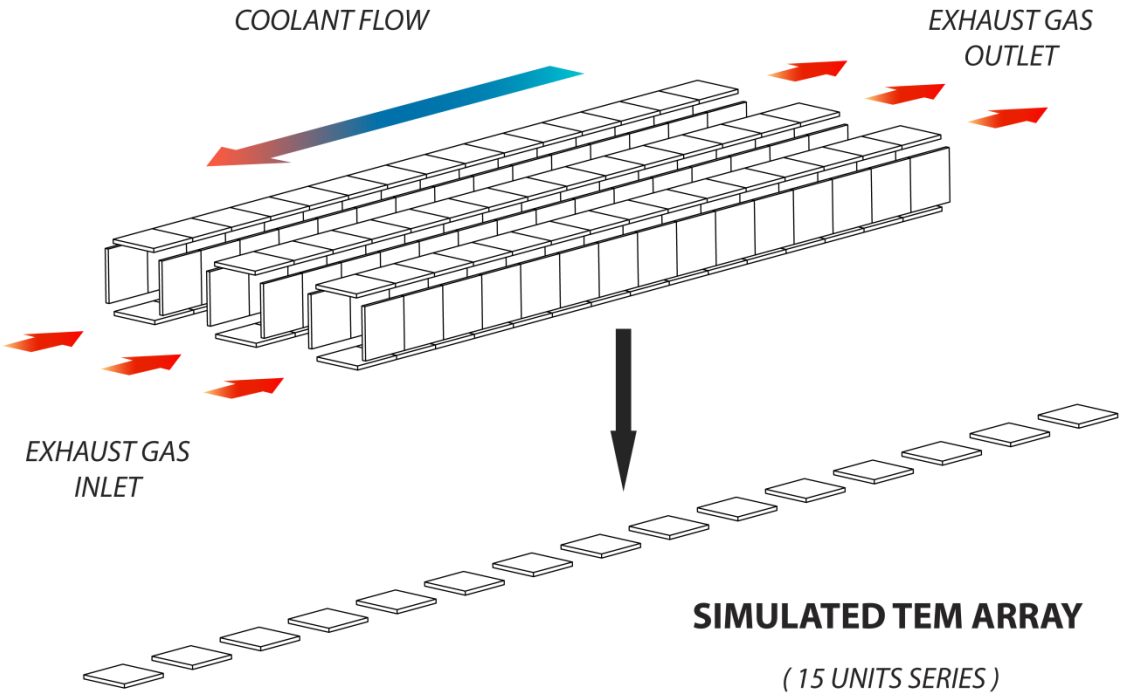

Figure 4.12. TEM distribution and total composition of theoretical ATEG simulated.

Heat exchange geometry applied to the model, is also taken from the same trusted model mentioned before. The hot side heat exchanger is composed of a holed aluminum block. This block has 5 identical holes through which exhaust gases flow. The interior cross-sectional area of each hole is 25mm^2 and the wetted perimeter of the pipe, used in the calculation of the hydraulic diameter, is 58mm. The surface roughness of the pipe is 0.002mm, corresponding to drawn metal. The same geometry is used for the cold side heat exchanger.

The simulation uses Chilton Colburn analogy to calculate the heat transfer coefficient of each case study, as it is the recommended option for laminar and liquid-gas flow simulation [60].

Heat transfer coefficients obtained are within standard values (400-1500 W/m^{2}K) and demonstrate that the simulation is reliable. Finally, we can have a precise lecture of the amount of energy recovered from the waste heat of this exhaust system. It covers a wide range of values (0.4-1.4kW) depending on the FTPP analysed.

It is important to note that the energy loss due to backpressure on the exhaust pipe and pressure loss in the cold side heat exchanger have not been considered. Following the considerations exposed in [37,46,47], the energy loss due to this two phenomenon should be subtracted from the power generated by ATEG to obtain the net power generated.

Table 4.6. Relevant data from ATEG simulation results.

CASE STUDY	Power (W)	Voltage (V)	Exhaust Outlet Temperature (°C)	Coolant Outlet Temperature (°C)	Heat Transfer Coefficient (W/m^{2}K)
1	425.22	36.22	64.72	28.42	409.41
2	514.21	41.85	87.58	28.95	549.85
3	442.68	38.67	85.55	28.64	574.78
4	392.40	36.28	83.59	28.41	592.88
5	435.70	38.73	92.78	28.64	667.42
6	546.68	44.25	109.67	29.17	786.05
7	729.58	52.32	133.90	29.96	955.78
8	1063.12	65.11	170.64	31.27	1183.07
9	1428.72	77.43	199.94	32.64	1213.10

A correlation of time can be established to supply the demanded power P_{EGH} , shown on Table 4.4, with the simulation results seen in Table 4.6. Here, test route conditions of a HDV are considered combining both stages of the system proposed using regime and speed data gathered from the previous tests. For the heating stage, we have selected the worst regime for SCR efficiency values (1000 rpm, 50 km/h). Indeed, it is during this cold start conditions when all the electric energy stored in the system must be transformed into heat using the EGH. For the recovery stage, the engine regime is set to 1500 rpm (80 km/h). With this route parameters, exhaust wasted energy is recovered by the ATEG and stored for being used in future EGH demands.

It is assumed that EGH is used the first 12 minutes after the engine start up. This time coincides with the cold start period for this particular vehicle. After this time, the standard aftertreatment system of the vehicle starts cutting NO_x emissions efficiently. Figure 4.13 shows

the working period required by the ATEG at 1500 rpm (recovery stage) to supply enough energy to the EGH (heating stage) during cold start. In addition, the recovery stage time depends on FTPP (%) and target power of the EGH (kW).

Regarding these results, it is observed a common pattern with two different zones. If we are moving into the lower range of FTPP (30%-45%), the recovery time needed for an ATEG is considerably long, as exhaust gas temperatures are too low to generate a great amount of power in a short period of time. Obviously the 5kW EGH is the longest to get fully supplied with 152 minutes if we consider that the ATEG is working continuously at 45% of FTPP. On the contrary, remaining with the same FTPP, it takes only 15 minutes to achieve its aim if the EGH supplies 0.5kW.

The second zone of the graphic shows a progressive descend in the time needed to power the EGH. With higher FTPP values, the exhaust gas temperatures are higher. Consequently, the ATEG energy recovered is also higher. This explains why less time of ATEG operation is needed with higher FTPP values. For a 0.5kW demand, it needs less than 5 minutes of the vehicle at 1500 rpm and 90% FTPP. Moving to the higher FTPP band, only 41 minutes is needed to fully supply an EGH of 5kW.

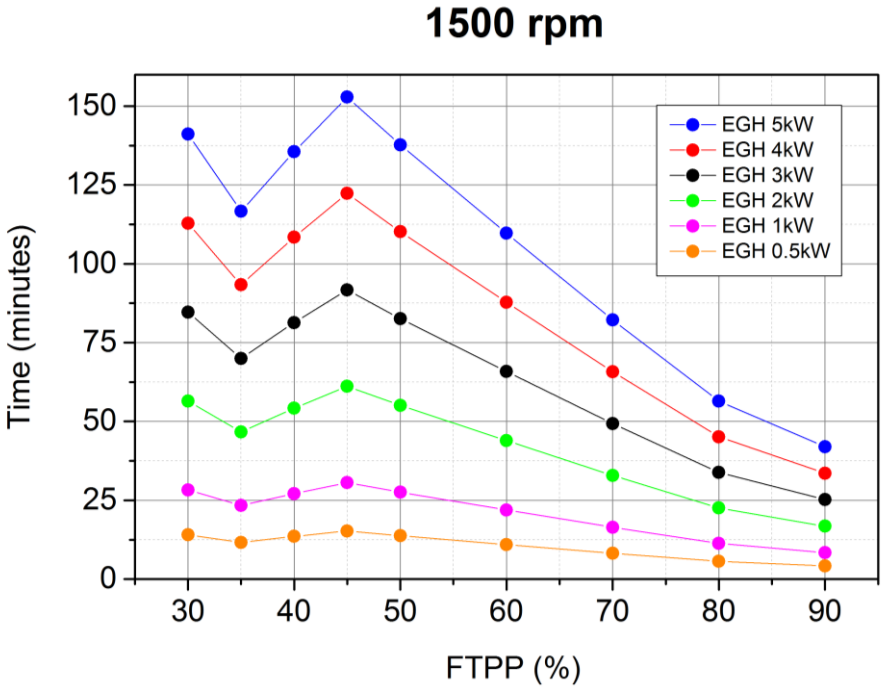

Figure 4.13. Time using ATEG to supply EGH power demand during cold start period at 1500 rpm.

As seen before, the majority of time figures are possible to achieve during a normal long-haul working journey of a HDV. However, it is important to add some light to the emission reductions obtained with this ATEG coupled to different EGH power configurations. Figure 4.14 quantifies the SCR efficiency improvement of the proposed EGH+ATEG system respect to the standard aftertreatment system of the HDV tested, both cases compared at 1000 rpm regime. Y-axis (time values in minutes) represents the duration of the recovery stage performed by the ATEG at 1500 rpm regime. These results confirm that EGH is required in lower or medium FTPP values, where major improvements are achieved, especially at high power demand of EGH (4 kW - 5 kW). Analysing results from high FTTP values to lower, we can see a progressive increase in SCR improvement, related with EGH power demand. From 65% FTPP onwards there is no remarkable efficiency improvement (<1%) of the catalytic system. Even for an EGH proposed of 0.5 kW, we can see that improvements in almost every FTTP can be dismissed. A poor efficiency improvement (5%-15%) is obtained for FTPP downwards until 50% for most EGH power values. However, EGHs of 0.5 kW and 1 kW are included totally in this improvement zone or even lower. The next efficiency improvement zone is more dynamic, which represents major values obtained adding few extra minutes of the ATEG recovery stage. Observing this medium improvement zone (15%-40%), we can conclude that includes low FTPP values (30%-45%). EGH power demand required for these improvements is in the range of 2 kW to 3 kW. The time needed to recover this energy through the ATEG is moderate (approximately 50-90 minutes). Moving on, we arrive to major recovery improvements (40%-55%). These figures can be obtained by EGH power values of 4 kW to 5 kW and can be applied for low FTTP values (30%-45%). Time figures for recovery stage of this power range are longer (95-155 minutes) but completely within HDV daily transportation routines.

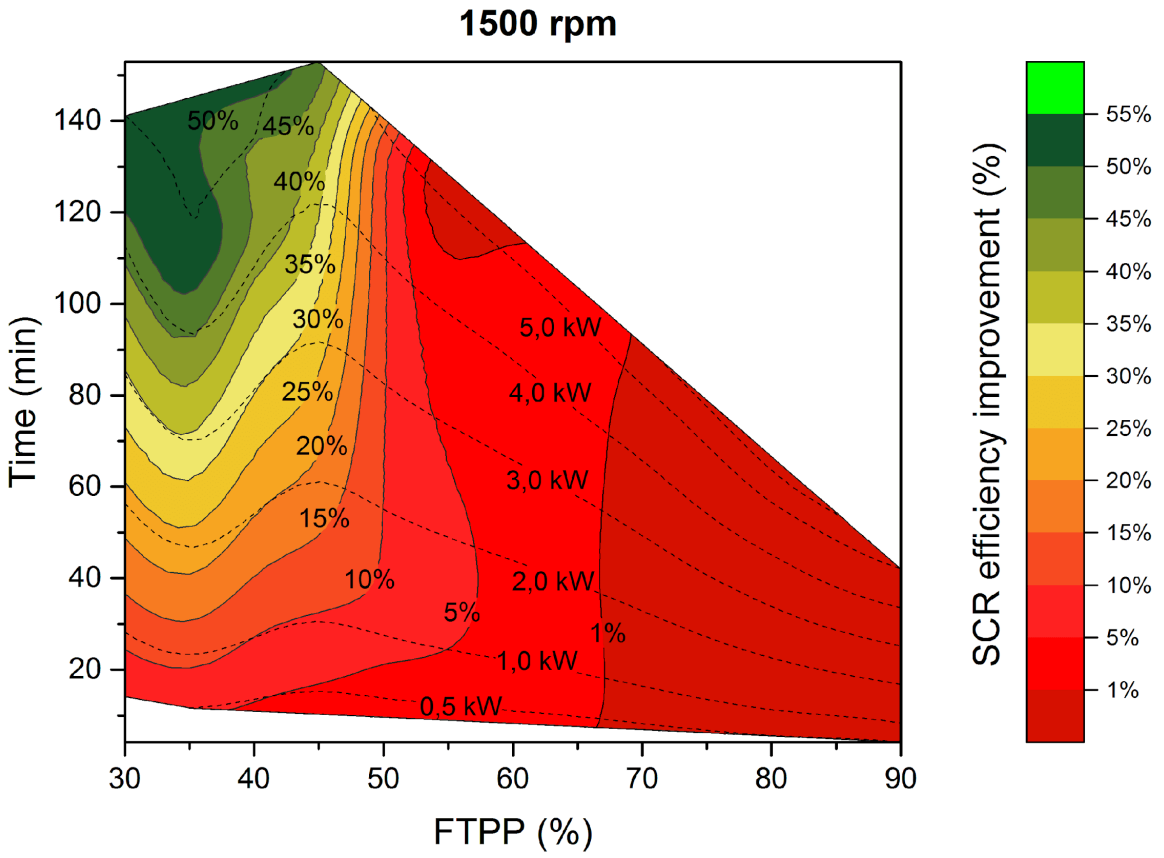

Figure 4.14. SCR efficiency improvement at 1000 rpm using different EGH power. Time using ATEG at 1500 rpm to supply respective EGH power demands at 1000 rpm.

4.6 Conclusions

This study experimentally demonstrates that the use of an EGH can reduce the NO_x emissions more than 80% in a Diesel-powered Euro VI Heavy Duty truck working at low engine regimes. The highest reductions were achieved at 1000 rpm and medium FTPP values. It also has been demonstrated that, at low engine regimes, EGH power higher than 5kW does not produce a significant impact on NO_x reduction. A conventional catalytic device heated using an EGH of 5 kW could improve the SCR efficiency from 65% to 95%. Consequently, exhaust gas heaters are a potential solution to the high emitting low engine regimes issue.

Numerical simulation of an ATEG demonstrate the viability of using the exhaust waste heat to produce electricity needed by the EGH. The designed ATEG layout consists of 180 commercial TEM units, distributed in 12 parallel groups of 15 consecutive cells. This ATEG generates a power range between 0.4 kW (at 30% FTPP) and above 1.4 kW (at maximum FTPP of 90%).

These values are obtained using an average engine regime (1500 rpm) scenario. Thinking about greater values of power generated by the same supposed ATEG is not reckless as HDV engine maximum power of this particular unit is reached between 1600 rpm to 1800 rpm.

The viability of energy supply during a cold start scenario (1000 rpm during 12 minutes) is positively demonstrated by time figures not exceeding of 155 minutes in the worst conditions possible (5 kW of EGH demand and generation at 45% FTPP). This viability guarantees the needed increment for exhaust gas temperature (T_{B_SCR}) in order to warm up SCR and start dosing urea solution in a shorter period of time. In consequence, the SCR efficiency is improved up to 55% using a proposed EGH of 5 kW and powered exclusively by an ATEG.

Deeper research concerning ATEG optimization for HDV specific characteristics is needed. Future work must focus on the system design, providing an accurate net energy balance after considering exhaust backpressure and pressure loss. Design geometry is fundamental to minimize backpressure as internal sharp edges tend to influence into mass flow rate behaviour.

It is also important to quantify cost and efficiency ratios in long haul case studies as they are the most common routes for these vehicles. At the same time, it is fundamental to make a calculation of the amount of energy generated with these optimized ATEG during a usual working period of time. Cold start scenarios could benefit from this electricity stored and generated when exhaust gas temperatures are optimal.

Chapter 5

NOx emissions below the prospective EURO VII limit on a retrofitted Heavy Duty Vehicle

---

This section is a full content transcription of the following paper (a copy of the published version can be found in Appendix B):

Ximinis J, Massaguer A, Massaguer E. NOx Emissions below the Prospective EURO VII Limit on a Retrofitted Heavy-Duty Vehicle. *Applied Sciences*. 2022; 12(3):1189. ISSN: 2076-3417. (Impact factor 3.021; 2nd quartile; Engineering).

https://doi.org/10.3390/app12031189

Abstract

In this study, a EURO VI HDV has been retrofitted with an exhaust gas heater (EGH) with the objective to cut NOx emissions below current EURO VI and EURO VII limits. Results show that an EGH of 5kW is enough to produce a significant NOx emissions abatement below EURO VI and EURO VII limits. A conventional after-treatment system heated using a 5kW EGH could work at its maximum catalytic conversion efficiency of 95% regardless of the engine operating speed. Consequently, exhaust gas heaters are a potential solution to high NOx emission at low engine regimes. With the use of an EGH, urea can be injected sooner, and catalytic reactions could cut much more NOx emissions. However, its incorporation would increase the vehicle's fuel consumption by 1.47% if it is connected directly to the vehicle's electrical system. Finally, it is also demonstrated that an automotive thermoelectric generator (ATEG) can supply the energy required by the EGH through the conversion of the waste heat from exhaust gases into electricity. This system could work electrically autonomous so there is no extra consumption of fuel.

5.1 Introduction

Over the last decades, the legislated maximum levels of emissions from engines were more and more tightened. Worldwide, in 2014, transport as a whole was responsible for 23% of total CO_2 emissions from fuel combustion and road transport was responsible for 20% [61]. The vast

majority of Heavy Duty Vehicles (HDVs) in Europe are powered by diesel engines and, although they account only for 4% of the vehicle fleet, they have been identified as important sources of both pollutant and Greenhouse Gas (GHG) emissions. Exhaust gases from diesel engines include carbon monoxide (CO), particulate matter (PMx), nitrogen oxides (NO_x) and Sulphur oxides (SO_x) [62]. NO_X contributes to serious environmental problems, such as acid rain and photochemical smog [63] and human health problems, especially respiratory disorders [64,65].

With the aim of reducing this contribution, the EU has adopted the strategy of supporting a mix of technologies, currently at high levels of maturity, depending on the transport modes and the travel range. The main response of the industry to the introduction of more stringent emission standards was the widespread use of Selective Catalytic Reduction (SCR) technology for reducing NO_X emissions at the tailpipe combined with Diesel Particle Filters (DPF) for PM reduction and Diesel Oxidation Catalysts (DOC) for the oxidation of incomplete combustion products [66]. The urea-based selective catalytic reduction (urea-SCR) technology, a lean NO_X after-treatment technology, has been widely used owing to its impressive NO_X reduction efficiency and compliance with newly rigorous specifications [67,68]. In SCR technique, the Urea Water Solution (UWS, 32.5% aqueous solution) is injected into hot exhaust gas using different strategies according to the manufacturer of the vehicle. After evaporation of water from UWS, the urea decomposes and gives out ammonia which is the reducing agent for the reduction of NO_X. Reduction of NO_X takes place when ammonia reacts with NOx over catalyst through different catalytic reactions.

However, exhaust temperature plays an important role in catalyst performance. It tends to be rather low in real driving cycles, which causes low catalyst efficiency [69]. In [34,35,70] authors showed the exhaust temperature history during NEDCs and WLTPs from cold and hot conditions. During the cold NEDC, the inlet temperature was below 130°C in the majority of the first 400s, and temperatures greater than 180°C were achieved only in a small portion of the hot driving cycle. This behaviour strongly affects the conversion efficiency of SCR devices because a minimum substrate temperature of 180°C is required to reach the SCR light-off. As a result, higher activity of SCR catalysts at low temperatures is mandated to effectively reduce real-world NO_X emission while fuel economy requirement has to be simultaneously met. A lot

of effort has also been made, but the main obstacle is that during low-speed urban driving and cold-starts, the low-CO_2 engines only generate exhaust gas temperatures below 200°C, which is not enough for the conventional urea-SCR based systems to reach the SCR light-off [71].

This issue is of great concern in combustion vehicles and several strategies for solving it are currently under development. These can be divided into 1) engine control and 2) catalyst control. Engine control strategies are focused on increasing the exhaust gas temperatures as fast as possible. Several ways are currently under study, such us retarding the ignition timing, increasing the idling speed, bypassing the turbocharger for creating a fuel rich mixture, alternating rich and fuel lean conditions, injecting more fuel at starting conditions in dual fuel vehicles, etc. [13,69,72–74].

However, all of these engine control techniques tend to strongly increase the fuel consumption and, therefore, reduce the net vehicle efficiency. Gao et al. reflected on the need to develop integrated and more advanced thermal management control strategies to reduce light-off time without significant energy penalty [5]. On the other hand, the catalyst control technologies are simpler and do not require modifying the engine's set up since they are focused on reducing the light-off temperature of the catalytic conversion by means of trying to develop alternative catalytic materials and/or reducing the time to reach the light-off temperature. This second and more realistic strategy is currently investigating several alternatives such as increasing the heat transfer inside the catalyst using higher cell densities and thinner wall designs, insulating the exhaust manifold and moving the SCR as close as possible to the engine's block or adding an electrical resistance to preheat the SCR. All in all, the simplicity of electrically preheated catalysts (EHCs) makes it the most cost-effective technology for solving the problem [4,5].

In this direction, several prototypes of a catalytic converter with an exhaust heater for preheating the catalyst specifically designed for CNG engines have been tested with very promising results [5,19]. These heat-integrated catalysts require a constant heating of 2.5 kW during 120 s in a 1.8 L CNG engine for a 90% reduction of CH_4 emissions in a New European Driving Cycle (NEDC) test in comparison with non-preheated TWC values. NEDC consists of repeated urban and extra-urban driving cycles usually performed on a roller test bench with a total duration of 1180 s. This 2.5 kW in 120 s is equivalent to a mean electrical power

consumption of 254 W during the NEDC that must be generated by the alternator and, hence, by the engine. This is the reason why this technical solution contributes to increasing the fuel consumption of the vehicle.

Massaguer et al. [17] analysed the use of an Automotive Thermoelectric Generator (ATEG) coupled to an Exhaust Gas Heater (EGH). This system could reduce up to 97% the NOx emitted by a light duty vehicle during cold starts. The ATEG is used to convert waste heat from exhaust gases, downstream of the aftertreatment system, into electricity. A battery is used to store the electricity generated, which can be used by the EGH later to shorten the time that urea is injected and reduce NOx emissions. This EGH+ATEG system, also known as Thermoelectric Aftertreatment Heater (TATH), was designed to be energetically autonomous, so there is no extra consumption of fuel. Note that the ATEG generates less power than the EGH. However, the EGH only works for a few minutes while the ATEG all the driving cycle. Therefore, the energy consumed and produced can be balanced.

This study is based on the developments presented in [17,75] but from a perspective of compliance with current EURO VI and future EURO VII regulations. The objective of this work is to experimentally quantify the energy required by an EGH to fulfill the EURO VI and EURO VII regulations. The EGH will be retrofitted upstream of the standard after-treatment system of a EURO VI certified HDV. The idea is to obtain the power and energy needed to make SCR work at its maximum efficiency. Then, the effect of the added weight, the additional back pressure caused in the exhaust pipe and the extra electricity consumption will be analysed. This will lay the groundwork for the future development of a thermoelectric recovery system capable to produce the energy required by the EGH in a real mission of a long-haul Euro VI HDV. The end goal is reducing the pollutant emissions without the need to increase the fuel consumption.

5.2 System proposed

In order to stablish the basement for this study, it was necessary to choose the optimal combination of elements that suited our requirements. In first place, it was clear that strict values of NO_x emission from Euro VI standard would be a good starting point. This pollution

limitation is a great challenge for all sorts of transport vehicles, specially for Heavy Duty Vehicles manufacturers. Man Truck & Bus A.G. is an example of how using sophisticated ECU (Electronic Control Unit) software, combined with catalytic chemical reactions, can obtain NO_x ppm values below Euro VI limits. The vehicle used in this article is a Euro VI certified Heavy-Duty Vehicle from MAN, model TGX 18.480 Efficient Line 2. The vehicle disposition and the main data acquired can be shown in Figure 5.1.

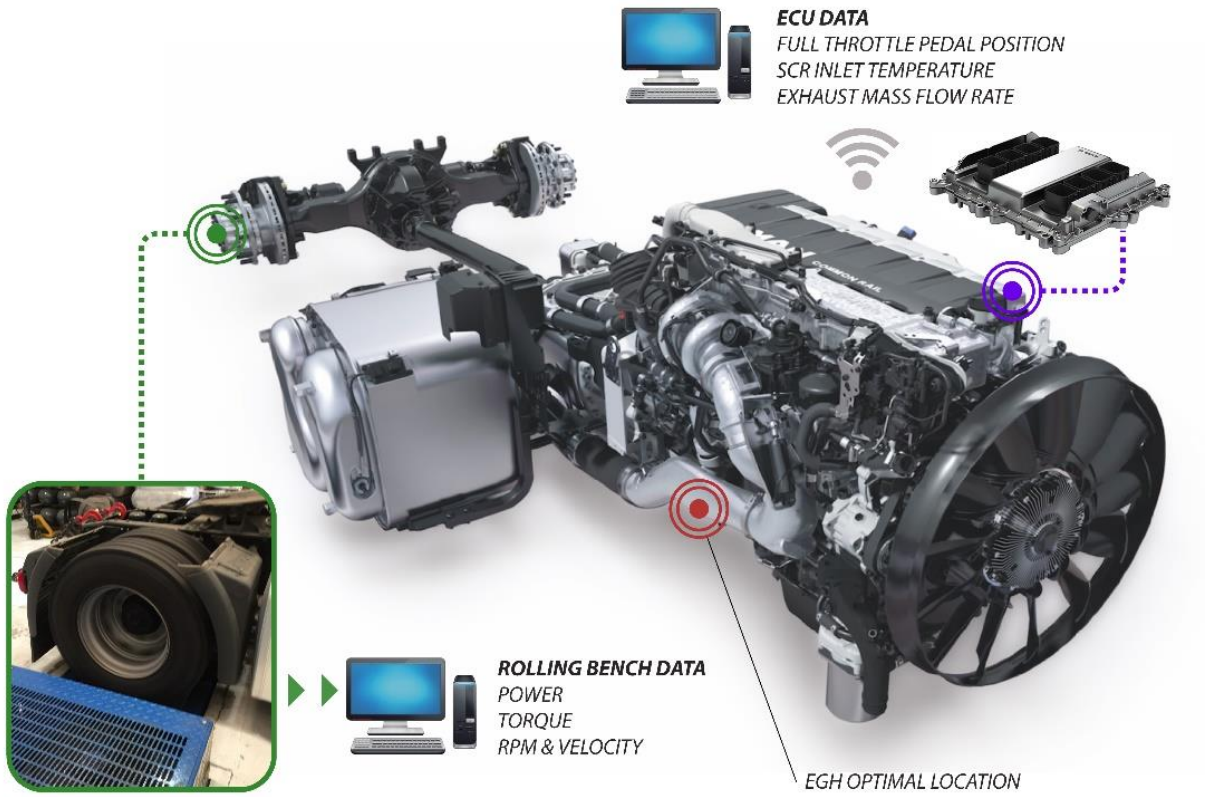

Figure 5.1. Efficient Line engine and transmission with ECU and rolling bench data parameters.

The system proposed is based on the existing ATS (aftertreatment system) retrofitted by an EGH. The EGH, shown in Figure 5.2, was located upstream of the ATS and, in essence, it is a 12kW electric coil temperature controlled by a PID system. To simplify the test, the EGH was not powered by the vehicle's battery, but it was connected directly to the electrical network. The control unit adjusted the power injected to the EGH according to the temperature set point. Apart from the data acquisition shown in Figure 5.1, it is also necessary to gather other important parameters such as EGH inlet and outlet temperatures, T_{B_EGH} and T_{A_EGH}

respectively and the electrical power consumption of the EGH $P_{EGH} = V_{EGH} \cdot I_{EGH}$. The EGH coupled to the standard exhaust system can be seen in Figure 5.3.

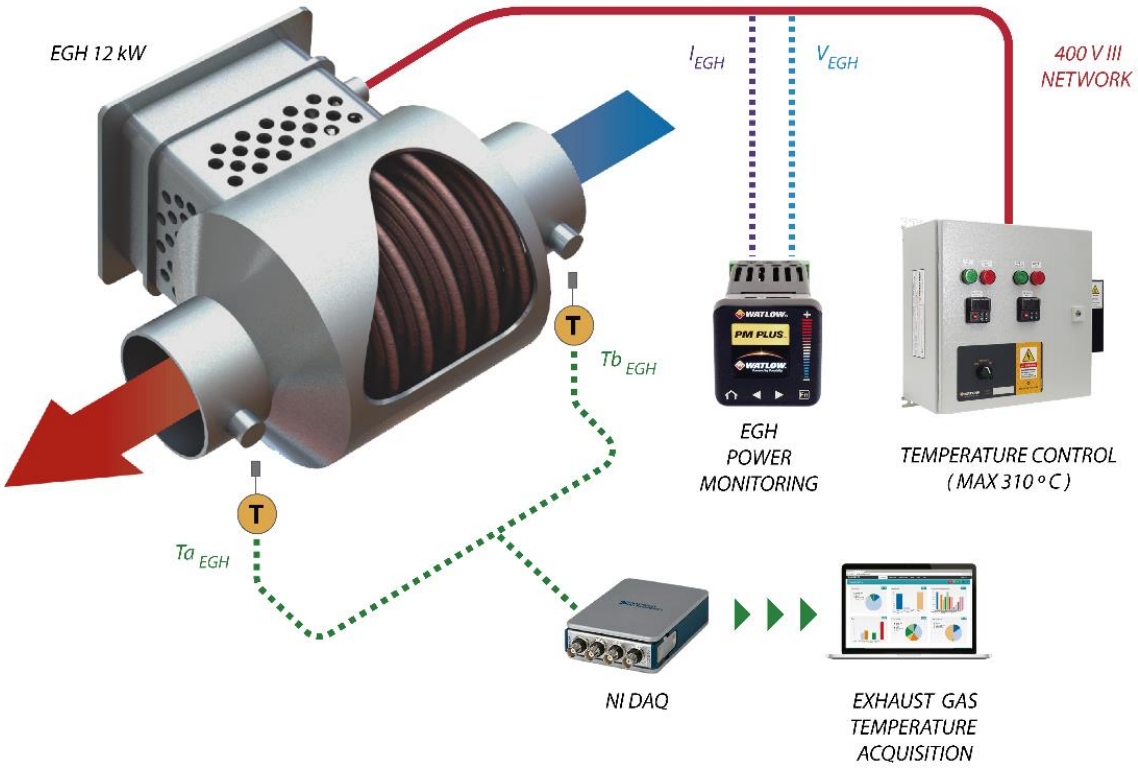

Figure 5.2. Scheme of the EGH installed upstream the ATS and its data acquisition.

As seen in Figure 5.3, EGH (number 1) has been located downwards the turbochargers, just before the standard ATS. The next element we find is the Diesel Exhaust Fluid (DEF) unit composed by a tank, a supply module, and a dosing module (number 2). The vehicle tested in this experiment uses AdBlue for NOx abatement. The ECU is the responsible of the AdBlue parameters, which is never injected into the system until the exhaust gas temperature exceeds 180°C. Inlet gas temperature and NOx content are read by the dosing unit to adjust the exact dose of AdBlue required to meet the EURO VI standard.

Next component we find is a closed unit composed by a Selective Catalytic Converter (SCR) and a Continuous Regenerating Trap (CRT). At this point a mix of AdBlue and exhaust gases enters into the SCR (number 3). Inside this device a catalytic reaction is produced to convert NOx into diatomic nitrogen (N2), and water (H2O). Carbon dioxide (CO2) is a subproduct of this reduction

when urea is used as DEF. Finally, it is necessary to eliminate NH3 produced by the reaction between AdBlue and NOx. Using an ammonia catalyst, included into SCR system, NH3 is converted into nitrogen and water.

Afterwards the SCR and within the same package the CRT (number 4) is divided into a DOC (Diesel Oxidation Catalyst) and a DPF (Diesel Particle Filter). The DOC is the responsible of CO and THC oxidation while the DPF is used to capture the unburned particles. Soot trapped in the DPF walls is burned when an excessive backpressure is reached. The same closed unit is the standard exhaust outlet were NOx sensor is coupled to acquire the vehicle emissions NOx_{EGH}.

Regarding Figure 5.3, there is a representation of an ATEG (number 5) to demonstrate which is going to be its suitable location, just at the end of the standard ATS. Its outlet manifold would be the collector of exhaust fumes where the NOx sensor is attached in this figure. This ATEG is a conceptual approach of size, location and design. The tested vehicle has its NOx sensor connected at the exhaust outlet, underneath the SCR+CRT unit.

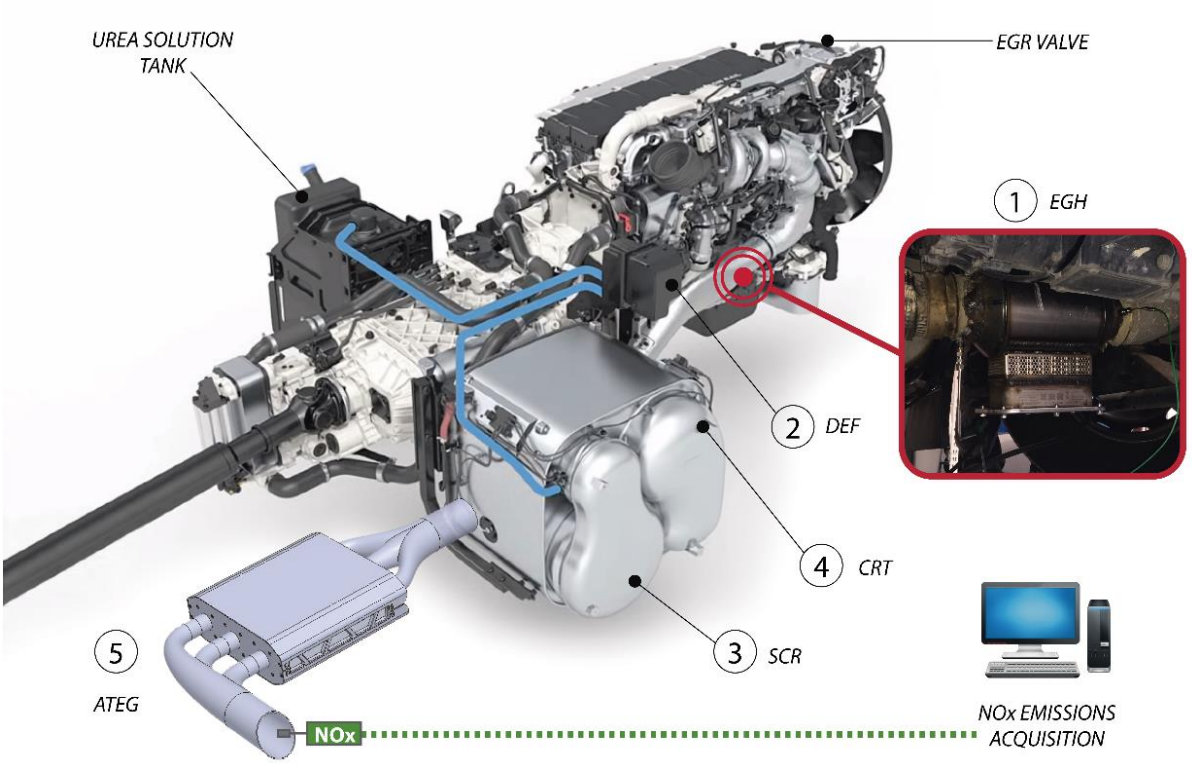

Figure 5.3. Scheme of the proposed system retrofitted in the tested vehicle with an ATEG representation.

5.3 Materials and Methods

To evaluate the influence of the EGH in NOx emissions reduction, a certified bench for Heavy Duty vehicles was used. The experiment series were held in EVARM S.L. facilities which had a certified test bench for testing HDVs (Maha Powerdyno R200/1) was used to put the vehicle in real operating conditions. This equipment was also used to capture the FTPP, NOx after and before the ATS, and exhaust temperatures from the ECU. The measurement of NOx emissions was done with a MIAC G4.0 located at the end of the exhaust pipe. This device presents a measure range from 0 to +5000ppm, an accuracy of ±5% of mv (+100 to +2000ppm) and ±5ppm (0 to +99.9ppm) with a resolution of 0.1ppm (0 to +500ppm). A Dranetz Power Explorer PX5 power meter was used to measure the EGH power consumption with the following specifications: voltage measuring range from 1-600Vrms with 0.1% rdg (reading) + 0.05% FS (full scale), 256 samples/cycle, 16 bit ADC; current measuring range from 1-6000Arms with 0.1% rdg + CTs (4), 256 samples/cycle, 16 bit ADC. Exhaust temperatures were recorded with a National Instruments DAQ with one NI 9211 acquisition module. This device presents a maximum measure error of 2.2°C (0-400°C) with a measurement sensitivity <0.07°C. All temperature probes used were type K thermocouples.

The method used to calculate absolute uncertainty values depends on the equipment accuracy. These parameters are obtained from datasheet provided by different manufacturers as exposed before. Thus, temperature and NOx measurement standard uncertainties have been calculated. Voltage and current (used to calculate EGH power consumption) are separately obtained and its uncertainties also calculated using the same method. As EGH power is an indirect parameter, its uncertainty is the result of both electrical magnitudes as it depends on these parameters [21]. Results presented in Figure 5.6 to 5.8 include error bars of data of less than 5% in all cases. Its small size (smaller than graphic symbology) makes it unable to represent it properly.

In this study, a Heavy-Duty Vehicle Euro VI TGX 18.480 Efficient Line 2 from MAN was used to carry out the tests. Its specifications are summarized in Table 5.1.

Table 5.1. Main specifications of tested vehicle.

Parameter	**Value**
Maker	MAN
Model	TGX 18.480 Efficient Line 2
Gearbox	Automatic (12 gears)
Max. rated power	353 kW (at 1800 rpm)
Max. rated torque	1500 Nm (at 930-1400 rpm)
Emission standards	Euro VI

Figure 5.4 shows the rolling bench with the vehicle tested. All tests were carried out using the same load.

Figure 5.4. Vehicle being tested on the rolling bench.

Three different engine regimes were selected to conduct the study: 1000rpm ($\approx 55 km/h$), 1250rpm ($\approx 65 km/h$) and 1500rpm ($\approx 80 km/h$). All these regimes, shown in Figure 5.5, can be found in a typical daily drive. The suitable gear to obtain all range of Full Throttle Pedal Position (FTPP) values was the eleventh. During all tests, the engine temperature stayed below 90°C to keep the same engine conditions. Before each test, the vehicle was warmed up at idle

for 20 minutes. NOx emissions were captured along the tests. Maximum FTPP tested is 90% to assure that can be reached equally in all conditions. In all tests, the setpoint temperature of the EGH was set to 300°C to ensure that the exhaust gas temperature at SCR inlet was above the SCR light-off temperature of 220°C.

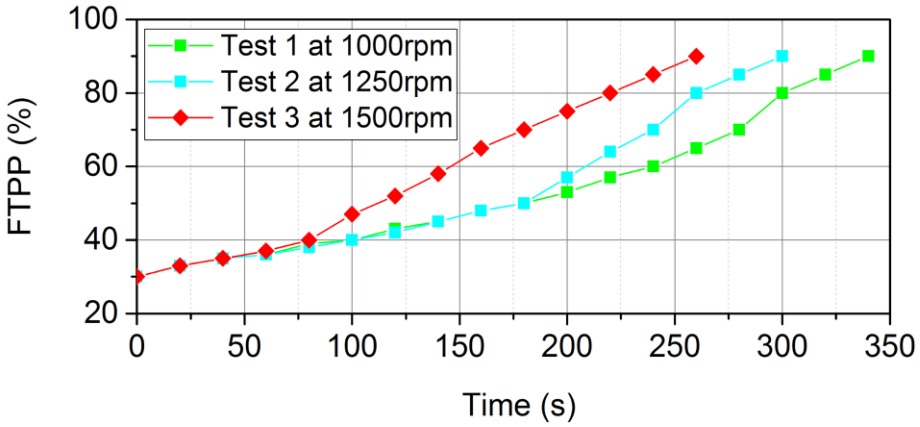

Figure 5.5. Transient tests carried out to analyse NO_x emissions.

5.4 Results

Figure 5.6 shows the NOx emissions and the EGH performance during the 1000 rpm test. The first thing that must be mentioned is the fact that the standard aftertreatment system (without the EGH) is not capable to fulfil the EURO VI regulation. EURO VI NOx limit has been calculated from the WHTC limit value multiplied by the conformity factor CF: $NOx_{limit}^{EURO\ VI} = 0.46 \cdot 1.5 = 0.69 g/kWh$. As can be seen in Figure 5.6, NOx emissions are higher than the limit $> 0.69 g/kWh$.

The new Euro 7/VII, which will be presented at the end of 2021 and expected to come into force on 2025 [76], will develop stricter CO2 and NOX limits, as well as new tests and limits for non-CO2 greenhouse gas emissions [77]. There is no decision yet, but some reports point out that NOX limits will be halved from Euro VI, placing the limit around 0.2g/kWh [78–80]. Then, the limit value will be $NOx_{limit}^{EURO\ VII} = 0.27 \cdot 1.5 = 0.41 g/kWh$.

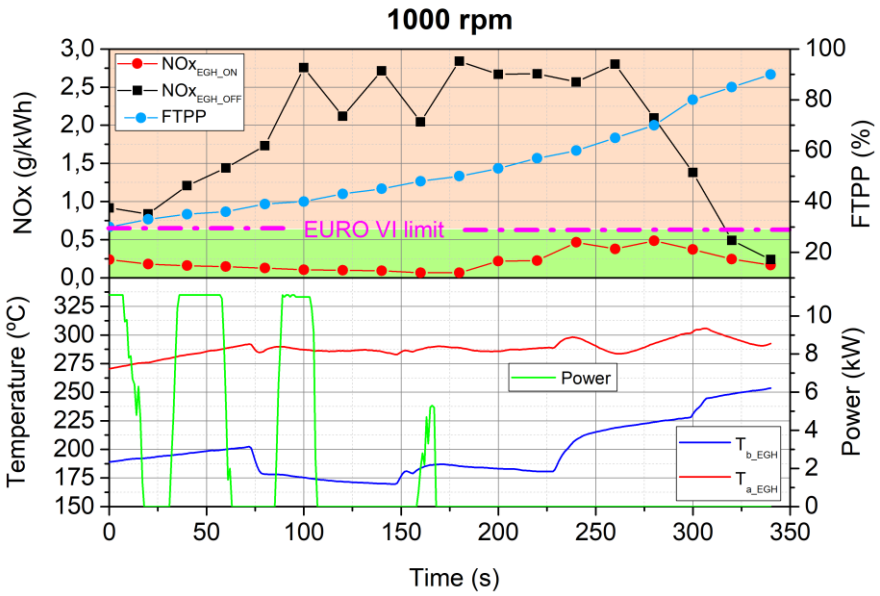

Figure 5.6. Results from Test 1 including NOx values, FTPP and gas temperatures at 1000 rpm.

Around 40% of FTTP, temperature T_{b_EGH} presents a great decline and it produces a significant increment of NOx emissions that is well maintained until 65% of FTPP. The vehicle catalytic system needs to achieve temperature much over these values to start its reaction. This explains also the importance of reaching the urea injection target temperature as soon as possible in order to start catalytic conversion at the standard ATS. Without enough temperature (lower than 225°C in this test) and without urea solution injected, NOx values remain high within medium range FTPP.

However, the inclusion of the EGH had a very positive impact. It can be noticed a significant NOx reduction, specially at medium FTPP range (40-65%). It is remarkable how NOx values without heater NOx_{EGH_OFF} descend drastically after temperature T_{b_EGH} exceeds the barrier of 260°C, onwards 65% of FTPP. This phenomenon can be explained by the injection of AdBlue that drastically increase the SCR efficiency. Ideally, AdBlue injection starts when SCR inlet temperature exceed 220°C. In this case it can be observed that the injection starts at 260°C. This difference can be explained by the heat loss in the section from the EGH to the SCR and also by the thermal inertia of the SCR substrate that needs a few seconds to reach the temperature injection threshold. It is important to note that this mismatch is present in all tests. Below 260°C, in EGH off mode, the trend of T_{b_EGH} is mostly influenced by EGR valve that is controlled by ECU manufacturer parameters.

On the other hand, using the heater, T_{a_EGH} temperatures were always far higher than the AdBlue injection threshold of 220°C (275°C minimum) and therefore NOx reduction is improved drastically. Note that during NOx_{EGH_OFF}, EGH was disabled and consequently temperatures $T_{a\_EGH} = T_{b\_EGH}$. This achievement is maximized at medium FTPP values as NOx_{EGH_ON} data registered is below 0.2g/kWh. This difference is minimized at 90% FTPP as thermal engine produced more heat and temperature values almost coincide in both cases. Consequently, as time passes and FTPP increases, power consumption decreases.

The second cycle was set at 1250 rpm, as shown in Figure 5.7. Unlike Figure 5.6, in this case the standard aftertreatment system is capable to fulfil the EURO VI regulation. Notice that NOx emission ranges from 0.1 to 0.3 until 65% FTPP. It is a narrow variation explained by the fact that this engine regime produces a greater impact in temperature increment as T_{b_EGH} numbers show. At the end of the test both temperatures present the same values (after 250s). The catalytic conversion benefits from these values over 300°C and NOx emissions provide a rapid decrease despite FTPP values are high.

On the other side, the use of the EGH continues to be beneficial in reducing NOx emissions below EURO VII limit. NOx_{EGH_ON} values decreased as FTPP increased and remained around 0g/kWh for almost the second half of the test. The main NOx reduction was performed at high FTPP values in contrast to test 1. However, they share the same drastic reduction of NOx_{EGH_OFF} values at 70% of FTPP that can be explained due to AdBlue injection. In this case it can be noted that, when EGH was disabled, the AdBlue injection started at 220°C approximately. When EGH was enabled, the AdBlue injection started at the beginning of the test. Apart from that, it can be observed that a higher T_{a_EGH} produce a higher SCR conversion and a higher NOx reduction. Both T_{a_EGH} and T_{b_EGH} temperatures converge at the end of the test.

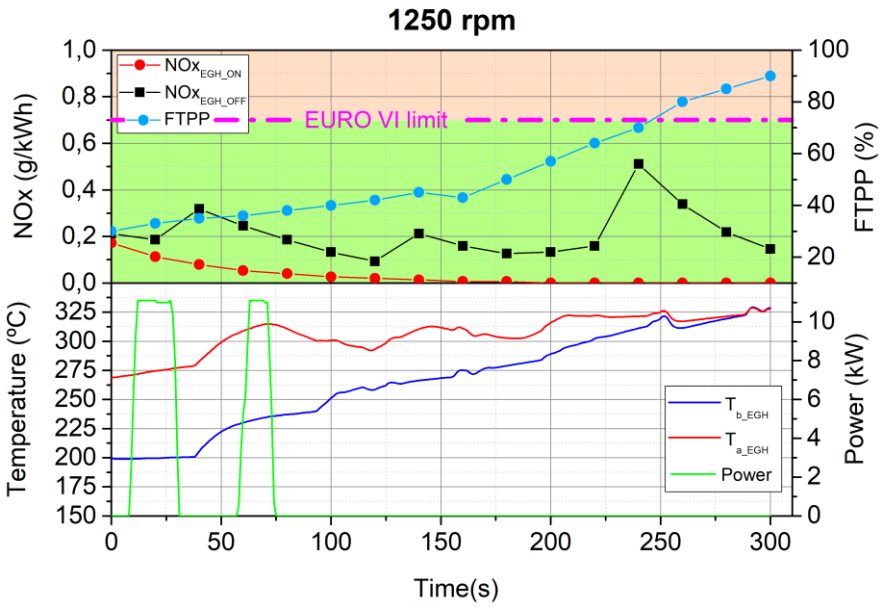

Figure 5.7. Results from Test 2 including NOx values, FTPP and gas temperatures at 1250 rpm.

Finally, Figure 5.8 shows the results at 1500rpm. Note that at 65% and 70% FTPP NOx emissions are higher than the EURO VI limit. Following the trend of the other cases, at 1500rpm the EGH maintains its capacity to abate NOx emissions and it can cut NOx emissions below EURO VII limit. During the first FTPPs, both NOx_{EGH_ON} and NOx_{EGH_OFF} emissions were very low. This phenomenon can be explained by the EGR activation until 50% FTPP that contributed positively to the NOx reduction, despite of the low exhaust gas temperature.

On the other hand, NOx reduction is also remarkable at second half of the test coinciding with lower energy consumption as heater is no longer needed thanks to T_{a_EGH} above target selected in the controller of the EGH. For FTPP values higher than 70%, NOx_{EGH_OFF} values are reduced in great numbers. This is due to the AdBlue injection according to the aforementioned injection threshold limit, which was clearly exceeded at 70% of FTPP. In contrast, the gap between 40-70% of FTPP is where NOx_{EGH_OFF} were higher. In this case, a moderate engine regime and medium FTPP range (around 50%) NOx emission values of the standard ATS increase rapidly. This phenomenon is a result of a combination between the greatest engine regime at moderate FTPP and relatively low exhaust gas temperature, both counterproductive in order to catch pollutants within the ATS. Consequently, it is in this range where NOx reduction, thanks to the inclusion of the EGH, was higher.

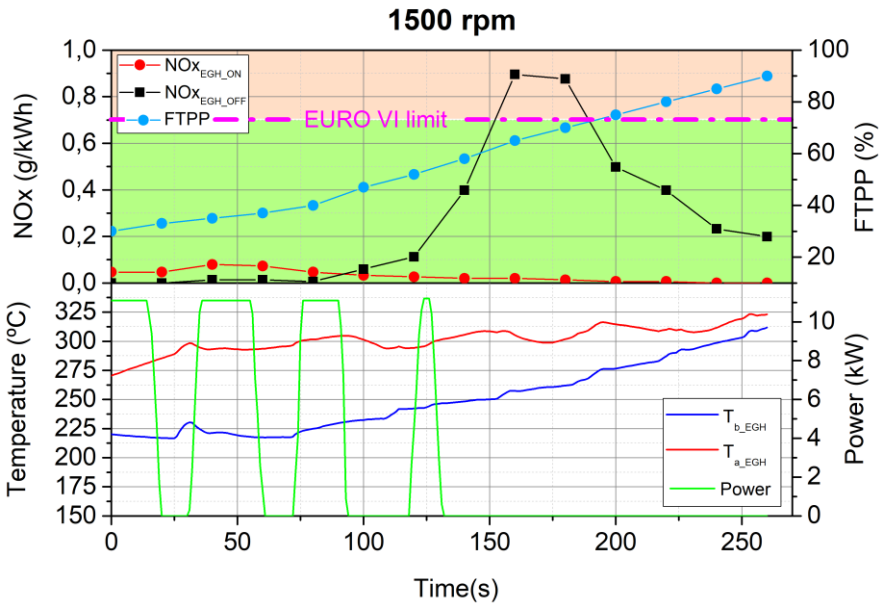

Figure 5.8. Results from Test 3 including NOx values, FTPP and gas temperatures at 1500 rpm.

Summarizing, NOx emissions are reduced in all cases but in different ways and conditions. As seen in Table 5.2, we find lowest exhaust temperatures and EGH highest consumption in Test 1. Low engine regimes produce low exhaust temperature. That is the reason why both NOx reduction and EGH consumption were the highest of the three tests. Under these conditions, the heater needed more electrical power to fill the temperature gap and also increased the AdBlue consumption. Once SCR light-off was achieved, the ECU started the AdBlue injection.

Table 5.2. EGH consumption and NO_x reduction results.

Test	Engine regime (rpm)	EGH energy consumption (kWh)	Duration (s)	Average EGH power consumption (kW)	NOx reduction (%)	Urea consumption increase (g)
1	1000	0.191	340	2.02kW	87.97	69.67
2	1250	0.098	300	1.18kW	83.46	19.59
3	1500	0.213	260	2.95kW	89.46	1.31

5.5 EGH optimization

From the results presented above, one can realize that a 12kW EGH, such as the one tested in this paper, is extremely disproportionate considering that this power should come from an on-board generator (i.e. alternator). Although this huge amount of power provides a great increase in T_{a_EGH} with initial values over 260°C, if we consider the manufacturer SCR efficiency curve represented in Figure 5.9, it can be observed that heating exhaust gases above 220°C has no sense. The SCR presents a maximum efficiency point of 95% at $T_{a\_EGH} = 220$℃. Temperatures above this value will not bring any improvement in NOx reduction but will cause the alternator to consume more fuel to feed the EGH.

From the experimental data presented in the previous section it has been possible to draw the experimental SCR efficiency curve. From Figure 5.9, it can be seen that when the EGH is active the curve maintains the efficiency above 90% for temperatures below 220°C. Note that the points within the circle cannot be taken into account since urea was not being injected at that moment. This can be explained by the fact that the urea injection decision is made from the temperature of the substrate, and not from the temperature of the gases going into the SCR, T_{SCR_IN}, used in Figure 5.9.

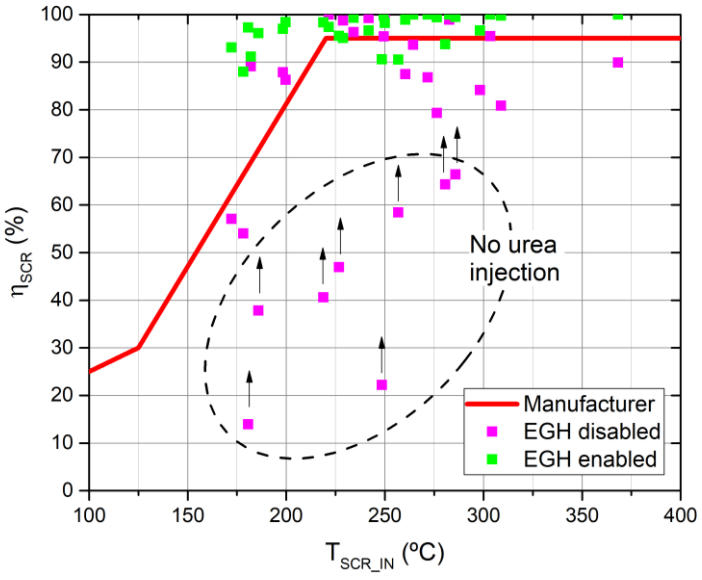

Figure 5.9. Theoretical and experimental SCR conversion efficiency as a function of catalyst temperature.

With T_{a_EGH} value set at 220°C, T_{b_EGH} and exhaust mass flow rate known from the previous tests it is possible to determine the theoretical power consumption to achieve 95% of SCR conversion efficiency.

Figure 5.10 shows the optimized EGH power that guarantees a SCR efficiency of 95%. Note that these values consider that all the electrical energy consumed by the EGH was exchanged as thermal energy into the exhaust gases. It can be observed that its consumption is lower than the EGH power used in previous tests. At 1000rpm, there is a top consumption peak of 5kW and it is remarkably lower than the 11 kW achieved during the test 1. Its consumption value is zero only at the end of the test when T_{b_EGH} is over 220°C and no extra energy is needed. At 1250rpm, the theoretical EGH power reach a peak of 2.2 kW during the first 50 s of testing and remains zero after T_{b_EGH} exceeds the 220°C target. Finally, in test 3 it can be seen a slightly different scenario as EGH power consumption remains below 0.5 kW. Note that the power required by the EGH depends on the exhaust gas conditions (i.e. mass flow rate and temperature), which fluctuate depending on the FTPP, engine regime and other ECU parameters that control EGR valve aperture, for instance.

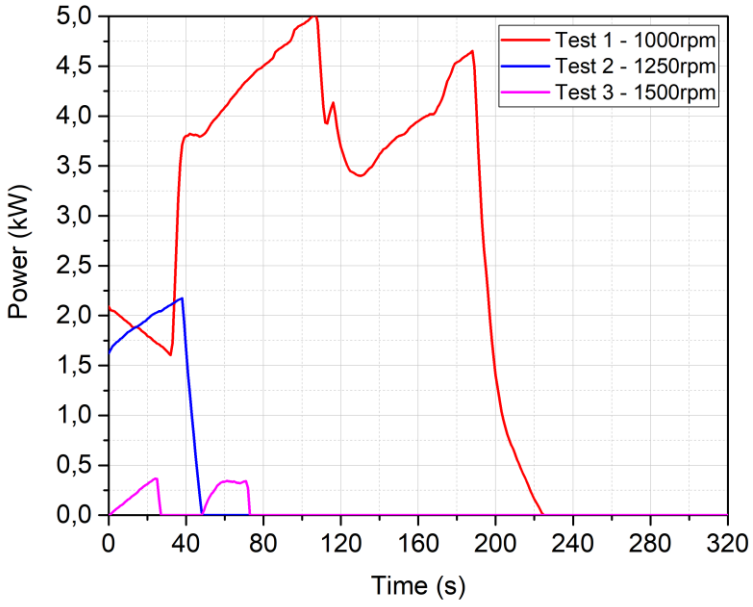

Figure 5.10. Theoretical power consumption of the EGH to achieve the SCR light-off temperature of 220°C at 1000rpm, 1250rpm and 1500rpm.

At this point, it is interesting to quantify the energy that a conventional HDV will require on a real operation profile. To do so it is necessary to determine the time a HDV spends at low engine regimes, typically during urban or suburban driving. Considering that the major part of the NOx emitted occur at low-speed, see Figure 5.6, this analysis will focus on the most demanding EGH regime of 1000rpm. Figure 5.11 presents a real mission profile of a long-haul heavy-duty vehicle. In this figure, it can be observed that the time a long-haul HDV spends at 1000rpm (50km/h) is about 12 minutes (suburban conditions).

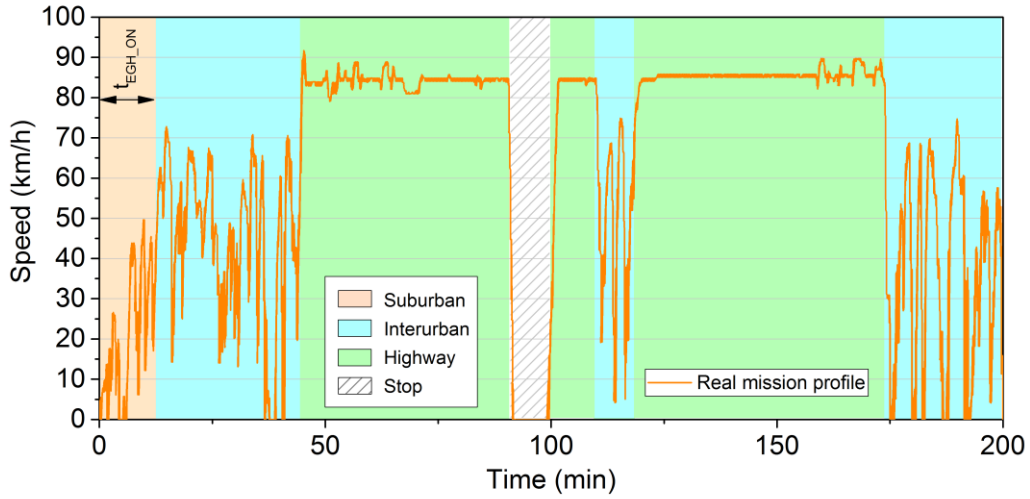

Figure 5.11. Speed profile of a long-haul heavy-duty vehicle [25].

Table 5.3 summarizes the power requirements of the EGH to achieve 95% of conversion efficiency.

Table 5.3. EGH power requirements to achieve 95% of SCR efficiency.

Test	Engine regime (rpm)	Speed (km/h)	Road	EGH peak power (kW)	EGH average power (kW)	Time*	EGH energy (kWh)
1	1000	55	Suburban	5.02	2.18	12 min	0.436kWh
2	1250	68	Interurban	2.17	0.28	61 min	0.285kWh
3	1500	82	Highway	0.36	0.05	115 min	0.095kWh

*Taken from the real speed profile of a long-haul HDV presented in Figure 5.11.

As seen in the Table 5.3, optimum consumption values are within a realistic range of an on-board generator, between 5.02kW and 0.36kW. These values have been extracted from

maximum points achieved in Figure 5.10 for each regime. Then, the average power and energy has been calculated considering the real mission profile presented in Figure 5.11. Note that the most demanding regime is the suburban driving, which contrasts with the fact that it is the shortest of the three. The total energy required by the EGH during the Figure 5.11 mission profile will be 0.816kWh.

The easiest solution to provide this additional energy would be the use of a supplementary alternator. Most factory alternators for HDVs are available with outputs ranging from 160 up to 320 amps (3.84 kW to 7.68 kW) and can handle the vehicle's basic necessities, such as headlights, gauges, fuel pumps, A/C, etc. Considering this power production range, the inclusion of a 5.02 kW EGH (i.e. to fulfil EURO VI) into the electrical system would require incorporating an exclusive alternator for the EGH, causing a significant increase in fuel consumption. A 200A alternator can produce the amount of power required by a 5kW EGH. However, its use will cause an increase on the vehicle's fuel consumption because when the alternator works under load conditions, it exerts an additional force on the engine shaft [34]. Under the worst conditions of Table 5.3, the fuel consumption would increase by 1.43%.

A hot air flow bench was used to analyse the backpressure caused by the EGH in the exhaust pipe. The maximum backpressure was 1.8mbar at 204 g/s. From this data, the hydraulic power, $P_{H_{EGH}} = Q_{EGH} \cdot \Delta p_{EGH}$, that the motor must exert to overcome the EGH additional back pressure is calculated. The greatest impact occurs during highway conditions (1500rpm and 90%FTPP) with $P_{H_{EGH}} = \frac{0.204kg/s \cdot 180Pa}{0.745kg/m\text{^}3} = 49.3\ W$. This means that the required engine power increase in 49.3W. Taking the power developed by the vehicle at that regime and the $P_{H_{TATH}}$, this would suppose a fuel consumption increase of 0.015%.

On the other hand, the additional weight that the EGH adds to the vehicle must also be considered. A heavier truck produces more rolling resistance than a lighter one, thereby increasing the power needed to move the vehicle. A 200 kg cut in vehicle weight can reduce fuel consumption by 0.5% on a regional delivery truck and 0.3% on a long haul truck [81]. Considering a EGH weight of 10 kg, this would suppose a fuel consumption increase of 0.025%. Other study [82] established that the average impact on mpg per tonne of increased payload of

a HDV with a fuel consumption of 8.15 mpg is 0.112 mpg. This supposes a fuel consumption increase of 1.3% per tonne. In this case, the TATH would increase the fuel consumption by 0.013%. Besides, the additional weight caused by the EGH would suppose an increase of 0.021% in fuel consumption according to the fuel economy assessment method of ref. [37].
Finally, the total fuel consumption increases due to the incorporation of an EGH into the exhaust system would be 1.47%.

The most interesting solution would be the use of a waste heat recovery system to produce the electricity needed by the EGH, such as an automotive thermoelectric generator (ATEG). These systems can convert waste heat, downstream of the after-treatment system, into electricity, and store it into a battery for later use. Many theoretical models [34,37,43–45] and experimental prototypes [35,46–49] have been developed which demonstrate the feasibility of this idea. Other authors have studied the use of ATEGs in heavy duty engines with a power production up to 1kW [40,83,84]. In Ref. [34], the same authors tested an ATEG in a light-duty vehicle (LDV) with a maximum power production of 200W. It has also been demonstrated that this kind of energy harvesters can reduce fuel consumption [17,36].

5.6 Conclusions

This study demonstrates that the retrofit of an exhaust gas heater upwards the after-treatment system can drastically reduce NOx emissions below EURO VI and even EURO VII limits. It also has been demonstrated that, an EGH of 5kW is enough to produce a significant NOx emissions abatement below EURO VI limit. A conventional after-treatment system heated using a 5kW EGH could work at its maximum catalytic conversion efficiency of 95% regardless of the engine operating speed. Consequently, exhaust gas heaters are a potential solution to the high NOx emission at low engine regimes. With the use of an EGH, urea can be injected sooner, and catalytic reactions could cut much more NOx emissions. However, the incorporation of an EGH into the exhaust system would increase the vehicle's fuel consumption by 1.47%.

Future work will focus on the potential capability of using the exhaust waste heat to produce the electricity needed by the EGH. Selecting a suitable automotive thermoelectric generator

(ATEGs), coupled downstream of the after-treatment system, is going to be our next challenge. This combination will avoid the need to consume more fuel to produce the extra electrical energy needed by the EGH.

Chapter 6

Towards compliance with the prospective EURO VII NOx emissions limit using a thermoelectric aftertreatment heater

---

This section is a full content transcription of the following paper (a copy of the published version can be found in Appendix C):

J. Ximinis, A. Massaguer, E. Massaguer. Towards compliance with the prospective EURO VII NO_x emissions limit using a thermoelectric aftertreatment heater. Submitted to *Applied Thermal Engineering*. ISSN 13594311. (Impact factor: 5.295; Journal 14 of 133; 1st quartile; Engineering).

Abstract

In this study, the use of a thermoelectric aftertreatment heater (TATH) to reduce NO_x emissions in low demanding regimes of diesel-powered HDVs has been analysed. This system is composed by an Exhaust Gas Heater (EGH) that heats up the exhaust gases in low engine regimes, in order to shorten the time that urea is injected. Besides, the TATH is fed by an Automotive Thermoelectric Generator (ATEG) that converts the waste heat from exhaust gases into electricity, so the system can work energetically autonomous.

Experimental results show that under low-speed regimes, a EURO VI certified HDV emits NOx pollutants 5 times above the EURO VI limit value. Results demonstrate that the use of a TATH reduces NOx emissions by up to 97.2%. TATH allows to a long-haul diesel-powered MAN Euro VI TGX 18.480 Efficient Line 2 to fulfil the current EURO VI and even the prospective EURO VII regulation when driving at low-speed regimes. Apart from that, it is also demonstrated that the ATEG can produce the energy required by the EGH in a long-haul mission profile. However, the added weight and the back pressure caused by the TATH is expected to increase the fuel consumption of the vehicle in 0.35%.

6.1 Introduction

Heavy duty vehicles (HDVs) have been recognised the world over as significant contributors to air pollution. Current tier legislation for the type approval of motorized vehicles with regards to (pollutant) emissions was adopted in 2013 with Euro VI standard for heavy duty. It has been

amended many times since then, culminating in 2020 with the current stage Euro VI-E (see Table 6.1).

Recently, the European Commission started the regulatory work aimed at setting the next stage of emissions standards, known as Euro 7 (for light-duty vehicles) and VII (for heavy-duty). The new Euro 7/VII, which will be presented at the end of 2021 and expected to come into force on 2025[76], will develop stricter CO_2 and NO_x limits, as well as new tests and limits for non-CO_2 greenhouse gas emissions [77]. There is no decision yet, but some reports point out that NO_x limits will be halved from Euro VI, placing the limit around 0.2g/kWh [78–80].

Table 6.1. EU Emission Standards for heavy duty diesel engines.

Tier	**Come into force**	**Stationary test**		**Transient test**		
		Test	**NO_X (g/kWh)**	**Test**	**NO_X (g/kWh)**	**CF**
Euro III	October 2000		5.0		5.0	
Euro IV	October 2005	ESC+ELR	3.5	ETC	3.5	-
Euro V	October 2008		2.0		2.0	
Euro VI (Euro VI-E)	January 2013 (Sept. 2020)	WHSC	0.4	WHTC	0.46	1.5
Euro VII*	2025	WHSC	0.2	WHTC	0.27	1.5

*Euro VII emissions regulations for trucks and buses is ongoing.

Since Euro VI, emissions have been tested through the World Harmonized Stationary Cycle (WHSC) and the World Harmonized Transient Cycle (WHTC). The Euro VI standards introduced off-cycle laboratory testing and on-road testing with portable emissions measurement systems (PEMS). The testing requirements for type-approval include: WHSC + WHTC test for diesel engines; WHTC test for positive ignition engines; Off-cycle emission (OCE) testing over the Work Not To Exceed (WNTE) control area of the engine map, and the on-road PEMS vehicle test. Additionally, the Euro VI regulation introduced in-service conformity (ISC) on-road PEMS testing.

A vehicle is deemed compliant if the average emissions, using the Moving Averaging Window (MAW) method, are below the ISC limit. The ISC limit is a function of the type-approval

limit over the WHTC (0.46 g/kWh for EURO VI), multiplied by a conformity factor (ISC limit = 0.46 g/kWh·1.5 = 0.69 g/kWh).

Although emission limits have been tightened and on-road measurements have been introduced, some studies point out that under specific engine regimes, emissions can exceed the regulatory limit.

Grigoratos et al. [25] tested five EURO VI diesel HDVs on-road under conditions that not necessarily comply with the official ISC test. They observed relatively high emissions for some of the pollutants over low-speed phases due to reduced effectiveness of the corresponding emission control systems. NO_x emissions of the tested HDVs ranged from 0.1 to 2.05 g/kWh at low-speed regimes. One of these vehicles exceeded the EURO VI engine certification limit (0.46 g/kWh) by a factor of 1.7.

TNO reported that despite most Euro VI HDVs emit overall low NO_x, in some cases under busy urban driving conditions they can emit NO_x over the conformity level of 1.5 [85], and confirmed this observation by measuring NO_x emissions of eight N3 Euro VI trucks (tractor semi-trailers and one rigid with trailer) over real world conditions [86].

Bishop et al. [87] reported that a large percentage of vehicles observed at a low speed location in California have catalytic devices functioning below a minimum temperature threshold restricting thus the potential effectiveness of SCR systems to further reduce NO_x emissions.

Vojtisek-Lom et al. [88] evaluated the prevalence of trucks with excess NO_x emissions on Czech motorways using an ordinary Customs Administration patrol vehicle temporarily fitted with a portable fast-response Fourier Transform Infra-Red (FTIR) analyser, acting as an impromptu chase vehicle. A total of 222 unique trucks were measured (66% were Euro VI). They found that about 10–25% of Euro VI trucks are believed to be excess emitters, with no SCR functionality on about 10–15% of Euro VI trucks.

Using on-board NO_x sensor data from two diesel transit buses, Kotz et al. [89] showed that these buses emitted NO_x at rates 3 to 9 times higher than the standard, primarily due to low load and low-speed operations. Tan et al. [90] reported the same.

Posada et al. [18] analysed five European trucks designed to meet the Euro VI NO_x standard. The analysis finds that European HDVs are better engineered than U.S. trucks to control NO_x emissions under low-speed, low-load, and idle conditions. The U.S. HDVs studied emit on average 1.4 times more NO_x per unit work than the European vehicles. During urban driving conditions, NO_x emissions were twice as much as their total route emission values.

In this regard, current emission standards should be improved to minimise the significant gap between real-world and certified NO_x emissions from heavy-duty diesel vehicles. As detailed above, this gap is especially wide during urban driving conditions and other low-load operations in diesel HDVs certified under the EURO VI.

This high NO_x emissions at low-speed, low load and idling are due to the fact that the SCR does not reach high enough temperature (i.e.>180 °C) to effectively abate engine out NO_x [25,26,75,91,92]. This occurs during cold starts and urban driving conditions, when the exhaust gas temperature is not high enough for SCR catalyst activation. Ammonia chemical reaction normally starts from 180°C, achieving its maximum reaction value around 350°C [27]. If exhaust gas temperature is roughly below 180°C, generation of derivatives such as ammelide, biuret, cyanuric acid and melamine create deposits on pipe walls as a decomposition of urea [28], being counter-productive for regular gas flow [93]. In fact, urea addition generally starts with exhaust gas temperatures around 220°C in order to avoid undesired products generation.

Therefore, even if the vehicle is EURO VI certified, it may emit pollutants above the regulatory limits if operates frequently in suburban areas, where traffic is mainly managed with traffic signs (traffic lights, stop signals, etc...) and the speed rarely exceeds 50 km/h.

Posada et al. [18] observed that a disproportionate amount of NO_x emissions from heavy-duty vehicles is emitted during the low-speed operation characteristic of urban driving. Vehicle operation at speeds of less than 40 km/h results in NO_x emissions of more than five times the

certification limit. Apart from that, a single line-haul truck emits the NO_x equivalent of 100 cars for each mile driven in urban driving. Based on 160 tests with a Portable Emissions Measurement System (PEMS), this study also shows that these trucks, which are optimized for highway driving, spend on average 43% of their time and emit 40% of the total mass of NO_x in urban-like operation, including low-speed driving and idling.

With the objective to improve SCR conversion during low-speed driving, some authors have studied the use of exhaust heaters. Some prototypes of catalytic converters that incorporate an internal electrical resistance for preheating the catalyst substrate have been tested with relevant results [13,14]. However, this solution is not as efficient as heating the exhaust gases directly. Mera et al. [94] implemented a system composed of an electric heating SCR and demonstrated that SCR inlet gas heating at 200 °C had the best deNO_x/CO_2 penalty trade-off. The minimum threshold of 200 °C resulted in the best NO_x/CO_2 trade-off, reducing on average 4.7 mg of NO_x per gram of CO_2. Culbertson et al. [16] analysed the ability of an electric heater to effectively increase the temperature of the exhaust and avoid the effect of moisture in low exhaust temperature, allowing NO_x conversion to start earlier. Results demonstrated that it is possible to achieve high NO_x conversion temperatures rapidly using robust heater technology for diesel applications. Sharp et al. [15] studied several options to reach extremely low NO_x values on a 361 kW Volvo HDV with a conventional turbocharged engine. Researchers investigated an electrically heated catalyst of 2 kW, coupled to a hydrolysis catalyst alone or combined with an additional heater of 5 kW assembled after the DPF and upstream the DEF. This system was compared to a mini-burner with adjustable-power from 8 kW to 20 kW. These configured ATS can provide a 45%, 70% and 80% in overall tailpipe NO_x emissions reductions respectively. However, these operating systems represent an increase of energy consumption that has to be carefully quantified.

However, in these systems it is assumed that the energy consumed by electrical heaters come from the vehicle's electrical system. In consequence, fuel consumption and overall vehicle efficiency must be studied in order to precise a fair evaluation of the system.

Massaguer et al. [17] proposed the use of an Automotive Thermoelectric Generator (ATEG) coupled to an Exhaust Gas Heater (EGH). This system could reduce up to 97% the NO_x emitted

during cold starts. The ATEG is used to transform waste thermal energy, afterwards the aftertreatment system, into electrical energy. The electricity generated is stored in a battery to be used by the EGH. This energy will be used when the EGH is required to heat the exhaust gas in low engine regimes, in order to shorten the time that urea is injected and reduce NO_x emissions. This EGH+ATEG system, also known as Thermoelectric Aftertreatment Heater (TATH), is developed to be energetically closed avoiding direct extra consumption of fuel for its use.

Recently, a new study [75] has experimentally demonstrated that a TATH could produce 80% NO_x emissions reduction in a Euro VI HDV at low engine regimes without the need of using extra energy. It also represents an improvement on SCR efficiency up to 55% for low engine regimes. The proposed system can be retrofitted in any Euro VI truck, which means that it can be installed without the need of replacing the existing aftertreatment system.

The objective of the present study is to assess whether a TATH allows a diesel-powered MAN TGX HDV EURO VI to comply with the current Euro VI regulation for low demanding regimes. It will also be studied if the use of a TATH allows the same vehicle to comply with the future Euro VII regulation.

To carry out this study, the vehicle will be subjected to different working conditions in order to obtain the emission map under standard operation on a dynamometer roller bench. The test will be repeated with the inclusion of an EGH before the ATS. NO_x reduction will be analysed with respect to the standard version without EGH. This study will determine which is the required EGH power to comply with EURO VI and EURO VII regulations. Finally, an ATEG will be sized to ensure that the system can work electrically autonomous. The power consumption of auxiliary equipment, the additional backpressure caused into the exhaust pipe and the additional weight on the vehicle will be considered.

6.2 Thermoelectric Aftertreatment Heater

As stated before, the proposed system to reduce NO_x emissions includes into the standard ATS two main components: the ATEG, located downwards the ATS, and the EGH, located upstream of the ATS. Figure 6.1 shows a detailed scheme of the exhaust pipe with the standard ATS and the proposed TATH. The estimated total weight of the TATH system (i.e. EGH, ATEG, battery and electronic system) is around 60 kg.

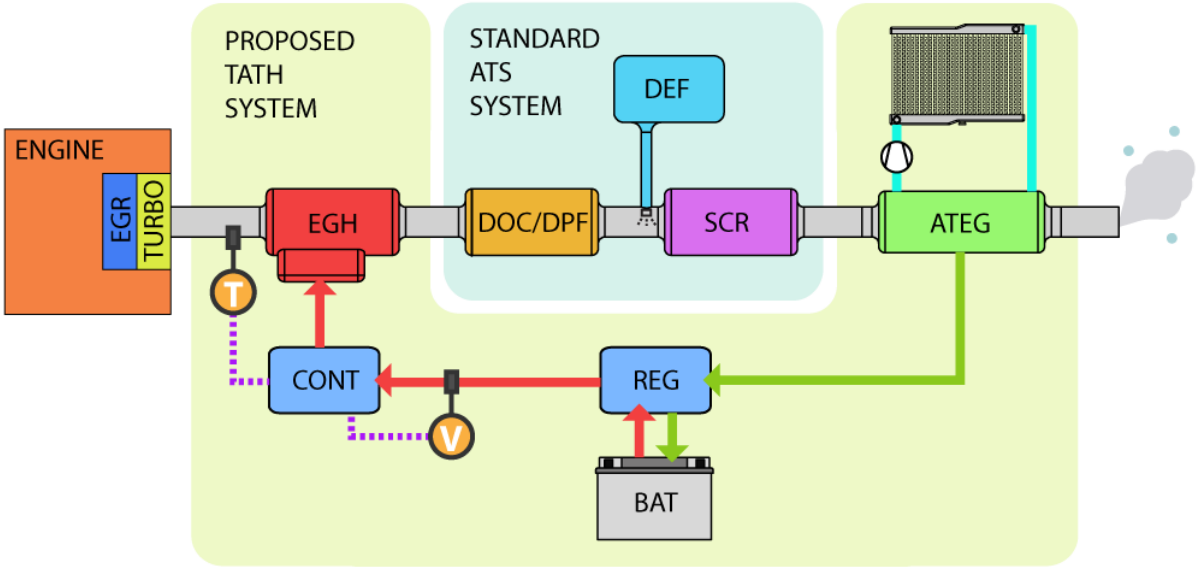

Figure 6.1. Proposed TATH system with the electrical energy flows: heating stage (red) and recovery stage (green).

Considering the exhaust gas flow, each component of the proposed TATH is assembled to maximize its functionality. The EGH is located after the turbocharger and the EGR valve. This element is assembled backwards the standard ATS of the vehicle, composed of a diesel oxidation catalyst (DOC), a diesel particle filter (DPF), a SCR and a diesel exhaust fluid (DEF) dosing system. The location of the EGH is crucial to help the standard NO_x reduction equipment as it provides higher exhaust gas temperature with minimal thermal loss. Despite the ideal location of the EGH is just before the SCR, it was impossible to achieve as the vehicle treated in this paper mounted a compact ATS (i.e. DOC, DPF and SCR in the same compartment).

Exhaust gas temperature is reduced while ATEG is converting energy by the thermoelectric effect. Meanwhile, this ATS performance principle is directly related to temperature increment. Taking this into account, the ATEG must be assembled afterwards the ATS.

As can be seen in Figure 6.1, the ATEG is complemented with a cooling system composed by a radiator and a hydraulic pump. Thermoelectric systems need to be cooled to achieve high temperature differences between hot and cold sides of thermoelectric modules (TEM). The lower the cooling temperature, the higher the efficiency of the ATEG [34]. In this study, the ATEG makes use of a refrigeration system independent of the vehicle to keep it cold. The additional power consumed by the hydraulic pump is supplied by the ATEG. The radiator is cooled by the flow of air onto it when the vehicle is in motion. Neither the aerodynamic loss due to the increased heat-exchanger surface of the radiator nor the hydraulic pressure loss in the refrigeration circuit have been considered.

The energy generated by the ATEG is send to the battery charging regulator (REG). To recover the maximum energy from exhaust gases, it is best to use a REG equipped with a maximum power point tracking system (MPPT) [95].

Additional weight of the system together with other counterproductive effects must be properly considered. We must take into account that the inclusion of the THAT cause a backpressure (BP) increase in the exhaust system. These effects will be analysed in chapter 4.5.

The TATH is designed to work in two different stages:

- **Heating stage:** in this stage the control unit (CONT) uses the energy stored into the battery to feed the EGH, which is used to rise the temperature of exhaust gases. The purpose of this stage is to rapidly heat the exhaust gases just before SCR. This stage begins when the engine starts, and it is maintained as long as the temperature of exhaust gases is lower than the light-off SCR temperature (i.e. <180°C). Reaching this target temperature as quick as possible is its main goal. When exhaust gases reach this point, urea solution could be dosed into the system causing a drastically abatement of NO_x. Time invested during this phase is related to achieve target temperature (=180°C). As it is demonstrated in the following subchapter, exhaust temperatures of a MAN TGX

HDV EURO VI are significantly lower than light-off temperature for regimes around 1000rpm (~ 55 km/h). Therefore, the heating stage will only take place at speeds below 55 km/h.

- **Recovery stage:** the recovery stage aims to charge the electrical battery with the residual heat from exhaust gases. This power will be used by the EGH during heating stage, mainly at low engine regime conditions. The ATEG is the responsible of converting waste heat into electricity during the operation of the vehicle. Unlike heating stage, which only takes place at certain moments along the way, the recovery stage lasts as long as the vehicle is running, even during the heating stage. It begins as soon as the engine is started and can last 270 minutes (equalling the maximum continuous drive time of 4.5 hours). As stated in other studies, the generated power of the ATEG (P_{ATEG}) increases directly with the engine regime as exhaust temperatures are higher at high engine regimes [34,35]. In consequence, the difference of temperature between the hot side and the cold side of each thermoelectric module (TEM) increases, $\Delta T = T_{HOT} - T_{COLD}$. If we consider $P_{ATEG} \propto \Delta T^2$, it can be stated that increasing engine regime, increases the ATEG generated power. Besides, the longer the mission time, the higher the energy recovered by the ATEG. In conclusion, the most suitable HDV to incorporate a THAT are long-distance transport vehicles.

To achieve emissions reduction without direct extra fuel consumption it must exist a balance between energy consumed (heating stage) and produced (recovery stage). In this regard, the mission profile of the HDV will play an important role in the TATH viability. A heavy-duty vehicle used in urban or suburban deliveries will spend the major part of its time at low-speed regimes. Mainly because traffic flow on urban and suburban routes has its speed limited around 50km/h and is frequently interrupted and delayed by traffic lights, stop signs, and intersections. This would cause the EGH to demand more energy than the ATEG could supply, making the use of TATH unviable. Contrarily, a long-haul HDV travels the major part of its time on highway at high engine regimes. Its speed profile is much more stable and closer to the highway limit speed, around 80km/h.

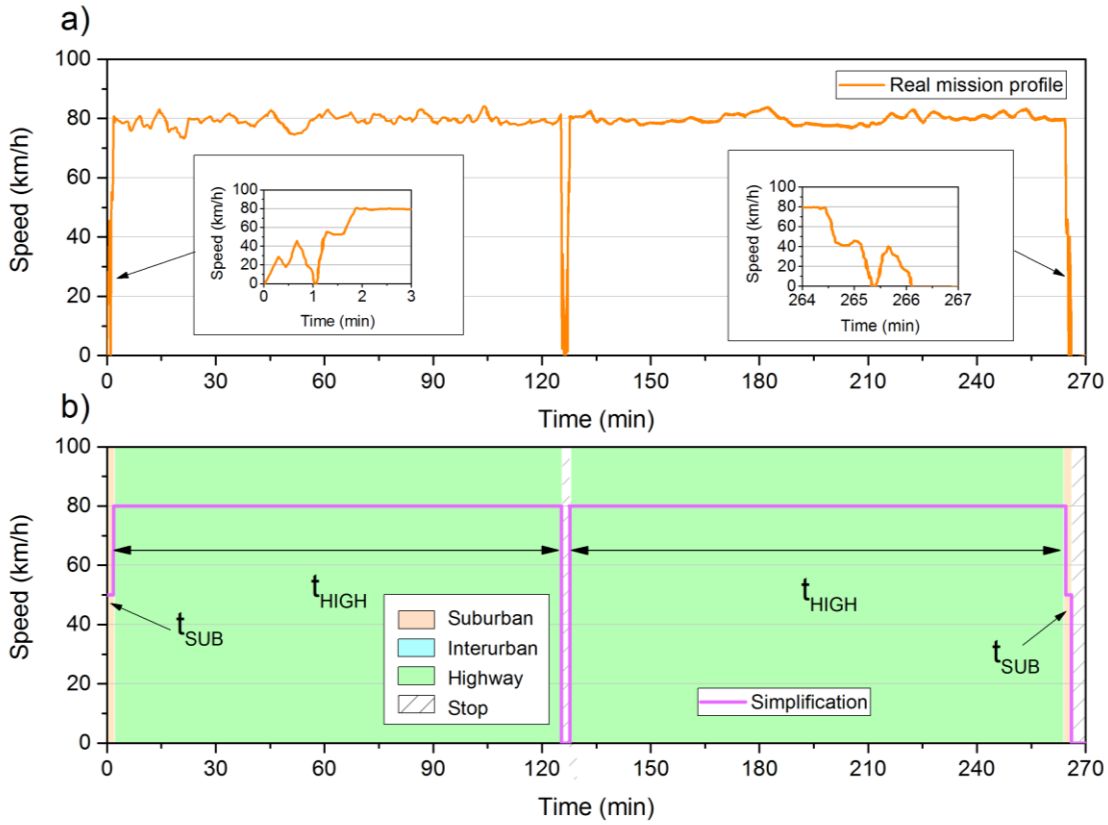

Figure 6.2. a) Speed profile of a long-haul heavy-duty vehicle[25]. b) Simplified speed profile.

Figure 6.2 shows a 266min long-haul mission profile of a HDV. Note that the vehicle spends $t_{HIGH} \approx 262min$ on highway conditions and just $t_{SUB} \approx 4min$ on suburban conditions. With long periods of time traveling in highway and interurban roads, the recovery stage can last long enough to store the energy required for the heating stage. This reason explains why in this study a long-haul HDV has been chosen as the target vehicle of the TATH.

To study the technical feasibility of the TATH system, two experiments were designed: the EGH and the ATEG experiment.

The EGH experiment was designed to study the effect of an EGH for NO_x emissions abatement. The ATEG experiment was designed to obtain the power generated by an ATEG under real exhaust conditions of temperature and mass flow in a HDV.

Two separate experiments were carried out due to the lack of information to correctly size the entire system. Note that at the beginning of the study we did not know what power the EGH needs to reduce NO_x emissions nor what power must be generated with ATEG to compensate the energy consumed by the EGH. The results of this study will allow us to size the complete system more efficiently in a future work. These two experiments are explained in detail in the following chapters.

6.3 EGH experiment

6.3.1 EGH experiment set up

The most restrictive antipollution standard for HDV in the European Union is the Euro VI standard, currently active. However, details of Euro VII (the next standard) will be announced in 2021 or 2022 and probably come into force in 2025. To obtain NO_x ppm values below antipollution regulation limits, manufacturers rely on a combination of a catalytic reaction system together with sophisticated ECU (Electronic Control Unit) software. In this study, a Heavy-Duty Vehicle Euro VI TGX 18.480 Efficient Line 2 from MAN was used to carry out the tests. Its most relevant characteristics are shown in Table 6.2.

Table 6.2. Main specifications of tested vehicle.

Parameter	**Value**
Maker	MAN
Model	TGX 18.480 Efficient Line 2
Gearbox	Automatic (12 gears)
Max. rated power	353 kW (at 1800 rpm)
Max. rated torque	1500 Nm (at 930-1400 rpm)
Emission standard	Euro VI

The whole system was disposed as presented in Figure 6.3. A certified test bench for testing HDVs (Maha Powerdyno R200/1) was used to put the vehicle in real operating conditions. This equipment was also used to capture the Full Throttle Pedal Position (FTPP), NO_x after and before the ATS, and exhaust temperatures from the ECU. Unfortunately, the on-board

acquisition system specifications were not available, so the accuracy of its measures is unknown. The EGH power consumption was measured by a Dranetz Power Explorer PX5 power meter with these specifications: measured current ranged from 1-6000 Arms with 0.1% rdg + CTs (4), measured voltage ranged from 1-600 Vrms with 0.1% rdg (reading) + 0.05% FS (full scale) both with 256 samples/cycle and 16-bit ADC. A National Instruments DAQ with a NI 9211 acquisition module was used to measure exhaust gas temperature. Its maximum measure error was 2.2°C (0-400°C) with measurement sensitivity <0.07°C. Type K thermocouples were used as temperature probes. A MIAC G4.0 was located at the end of the exhaust pipe to register NO_x emissions. This sensor provides a measure range from 0 to +5000 ppm with a resolution of 0.1 ppm (0 to +500 ppm), an accuracy of ±5ppm (0 to +99.9 ppm) and ±5% of mv (+100 to +2000 ppm).

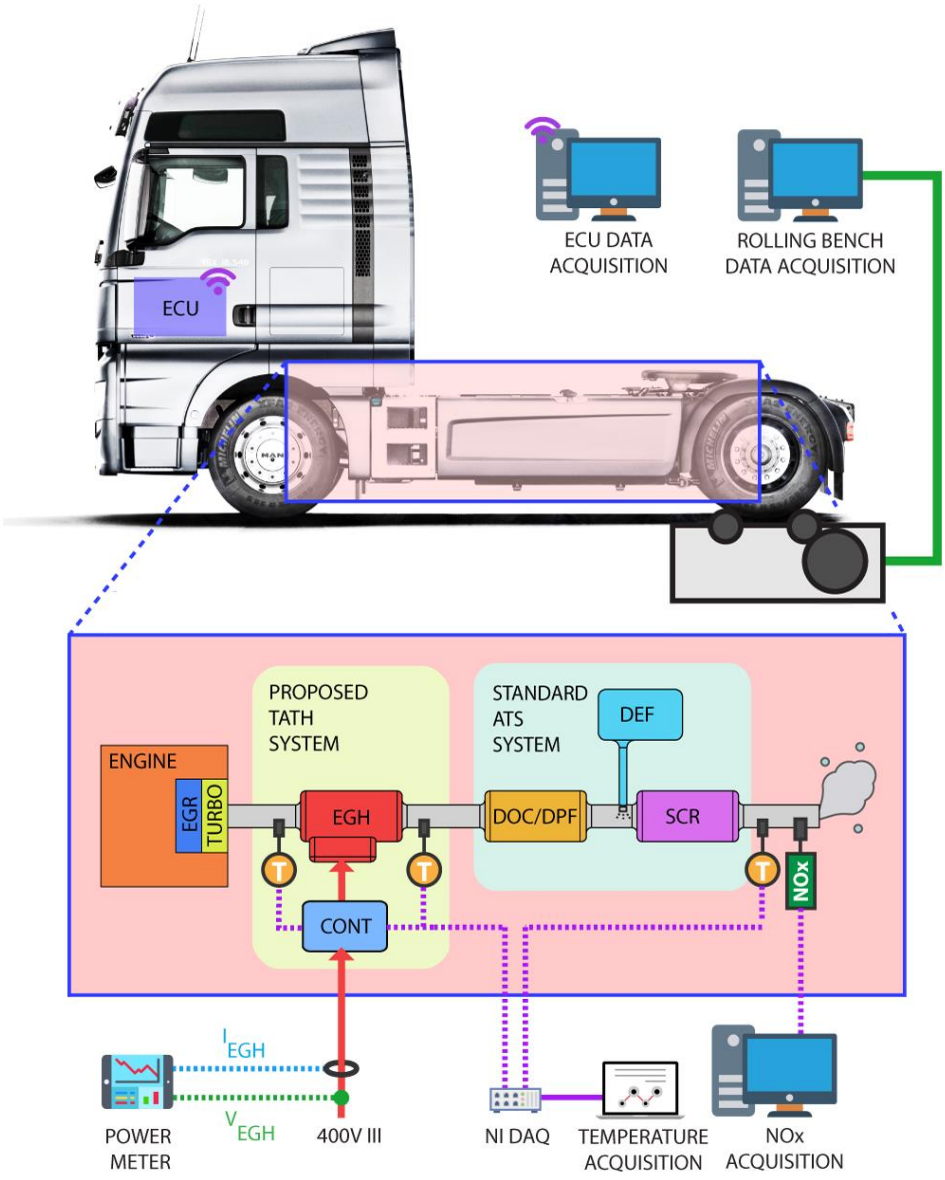

Figure 6.3. Scheme of the EGH experiment with data acquisition modules.

In order to prevent rear wheel sliding, the rolling bench was preloaded before testing as it can be seen in Figure 6.4 a). This same load was used in all tests within the experiment.

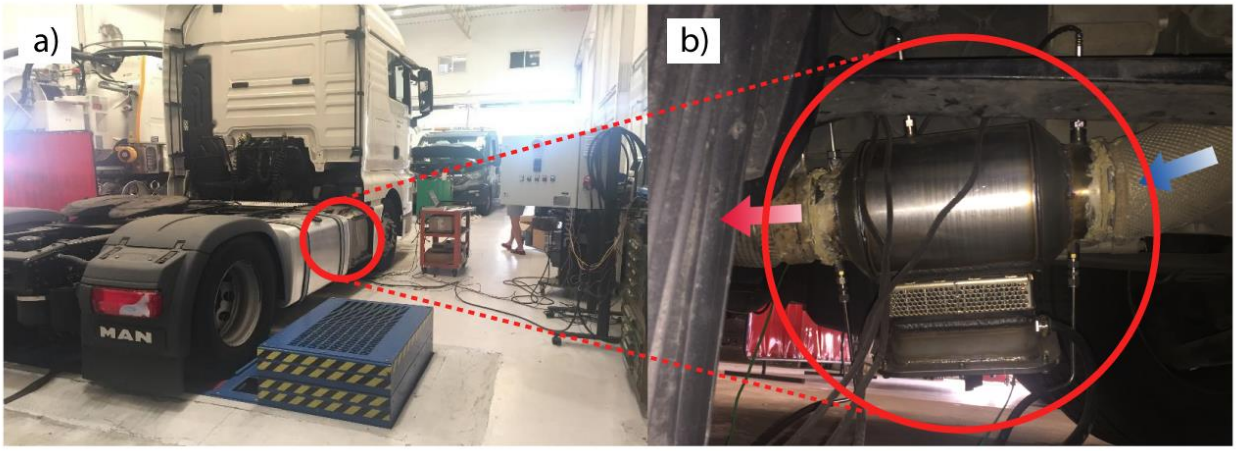

Figure 6.4. a) Vehicle placed on the test bench and b) EGH installed on the exhaust pipe.

To avoid gas flow alterations, the EGH seen in Figure 6.4 b) was installed preserving the original exhaust pipe and minimizing its deviation. Thermocouple sensors presented in Figure 6.3 can be seen in Figure 6.4 b) at inlet and outlet of the EGH. They respectively measure temperatures before EGH ($T_{B_{EGH}}$) and after the EGH ($T_{A_{EGH}}$), both fundamental parameters to study the whole performance of the ATS.

The selected EGH was a Watlow ECOTEG unit with a maximum heating power of 12 kW. This component contains an electric heating coil externally powered by a three-phase circuit and controlled by a temperature regulation system (CONT) specifically designed for this purpose. This system adjusted the power injected to the EGH according to the temperature set point (i.e. 300°C). Note that the power consumed by the EGH to heat the fumes to SCR light-off temperature depends on the exhaust gas conditions. As explained in the results chapter, the power consumed by the EGH ranges from 4 to 10 kW. Selected key parameters such as NO_x ppm, temperatures or engine regime, were synchronized, monitored, and registered.

Downwards the exhaust pipeline, it follows a compartment shared by a DOC and a DPF. The first one handles oxidation of carbon monoxide (CO) and unburned hydrocarbons (HC). Besides, it provides a permanent regeneration of the DPF. The particles filter must capture as many organic fraction (OF) of diesel particles as possible. Soot is also trapped in the filter surface and it is burned when maximum backpressure is reached. The induced regeneration injects more

fuel to rise exhaust gases temperature and burn the undesired particles. Threshold value is fixed by each manufacturer.

In second place of the standard ATS system, there is a package of components related to the Diesel Exhaust Fluid (DEF) function. This set includes the fluid tank and the supply and dosing modules. The mentioned fluid is a commercial urea solution which is injected into the system after exhaust gas temperature is over 180°C. DEF management is controlled by ECU parameters specifically designed for this vehicle. The dosing module is connected to temperature and NO_x sensors (one installed before the DOC and another located after the SCR) providing real time precise dose of urea solution to fulfil a particular standard (i.e. Euro VI). Finally, the exhaust gases combined with this solution enter the SCR (Selective Catalytic Reduction) unit. A catalytic reaction is produced inside to transform NO_x into water (H_2O) and diatomic nitrogen (N_2).

The main parameters acquired from the ECU and the rolling bench are: the FTPP, the engine torque, the vehicle speed and the SCR inlet temperature, which are necessary to carry out the subsequent analysis. Other data, like the EGH inlet and outlet temperatures ($T_{B_{EGH}}$ and $T_{A_{EGH}}$ respectively), the heater electrical power consumption ($P_{EGH} = \sqrt{3} \cdot V_{EGH} \cdot I_{EGH} \cdot \cos\varphi$ being V_{EGH} the voltage and I_{EGH} the current) and the NO_x emissions (NOx_{EGH}) are obtained from external equipment modules. A scheme of these acquisition modules is also shown in Figure 6.3.

With this combined ATS layout, a rise in exhaust gases temperature can increase the SCR efficiency in cold start conditions and low demanding urban routes. In addition, this temperature increment produces an improvement for DPF regeneration. Consequently, this configuration can improve fuel consumption, as less fuel will be required to burn particles inside the DPF. Afterwards the SCR is the ideal location for coupling an ATEG to harvest thermal energy, thus alterations of exhaust gas temperatures and flow are minimized.

The experiment is divided into three different stationary points. All of them present low or medium rpm values analysing low demanding engine speed. In order to obtain all FTPP range in driving conditions it has been permanently selected the eleventh gear. In each particular test,

point data has been registered only after stabilizing the desired stationary regime. In order to equal engine conditions during all tests, engine temperature has been kept below 90°C, simulating cold start conditions. Consequently, short periods of time between tests were required to cool down the engine temperature. Table 6.3 shows all regimes selected for this experiment, being found all of them in a typical daily drive. It also shows all FTPPs used to analyse NO_x emissions and a correlation between engine regime and vehicle speed.

Table 6.3. Stationary points selected for the tests.

Test	Engine regime (rpm)	FTPP (%)	Vehicle speed (km/h)
1	1000	30, 35, 40, 45, 50, 55, 60, 70, 80, 90	55
2	1250	30, 35, 40, 45, 50, 60, 70, 80, 90	68
3	1500	30, 35, 40, 45, 50, 60, 70, 80, 90	82

6.3.2 EGH experimental results

To analyse if the incorporation of an EGH is beneficial or not for the abatement of NO_x emissions, two NO_x emissions maps are confronted in Figure 6.5. On one side, Figure 6.5a shows the NO_x emissions map of a MAN TGX 18.480 Efficient Line 2 EURO VI HDV with its standard ATS (i.e. EGH was disabled). On the other side, Figure 6.5b shows the NO_x emissions map of the same vehicle but with the EGH enabled. On both maps the boundary regions for compliance with the EURO VI and VII regulations have been marked. According to Table 6.1, these limits have been calculated from the WHTC limit value multiplied by the conformity factor CF: $NOx_{limit}^{EURO\ VI} = 0.46 \cdot 1.5 = 0.69 g/kWh$ and $NOx_{limit}^{EURO\ VII} = 0.27 \cdot 1.5 = 0.41 g/kWh$.

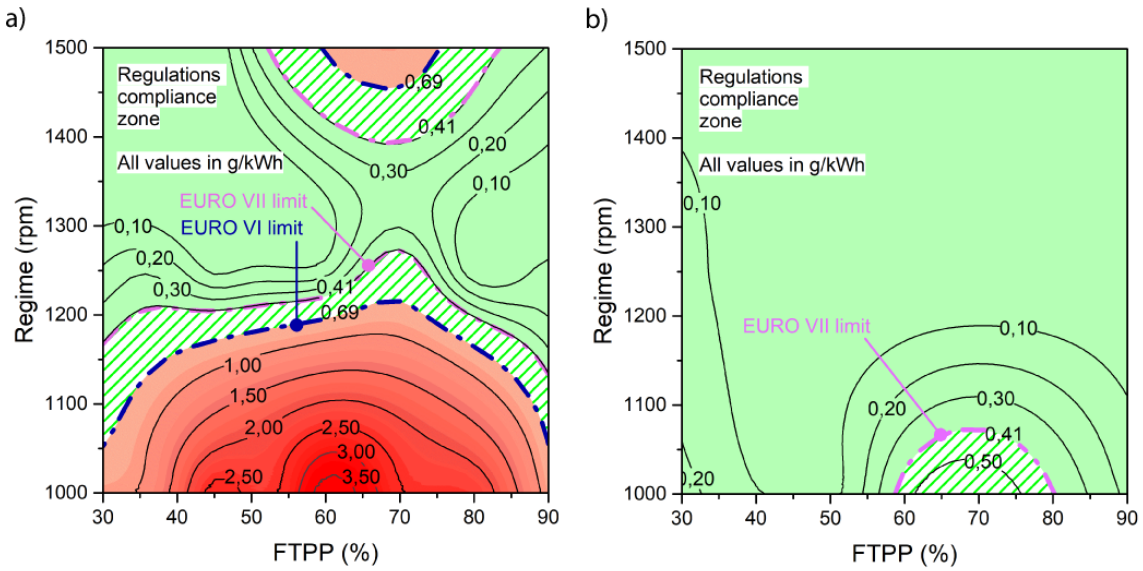

Figure 6.5. NO_x emissions map of a MAN TGX 18.480 Efficient Line 2 EURO VI HDV with the EGH a) disabled and b) enabled.

From Figure 6.5a, it can be observed that under certain engine regimes, mainly low-speed regimes, an EURO VI certified HDV emits NO_x pollutants above the limit value. This agrees with what authors in ref. [25,85–87] observed. The highest NO_x emissions appear at regimes around 1000 rpm, which correspond to suburban driving conditions. The highest value is located at 1000 rpm and 60% FTPP, where NO_x emission reach 3.83 g/kWh, surpassing 5 times the regulation limit. In mid demanding regimes, such as 1200—1500 rpm, is where EGH is less required because the engine produces enough heat to reach the SCR light-off temperature and make the catalytic conversion highly efficient [75]. Note how the over-emission area grows with the inclusion of the EURO VII limit. This evince that there is still a lot of work to be done.

Fortunately, Figure 6.5b demonstrates that the incorporation of a 12 kW EGH allows the HDV to comply with the EURO VI and most of EURO VII emissions limit. Observe that all points in the map fulfil the EURO VI regulation. The EURO VII limit is also fulfilled except in a small region between 1000—1100 rpm and 60—80% FTPP.

A more detailed analysis shows that NO_x emissions achieved 3.83 g/kWh when the EGH was disabled at 1000 rpm and 60% FTPP. Under the same conditions, NO_x measured with the EGH enabled, was about 0.46 g/kWh. This represents the maximum reduction found in all tests. In

absolute terms, it represented a NO_x reduction of 3.37 g/kWh. This, translated to relative terms, can be read as a 97.2% of NO_x reduction at 50% FTPP.

Regarding the EURO VI compliance, note that all combinations of values in Figure 6.5b are lower than the limit value of 0.69 g/kWh. This means that the heat delivered by the EGH to exhaust gases was excessive to fulfil EURO VI regulation, therefore, a smaller EGH could be used. The EURO VII case is a little bit different because in some cases, the heat delivered by the EGH to exhaust gases was excessive (i.e. <0.41 g/kWh) and in other cases it was insufficient (i.e. > 0.41 g/kWh).

Figure 6.6a and b show the strictly necessary power required by the EGH to comply with EURO VI and EURO VII regulations, respectively. These values were obtained by interpolating the experimental values with the regulation limit. Note that the EGH power is not static because it depends on the temperature and mass flow rate of the exhaust gas. In both cases, the maximum power values delivered by the EGH are at 1000 rpm.

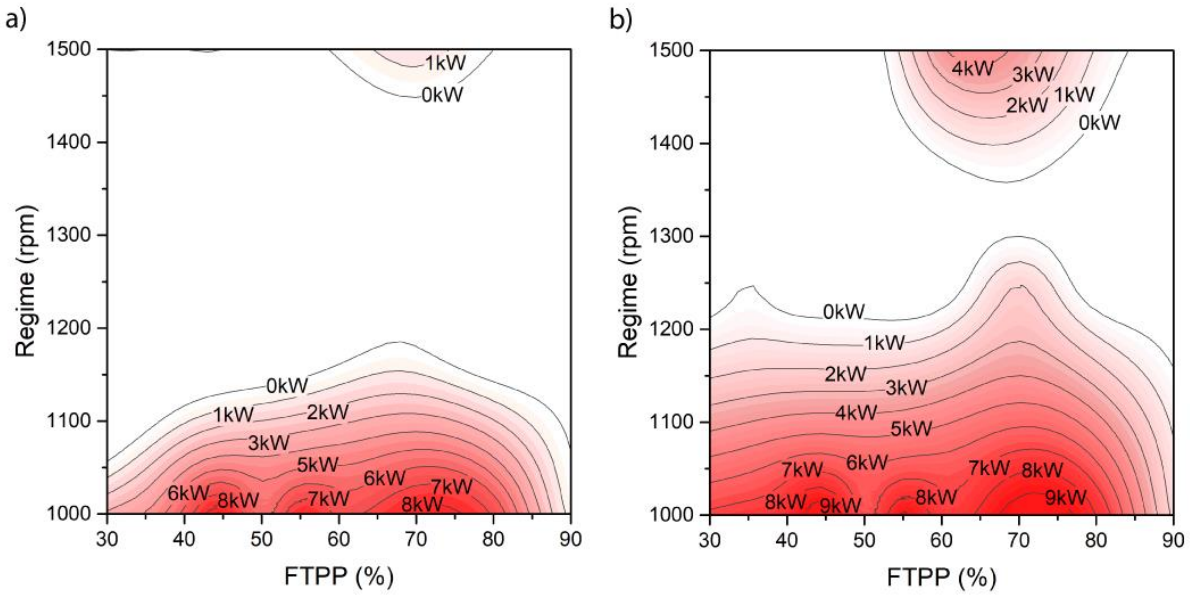

Figure 6.6. EGH power demand map to fulfil a) EURO VI and b) EURO VII regulations in a MAN TGX 18.480 Efficient Line 2 EURO VI HDV.

In Table 6.4., a comparison of the average power required by the EGH to comply with EURO VI and EURO VII regulations under three driving conditions are summarized. The most demanding regime is the suburban driving with an average EGH power requirement of 5.84kW and 7.52kW to accomplish EURO VI and EURO VII regulations, respectively. Furthermore, it is the most pollutant regime, emitting 10 times more NO_x on average than the interurban driving and 7 times more compared with a highway driving.

Table 6.4. Comparison of the average power required by the EGH to comply with EURO VI and EURO VII regulations under three driving conditions.

DRIVING CONDITION	**Vehicle speed**	**Time***	**Average NO_x emissions of the standard ATS (g/kWh)**	**Average EGH power required to fulfil EURO VI $P_{EGH}^{EURO\ VI}$ (kW)**	**Average EGH power required to fulfil EURO VII $P_{EGH}^{EURO\ VII}$ (kW)**	**Average exhaust temperature downwards ATS (°C)**	**Average mass flow rate downwards ATS (kg/s)**
SUBURBAN	55 km/h (1000rpm)	1,5% (4 min)	2.09	5.84	7.52	159	0.147
INTERURBAN	68 km/h (1250rpm)	0% (0 min)	0.19	0.00	0.22	228	0.172
HIGHWAY	82 km/h (1500rpm)	98.5% (262 min)	0.30	0.19	0.95	196	0.204

*Taken from the real speed profile of a long-haul HDV presented in Figure 6.2.

Considering the time spent and the average NO_x emissions at each driving condition in Table 6.4., it can be observed that the amount of NO_x emitted during the suburban driving represents the 10% of the total NO_x emitted during the mission. In other words, driving 4 minutes in suburban roads generates the same amount of NO_x than driving 28 minutes in the highway. This justifies the need to focus on developing technologies that allow reducing NO_x at this working regime. This is the purpose for which the TATH has been designed.

Table 6.4. also presents the average exhaust temperature and mass flow rate measured downwards the ATS. These values will be used in the following chapter to size and test the ATEG system.

At this point, it is important to remark that it is not necessary to install a 12 kW EGH in a HDV to effectively reduce NO_x emissions. Considering that the SCR light-off temperature for urea solution injection is 180°C, it is demonstrated that the EGH device should only heat the exhaust gases to reach this target value. To provide extra thermal power to the exhaust gases is unnecessary and counter-productive.

Finally, the EGH was tested in a hot air flow bench under the highway conditions to analyse its backpressure. The results from this test showed a maximum pressure loss of 1.8mbar at 204 g/s. From this data, the hydraulic power, $P_{H_{EGH}} = Q_{EGH} \cdot \Delta p_{EGH}$, that the engine must provide to overcome the EGH additional backpressure is calculated. The greatest impact is presented in highway conditions with $P_{H_{EGH}} = \frac{0.204kg/s \cdot 180Pa}{0.745kg/m\text{^}3} = 49.3\ W$.

6.4 ATEG experiment

Conventional internal combustion engine vehicles use an alternator to produce the electricity needed by the vehicle. This electricity is generated at expense of consuming more fuel. Some studies have reported that alternators are the responsible of $4{\sim}6\%$ of the total fuel consumption of the vehicle [34,96].

Most factory alternators for HDVs are available with outputs ranging from 160 up to 320 amps (3.84 kW to 7.68 kW) and are capable of handling the vehicle's basic necessities, such as headlights, gauges, fuel pumps, A/C, etc. Considering this power production range, the inclusion of a 5.84 kW EGH (i.e. to fulfil EURO VI) into the electrical system would require incorporating an exclusive alternator for the EGH, causing a significant increase in fuel consumption.

To avoid this extra fuel consumption, this chapter is focused on analysing the feasibility of using an ATEG as the main and only power supplier for the EGH. An ATEG is a heat recovery system

designed to convert waste heat form exhaust gases into electricity. Many theoretical models [34,37,43–45] and experimental prototypes [35,46–49] have demonstrated the feasibility of ATEGs as on-board power suppliers.

6.4.1 ATEG experiment set up

The aim of this experiment is to find out how much power could be recovered from the exhaust fumes of a HDV, downstream of the ATS, under the real working conditions presented in Table 6.4.

Figure 6.7 shows the ATEG layout designed in this study. It has been engineered to feed the TATH electrical system based on the data collected in previous developments [34,35]. These studies demonstrated the importance of keeping the backpressure as low as possible to minimize the engine extra effort. Considering that, the proposed ATEG is composed by six ATEG single units (ATEG_su) arranged in parallel with respect to the fumes. Each one is identical to the one tested on [34]. The dimensions of the ATEG are 950x420x340mm (WxLxH), it weights around 40 kg and make use of 204 Bismuth Telluride thermoelectric modules.

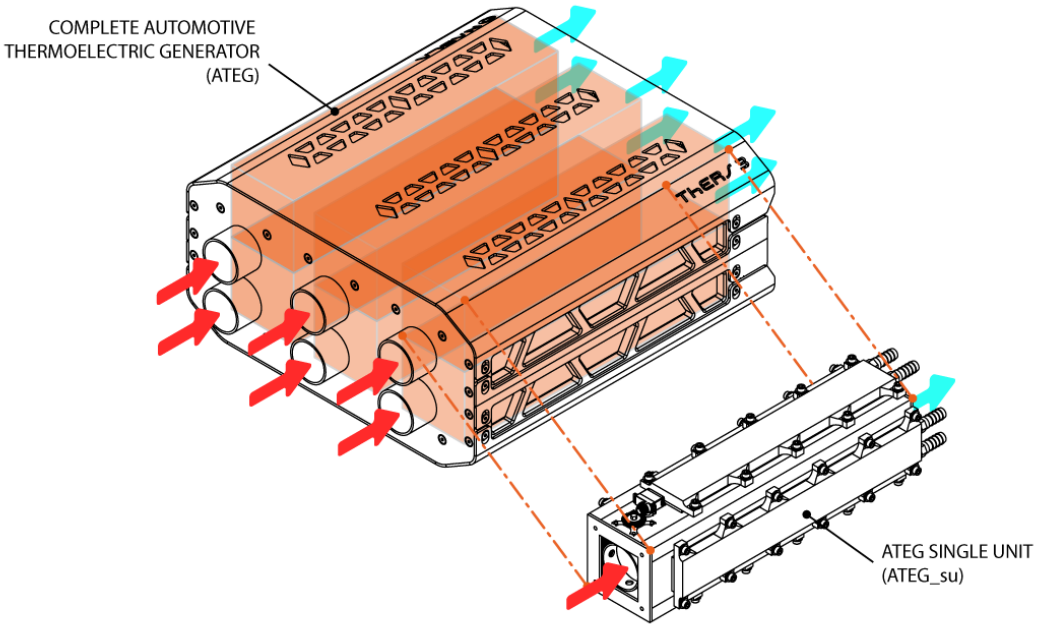

Figure 6.7. Complete ATEG composed of six ATEG_su.

To simplify the execution of the experiment, only one of the six ATEG_su was tested. The ATEG_su inlet temperatures and mass flow rates used in the experiment are presented on Table 6.5. Note that temperatures are quite similar to ones shown in Table 6.4. However, mass flow rates are one sixth of those described in Table 6.4, in order to consider the flow distribution.

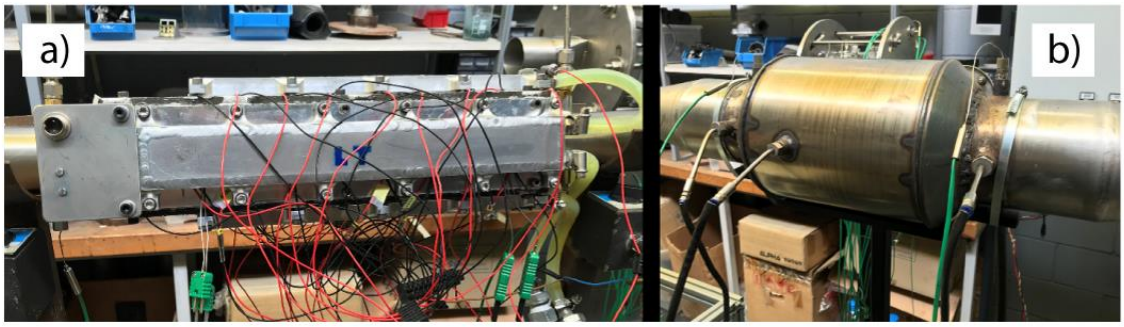

Figure 6.8. a) ATEG_su prototype attached to the b) EGH.

Figure 6.8a shows the ATEG_su with this cooling plate in first term and its connections to the cooling circuit. Figure 6.8b presents the EGH coupled upstream to the ATEG_su. Inlet and outlet thermocouple sensors and the electrical power supply cable can also be seen.

The dimensions of the ATEG_su are 170x420x170mm (WxLxH) and weights around 8kg without considering cooling fluid. It includes 34 thermoelectric modules (TEMs) configured in two parallel branches (of 8 and 9 individual TEMs) each one electrically connected in series. TEMs are composed of Bismuth Telluride and they are assembled with graphite pads on their contact sides to provide low thermal resistance. Hot sides of these modules contact the surface of an aluminum heat exchanger, through which the exhaust gas flows. Cold sides are in contact with an aluminum plate with an interior cooling circuit. For more information about the ATEG_su, see [34].

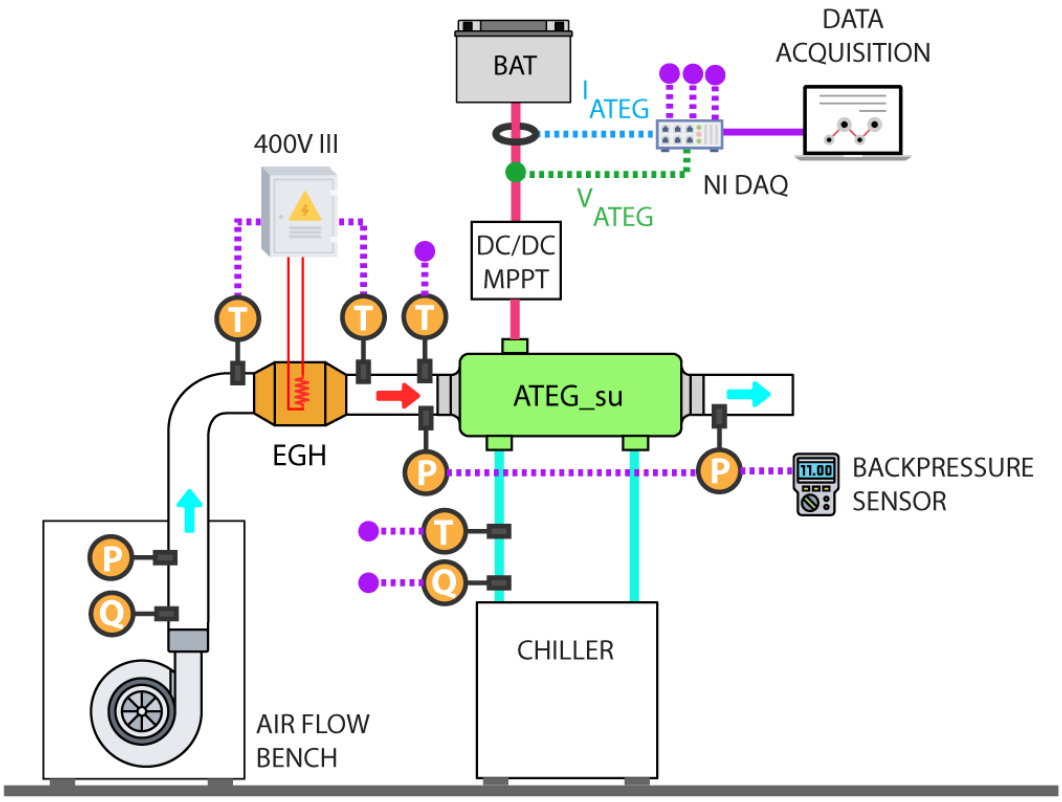

Figure 6.9. Scheme of the test bench for ATEG_su.

Figure 6.9 shows a scheme of the experimental bench used to test the ATEG_su, which consist of an air flow bench and a 12 kW EGH controlled by a PID. This apparatus has the capacity to generate air flow rates up to 150 g/s at temperatures between 25°C to 400°C. This equipment is complemented by a National Instruments DAQ data acquisition system, with thermocouple slots, RTDs, analogic and digital inputs, voltages 0-10 V, voltages 0-60 V and currents up to 5 A. A cooling system composed of a Thermo Scientific ThermoChill II chiller, shown in Figure 6.10a, was used to emulate a real vehicle cooling system. It can control the temperature of the cooling circuit between -10°C and 30°C, with a flow rate of 2.5 gpm @ 60 psid (9.4 lpm @ 4.1 bar) with an accuracy of +/-0.1°C. This equipment incorporates temperature, flow rate, and pressure sensors. The energy generated by an ATEG_su was regulated and maximised by a Victron BlueSolar 130/35 DC/DC converter with MPPT and then stored to a 12 V battery. The backpressure caused by the ATEG_su was measured by a WIKA A2G-50 differential pressure sensor. Real operating conditions have been reproduced in the refrigeration circuit [34]. A pump, with a power consumption value of 20 W, is the responsible of moving the water

through the cold plates of the ATEG_su. A Saenz J-600 flow bench was coupled directly to the EGH inlet as seen in Figure 6.10b.

Figure 6.10. a) The chiller and b) the air flow bench unit.

This equipment allows us to experiment with ATEGs cheaply and quickly. It allows us to modify the ATEG on the fly, a very interesting option when you are starting from an incipient and unvalidated design. It also allows us to quickly set up any working regime and test ATEGs at small-scale without having to build the complete set. It is for this reason why, at this stage, we refused to do the test directly on the vehicle. All data collected in this study will minimize risks during the future design and construction of the complete TATH system. In this way it will be possible to face the future tests in a real vehicle with maximum guarantees.

6.4.2 ATEG experimental results

Table 6.5 shows the net power generation of the tested prototype in different real conditions. Note that the ATEG_su inlet mass flow rate is one sixth the average mass flow rate downwards ATS presented in Table 6.4.

Table 6.5. Net power generation of an ATEG under three different driving conditions.

DRIVING CONDITION	Vehicle speed	Time*	ATEG inlet T (°C)	ATEG_su inlet mass flow rate (kg/s)	ATEG_su power generated (W)	ATEG power generated (W)	Hydraulic pump power (W)	ATEG net power generation P_{ATEG} (W)
SUBURBAN	55 km/h (1000rpm)	1,5% (4 min)	162	0.025	23	138	20	118
INTERURBAN	68 km/h (1250rpm)	0% (0 min)	225	0.028	34	204	20	184
HIGHWAY	82 km/h (1500rpm)	98.5% (262 min)	210	0.035	53	318	20	298

*Taken from the real speed profile of a long-haul HDV presented in Figure 6.2.

From Table 6.5, it can be observed that the low exhaust temperatures at the end of the ATS generate a humble power production on the ATEG. Note that, with the increase of the exhaust gas temperature or mass flow rate, the power production also increases but exponentially. Consequently, it is recommended to thermally isolate the exhaust system in order to minimize heat losses upwards the ATEG.

Figure 6.11 shows the pressure drop of the ATEG_su under the three driving regimes. As seen in the figure, the curve fits to a linear function with a R-Square factor of 0.999.

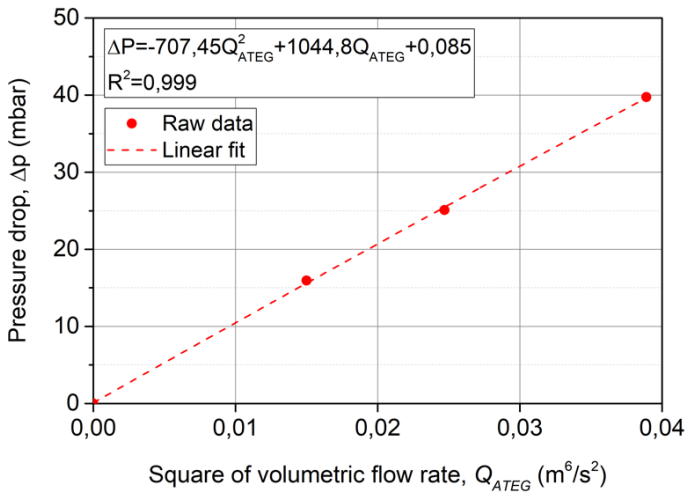

Figure 6.11. ATEG_su pressure drop with respect to the square of volumetric flow rate.

Note that the maximum backpressure is 40 mbar at highway conditions. From this data, the hydraulic power, $P_{H_{ATEG}} = Q_{ATEG} \cdot \Delta p_{ATEG}$, that the engine must exert to overcome the backpressure is calculated. Note that Q_{ATEG} is the exhaust volumetric flow rate through the ATEG and Δp_{ATEG} the backpressure on the ATEG. The greatest impact occurs during highway conditions with $P_{H_{ATEG}} = \frac{0.204kg/s \cdot 4000Pa}{0.745kg/m\text{^}3} = 1095.3\ W$.

6.5 Discussion

As explained in Chapter 6.3.2, the 10% of the total amount NO_x produced during the mission was emitted during the suburban drive, which took the 1.5% of the mission time. These values demonstrate the need of a TATH system, which was designed to reduce these emissions at this regime. It heats up the exhaust gases only during the suburban driving and recover energy during the entire mission.

Once the performance of both, the EGH and the ATEG, have been obtained, it is the turn to analyse the capacity of the whole system to be energetically self-sufficient. To guarantee that the TATH system can feed itself autonomously, the energy consumed in the heating stage must be lower than the energy recovered, $E_{HEATING} \leq E_{RECOVERY}$. Eq. 1 details this relationship based on the parameters collected in the previous chapters.

$$0 \leq P_{ATEG_{HIGH}} t_{HIGH} + P_{ATEG_{INT}} t_{INT} + \left(P_{ATEG_{SUB}} - P_{EGH_{SUB}}\right) t_{SUB} \quad \text{Eq. 1}$$

Where $P_{ATEG_{HIGH}}$, $P_{ATEG_{INT}}$ and $P_{ATEG_{SUB}}$ are the power recovered by the ATEG during the three driving conditions; and $P_{EGH_{SUB}}$ is the heating power of the EGH at suburban driving conditions. Finally, t_{HIGH}, t_{INT} and t_{SUB} are the times spent by the vehicle at highway, interurban and suburban routes, respectively. Those values are obtained using Eq. 2 to 4.

$$t_{SUB} = \sum_{i=0}^{200} t_i = f(v)\ \ if\ v \leq \frac{50km}{h} \quad \text{Eq. 2}$$

$$t_{INT} = \sum_{i=0}^{200} t_i = f(v)\ \ if\ \frac{50km}{h} < v < \frac{80km}{h} \quad \text{Eq. 3}$$

$$t_{HIGH} = \sum_{i=0}^{200} t_i = f(v)\ \ if\ v \geq \frac{80km}{h} \quad \text{Eq. 4}$$

Substituting the power values by those obtained in Table 6.4 and 6.5, the limit time relationships that satisfy the energy balance can be obtained. Table 6.6 conditions must be fulfilled to comply with the EURO VI or EURO VII regulations in suburban conditions. Note that these relations do not consider the power losses in the power converters, battery charge-discharge and regulation.

Table 6.6. Time relationships to comply with EURO VI and VII regulations in suburban conditions.

Regulation	**Condition to comply with EURO regulation for suburban conditions**	**Percentage of time spent in suburban conditions with respect to mission time to comply with EURO [%]**
EURO VI	$0 \leq 298t_{HIGH} + 184t_{INT} - 5722t_{SUB}$	$r_{SUB\_MAX}^{EURO\ VI}$ < 3.1 - 4.9%
EURO VII	$0 \leq 298t_{HIGH} + 184t_{INT} - 7402t_{SUB}$	$r_{SUB\_MAX}^{EURO\ VII}$ < 2.4% - 3.9%

These equations demonstrate that, to comply EURO VI regulation in suburban conditions, it is necessary that the HDV spends a maximum of 3.1% of the mission time in suburban conditions. This value is obtained considering that the recovery stage is exclusively limited to interurban driving. If the recovery stage is limited to highway conditions, this value is slightly higher, achieving a maximum of 4.9%. This can be explained by the higher power recovered in highway conditions compared to the same period in interurban conditions. A route that mixes highway and interurban driving would give an intermediate value between 3.1% and 4.9%. The same happens for EURO VII fulfilment, where this maximum stays between 2.4−3.9%, depending on the driving conditions during the recovery stage. Note that these two conditions are fulfilled in the mission profile described in Figure 6.2, where the time spent in suburban conditions was 1.5%. Therefore, the incorporation of the TATH presented in this study would allow a EURO VI HDV to comply with not only EURO VI but also EURO VII in suburban conditions.

However, the HDV usage or routing map is crucial in the viability of the TATH system. Figure 6.12 shows six HDV mission profiles depending on the usage of the vehicle. These mission profiles have been extracted from VECTO software and reflect the current European fleet. VECTO is a simulation tool that has been developed by the European Commission and is used for determining CO_2 emissions and Fuel Consumption from Heavy Duty Vehicles (trucks, buses and coaches) with a Gross Vehicle Weight above 3500 kg.

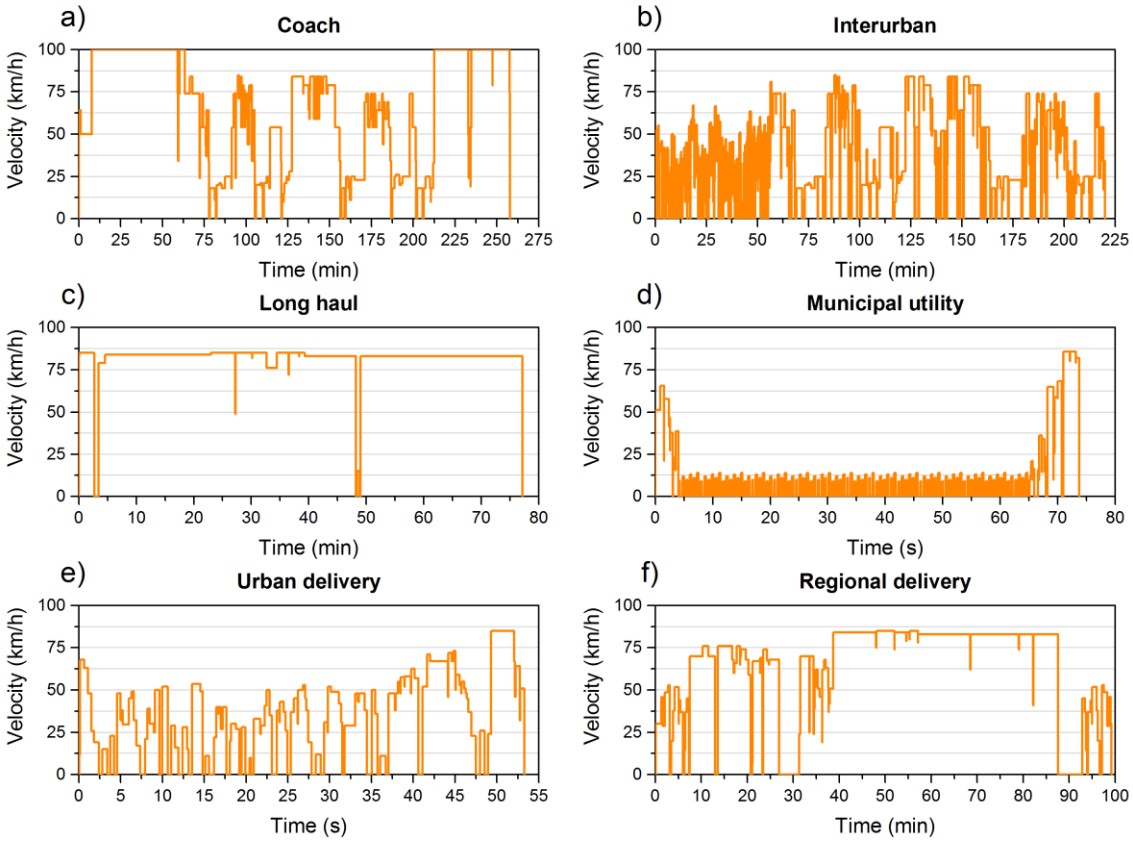

Figure 6.12. Typical mission profiles of different HDVs.

From Figure 6.12, the percentage of time spent in suburban conditions can be calculated with respect to the mission time, $r_{SUB} = 100t_{SUB}/t_{MISSION}$, for each mission profile. Table 6.7 summarizes these values.

Table 6.7. Percentage of time spent in suburban conditions with respect the mission time for each mission profile.

Mission profile	r_{SUB}
Coach	25.02%
Interurban	44.15%
Long haul	0.64%
Municipal utility	32.74%
Urban delivery	48.65%
Regional delivery	11.20%

Note that only the long-haul mission profile satisfies the time requirements that makes the TATH system technically viable for both EURO regulations, $r_{SUB} < r_{SUB\_MAX}^{EURO\ VI}$ and $r_{SUB} < r_{SUB\_MAX}^{EURO\ VII}$. Long-haul transportation refers to a long-distance driving transportation system wherein the drivers undertake a single delivery by driving a commercial vehicle for a distance of 250 km or more. Typically, long-distance vehicles connect logistics centres that are close to major transportation routes, so they spend most of the journey on the highway. This is the reason why this type of vehicle is the most appropriate to incorporate the TATH system.

As explained in previous chapters, the maximum backpressure caused by the EGH and ATEG were 1.8 mbar and 40 mbar, respectively. This means that the TATH system increases the pressure drop in 41.8 mbar and the required engine power in $P_{H_{TATH}} = P_{H_{EGH}} + P_{H_{ATEG}} = 1144.3\ W$. Taking the power developed by the vehicle at that regime and the $P_{H_{TATH}}$, this would suppose a fuel consumption increase of 0.2%.

On the other hand, the additional weight that the TATH adds to the vehicle must also be considered. A heavier truck produces more rolling resistance than a lighter one, thereby increasing the power needed to move the vehicle. A 200 kg cut in vehicle weight can reduce fuel consumption by 0.5% on a regional delivery truck and 0.3% on a long haul truck [81]. Considering a TATH weight of 60 kg, this would suppose a fuel consumption increase of 0.09%. Other study [82] established that the average impact on mpg per tonne of increased payload of a HDV with a fuel consumption of 8.15 mpg is 0.112 mpg. This supposes a fuel consumption increase of 1.4% per tonne. In this case, the TATH would increase the fuel consumption in a 0.08%. Besides, according to the fuel economy assessment method of ref. [37], the additional weight of the TATH would suppose an increase of 0.13% in fuel consumption.

Finally, the total fuel consumption increase due to the incorporation of TATH into the exhaust system would be 0.35%. It is clearly lower than the use of an exclusive alternator, that would suppose a 4-6% fuel consumption increase. With this information it can be concluded that the use of an ATEG is a better option than using an alternator to feed the TATH. Besides, the inclusion of the TATH into the exhaust system will not negatively affect the engine performance.

6.6 Conclusions

In this particular research, the use of a thermoelectric aftertreatment heater (TATH) to reduce NO_x emissions of diesel-powered HDVs in low demanding regimes have been analysed. This system includes an Exhaust Gas Heater (EGH) that heats up the exhaust gases in low engine regimes, to shorten the time before urea is injected. Additionally, the TATH receives energy by an Automotive Thermoelectric Generator (ATEG) previously transforming wasted heat from exhaust gases into electricity, so the system can work energetically independent.

This study demonstrates that under certain engine regimes, mainly low-speed regimes, a EURO VI certified HDV emits NO_x pollutants above the limit value. The highest NO_x emissions occur at regimes around 1000rpm, which corresponds to suburban driving conditions. The highest value can be found at 1000rpm and 60% FTPP, where NO_x emission reached 3.83 g/kWh, 5 times higher than the regulatory limit.

One of the most significative findings is that the use of a TATH allows to a long-haul diesel-powered MAN Euro VI TGX 18.480 Efficient Line 2 to fulfil the EURO VI and even the prospective EURO VII regulation when operating in suburban conditions. The suburban driving is the most demanding regime with an average EGH power requirement of 5.84 kW and 7.52 kW to fulfil EURO VI and EURO VII regulations, respectively. It is also the most pollutant regime, emitting 7 times more NO_x on average than the highway driving.

Besides, this study also demonstrates that an ATEG is capable to produce the energy required by the EGH in a long-haul mission profile. However, the added weight and the backpressure caused into the exhaust system increased the fuel consumption of the vehicle by 0.35%, which is lower than the expected of an exclusive alternator, that would suppose a 4-6% fuel consumption increase.

To guarantee the energetic autonomy of the THAT, and to comply with the EURO VI regulation in suburban conditions, it is necessary for the HDV to spend a maximum of 3.1% of the mission time in suburban conditions, $r_{SUB\_MAX}^{EURO\ VI} = 3.1\%$. This value is obtained considering that the

recovery stage occurs exclusively in interurban driving. If the recovery stage occurs only in highway conditions, this value is moderately higher, reaching a maximum of 4.9%, $r_{SUB\_MAX}^{EURO\ VI} = 4.9\%$. This can be explained by the fact that in highway conditions, the power recovered is higher than in interurban conditions. The same occurs for EURO VII fulfilment, where r_{SUB} maximum remains between $r_{SUB\_MAX}^{EURO\ VII} = 2.4 - 3.9\%$, depending on the driving conditions of the recovery stage.

Finally, this study has demonstrated that the TATH can work energetically autonomous for long-haul HDV. Among the vehicles analysed, long-distance transportation vehicles are the most appropriate to incorporate the TATH system due to the lower r_{SUB} ratio, which is $r_{SUB} = 0.64\% < r_{SUB\_MAX}^{EURO\ VI}$ and $< r_{SUB\_MAX}^{EURO\ VII}$. However, the viability of TATH could be extended to other HDV uses if the efficiency of ATEGs improved.

Chapter 7

Results and discussion

As explained in Chapter 2, the first part of this study was focused in analyzing the effect of an EGH into the standard ATS. As exposed in Chapter 4, a comparative analysis was designed choosing three engine regimes: 1000rpm, 1250 rpm and 1500 rpm for two stage comparison. In first term to directly compare the heating effect of the EGH at the same regime and FTPP. The second stage of this analysis was focused in finding common patterns between the three regimes and its particularities.

In all cases, average NO_x emissions were reduced significatively (from 53.94% to 86.35%) as summarized in Table 4.3. However, these tests also quantified a significant average power demand of the EGH (from 6.58 kW up to 8.55 kW) to reach its target temperature set at 300°C. Highest NO_x reduction corresponds to test 1 with an engine regime of 1000 rpm. The same test presented the highest average EGH power consumption, thus exhaust gas temperatures were increasing at the lowest pace. Then EGH had to inject more thermal energy to reduce urea solution threshold, 220°C in this particular test.

EGH power consumption exceeded the maximum capabilities of an ATEG (efficiencies are around 2.5%). To design an energetically closed TATH was necessary to balance the system. At that point, research efforts were centered to determine the SCR efficiency improvement with more affordable EGH power values (P_{EGH} ranging from 0.5 to 5kW). Test 1 scenario (1000 rpm) was chosen as exhaust gas temperatures were the lowest among all to determine if an ATEG can theoretically supply enough energy for the EGH during worst conditions (low range FTPP from 30% to 45%). These comparative results showed that standard SCR performed at 60-68% while coupling to the system an EGH of 4-5kW it could achieve an efficiency of 95% in all calculated FTPP. Complete results are summarized in Table 4.5.

Next step of our research was to determine a theoretical model for the ATEG that could supply enough power to the EGH. First part was to stablish the system behaviour during a normal transportation routine. Engine parameters (such as exhaust gas temperature, FTPP and regime) differ significatively depending on HDV routine point (urban areas, highway or initial cold start). The 1500 rpm regime is chosen for this simulation as it provides high exhaust gas temperatures without surpassing TEMs maximum working temperature stablished at 230°C. These conditions are defined as recovery stage) of the system (1500 rpm and 80 km/h) while heating stage is

when EGH is enabled (i.e. 1000 rpm, 50 km/h and cold engine conditions). For the commercial TEM it was selected a Marlow Industries TG-12-08 which parameters were successfully calculated (R^2 > 0.95).

ATEG simulated represented a total layout of 180 TEMs distributed into 3 identical subassemblies. Each subassembly was composed of 4 rows of 15 TEMs connected in series and interconnected each row in parallel. For simulation optimization a single row was used and the result was extrapolated to obtain the total energy produced by an ATEG of 180 TEM. In these results neither backpressure nor energy loss were considered as explained in Chapter 4.5.

After validating the simulation results, an important correlation of time between both stages was stablished. In other words, we have calculated for each FTPP how many minutes the ATEG needs (recovery stage) to supply the demanded power P_{EGH} (heating stage) for EGH values ranging from 0.5-5 kW. It is assumed that EGH is enabled during the first 12 minutes as it coincides with cold start period on the tested vehicle. Afterwards, the standard ATS starts working efficiently as urea solution is dozed into the system.

All recovery stage time values are represented in Figure 4.13. To summarize recovery time results, it can be simplified into two different zones. The first zone is related to low range FTPP (30%-45%), where exhaust gas temperatures are relatively low to help the ATEG in a short period of time. In this case it needs a maximum of 152 minutes at 45% of FTPP to supply the power demand of a 5 kW EGH for a single heating stage. On the other hand, it takes 15 minutes to supply an EGH of 0,5 kW while FTPP is constantly at the same FTPP. The second zone of time figures are diminishing rapidly as FTPP increases due to exhaust gas temperatures. The simulated ATEG needs a recovery time of 41 minutes to supply a 5 kW EGH and only 5 minutes to supply a 0.5 kW EGH for its heating period. Finally, it is remarkable that all time figures are within the maximum driving time permitted of 4.5h, according to the EU Road Safety Authority.

Finally, a comparison of SCR improvement was held to determine in which conditions the proposed EGH+ATEG system contributes to a better SCR performance. For relatively high FTPP values over 65% the any EGH contribution to SCR improvement its irrelevant (<1%). For 0.5 or 1kW EGH regardless of any particular FTPP they present a low SCR improvement of 5%-15% of

its efficiency. For EGH of 2 or 3kW there is a relevant SCR improvement (15%-40%) for a relative short ATEG performing time (50-90 minutes). Finally, as we move to low range FTPP of 30% to 45% combined with EGH values of 4 or 5kW is when SCR improvements are relevant (40%-55%). Logically, these greater power demands require longer recovery time of the ATEG (95-155 minutes).

Second part of our research was focused in quantify the impact of the proposed system compared to the standard ATS concerning EURO VI-VII regulations fulfilment. EURO VI NO_x limit was obtained from the WHTC limit value multiplied by the conformity factor CF: $NOx_{limit}^{EURO\ VI} = 0.46 \cdot 1.5 = 0.69 g/kWh$. As explained in Chapter 5.4., EURO VII limits were halved from EURO VI, resulting the limit value as $NOx_{limit}^{EURO\ VII} = 0.27 \cdot 1.5 = 0.41 g/kWh$.

Three transient tests were held at following engine regimes: 1000 rpm, 1250 rpm and 1500 rpm. Each respective duration was: 340 s, 300 s and 240s. Results for the first test at 1000 rpm showed that the tested vehicle did not fulfill EURO VI regulation using the standard ATS except for 80% and 90% of FTPP. Results showed that when EGH is disabled, there was a time coincidence between NOx decrease after 65% of FTPP and temperature T_{b_EGH} exceeding threshold injection of urea solution (over 220°C).

On the other hand, when EGH was enabled, it contributed to maintain NOx values lower than this regulation maximum levels during all cycle. EGH most significant contribution was at FTPP range from 40% to 65%. These significant results are explained by the rise on exhaust gas temperature that moved forward the SCR ideal performance conditions. Thus, initial test temperature T_{a_EGH} was around 270°C.

Second transient test presented was a cycle set at 1250 rpm and the standard ATS maintained all registered NO_x values within EURO VI regulation limits. These figures were possible because this engine regime raised exhaust temperature faster than test one and SCR performed earlier. Thus, both T_{a_EGH} and T_{b_EGH} temperatures coincide at the cycle ending (250 s). EGH contribution was also relevant to maintain NOx values even within EURO VII prospective maximum levels (0.41g/kWh). NOx_{EGH_ON} maximum value was registered at the beginning of

the test (0.2g/kWh) with T_{b_EGH} temperature around 200°C being the lowest and below threshold DEF temperature.

Third cycle was set at 1500 rpm and the standard ATS fulfilled EURO VI limits except for one small zone around 70% of FTPP with values of 0.9g/kWh. On the contrary, EGH continued to fulfill EURO VI-VII despite this engine regime emitted more pollutants. This is explained by the fact that rise in exhaust temperature was the highest of the comparative with T_{a_EGH} initial value around 275°C.

Overall, these comparative cycles showed that EGH contributed to fulfill antipollution standards with NOx reduction over 80% in all tests. Energy consumption values are summarized in Table 5.2 and ranged from 0.098 kW/h for test 2 (1250 rpm) up to 0.213 kW/h for test 3 (1500 rpm). This energy consumption disparity was analyzed and contributed to define next step as EGH optimization as explained in Chapter 5.5.

To optimize EGH, target temperature was reset at $T_{a\_EGH} = 220$°C. Heating exhaust gases at higher values has no sense as regulations can be already fulfilled if SCR is at its maximum efficient point of 95%. Thus, the theoretical maximum demand of P_{EGH}, is calculated being 5 kW for 1000 rpm, 2.2 kW for the first 50 s at 1250 rpm and below 0.5 kW located during first 70 s at 1500 rpm. These results considered a full energy conversion without losses.

An EGH power consumption to achieve 95% SCR efficiency during a simulated real HDV driving profile was then analyzed. This driving profile was segmented and quantified into three types of road conditions. Suburban (1000 rpm for 12 minutes), interurban (1250 rpm for 61 minutes) and finally highway (1500 rpm for 115 minutes). These relatively low regimes selected can vary depending on each driver and vehicle particular conditions. Despite comparatively lower exhaust gas temperatures, EGH peak power demands were reasonable with 5.02 kW for its maximum demand (1000 rpm suburban road). The total energy required for all the mission driving profile was 0.816 kWh.

This extra energy consumption could be provided by an onboard system such as a specific 200 A alternator. A study of extra fuel consumption was developed to quantify its impact. Results

showed a total increment of 1.47% in fuel consumption that came from 1.43% (additional force under worst load conditions from alternator), 0.015% (backpressure effects) and 0.021% (extra weight).

Finally, third part of our research presented two experiments. First one was an EGH experiment to define and quantify which are the best driving profiles that fit with the proposed TATH system. Furthermore, it is calculated the exact P_{EGH} to comply with EURO VI and EURO VII in three different scenarios. Results are presented in Figure 6.6. and Table 6.4. and showed in worst scenario (1000 rpm) a power requirement of 5.84kW and 7.52 kW to accomplish EURO VI and EURO VII respectively. Afterwards, the EGH was tested in a hot air flow bench under highway conditions to quantify backpressure effects. Results showed a maximum pressure loss of 1.8 mb at 204 g/s. The hydraulic power $P_{H_{EGH}}$ that must be provided from the engine to overcome this effect is quantified for highway conditions (worst scenario) being 49.3 W.

Second experiment was an ATEG single unit test (ATEG_su) using a flow bench and a chiller to simulate real HDV conditions. As explained in Chapter 6.4. the ATEG layout for HDV is composed of 6 identical ATEG_su units. In order to simplify the experiment set up, it was tested only a single unit taking into account the proportion of mass flow rate (1/6) simulating a long-haul driving profile (suburban and highway conditions). Results showed an ATEG net power generation P_{ATEG} of 118 W and 298 W, under suburban and highway conditions respectively. Engine hydraulic power $P_{H_{ATEG}}$ to overcome ATEG backpressure (40 mb) is calculated in worst conditions possible (highway conditions) resulting in 1095.3 W.

In Chapter 6.5 we quantified the boundaries to make the proposed TATH system energetically self-sufficient when energy recovered (interurban and highway) is greater than energy consumed in heating stage (suburban). In this regard, to comply EURO VI-VII in suburban conditions, time spent in this road environment must not exceed the following:

- EURO VI: 3.1-4.9% of the complete mission time ($r_{SUB\_MAX}^{EURO\ VI}$ < 3.1 - 4.9%).
- EURO VII: 2.4-3.9% of total mission time ($r_{SUB\_MAX}^{EURO\ VII}$ < 2.4% - 3.9%).

Lower maximum levels are the result of considering energy recovery stage only during interurban conditions. On the other hand, highway conditions produce greater energy recovery figures and this provides more time for the heating stage.

To conclude with HDV routines study, we demonstrated in Table 6.7 that the energy equation $E_{HEATING} \leq E_{RECOVERY}$ is only valid for long-haul routines as suburban time is within its limits being $r_{SUB} = 0.64\%$.

Finally, total TATH extra fuel consumption for a long-haul HDV is calculated in 0.35%. This result comes from the sum of backpressure effects (0.2%) added to the extra weigh contribution (0.13%).

Chapter 8

Conclusions

This research study is focused in developing a valid TATH system energetically closed and with the possibility of being retrofitted to a current HDV in order to improve its standard SCR efficiency. As objectives presented in Chapter 2 suggest, our research has evolved and sharpened as results added more and more relevant information.

First approach related to NOx emissions reduction using an EGH and SCR efficiency showed us the following relevant information:

- NOx abatement is directly related to T_{a_EGH}.
- Heating exhaust gases after T_{a_EGH} has reached threshold urea injection point (T>180°C; depending on each vehicle) is useless.
- P_{EGH} of 5 kW EGH could be supported by an onboard generator (alternator or ATEG).
- Recovery stage is stablished at 1500 rpm as maximum regime without surpassing TEM maximum temperature (230°C).
- Heating stage is stablished at 1000 rpm as exhaust gas temperatures remain increase slowly as FTPP increase too.
- SCR worst performance (60-65%) is presented at 40-45% of FTPP during heating stage. Using an EGH of 4-5 kW its performance reach 95%.
- ATEG layout of 180 TEMs distributed in 3 subassemblies is simulated and validated through tested vehicle parameters and commercial TEM parameters.
- A 5 kW EGH is fully supplied for a heating stage of 12 minutes (defined as cold start) in 152 minutes at 45% FTPP. According to simulated model.
- Using P_{EGH} of 2-3 kW, SCR improvement of 15-40% is achieved with ATEG performing from 50 to 59 minutes.
- SCR improvement of 40-55% is achieved when P_{EGH} of 4-5 kW is used at low FTPP (30-45%).

An exploration of both systems concerning EURO VI-VII compliance shows us some useful conclusions that can be summarized as follows:

- HDV tested at 1000 rpm with standard ATS exceeds EURO VI maximum limits during all test (except for 80-90% of FTPP).

- Prospective EURO VII is fulfilled at 1250 rpm with EGH enabled while standard ATS only accomplish EURO VI regulation.
- Target temperature was reset at $T_{a\_EGH} = 220℃$ in order to optimize the EGH for this particular HDV model.
- A simulated real driving profile combining suburban, interurban and highway roads; showed EGH peak power demands of 5.02 kW and an energy requirement for all the mission of 0.816 kWh.
- A specific on-board alternator could supply EGH power demand, for this specific mission, with an extra fuel consumption of 1.43%.

Last step forward of this research quantified the viability on an EGH-ATEG system and its need for NO_x abatement considering transportation routines characteristics. It also provided these conclusions:

- The exact EGH power demand P_{EGH} to fulfill EURO VI-VII at 1000 rpm is 5.84 kW and 7.52 kW respectively.
- Tested EGH produced an engine hydraulic power $P_{H_{EGH}}$ of 49.3W in highway conditions.
- Tested full ATEG with 6 ATEG_su, produced an engine hydraulic power $P_{H_{EGH}}$ of 1095.2 W in highway conditions.
- To fulfill EURO VI, suburban maximum time must not exceed 3.1-4.9% of total mission time.
- To fulfill prospective EURO VII, suburban maximum time must not exceed 2.4-3.9% of total mission time.
- Long-haul routine for HDV is the only mission profile that can benefit from the system proposed in order to accomplish EURO VI-VII regulations.
- TATH extra fuel consumption is 0.35%, clearly a better value than the one calculated for a specific alternator.

Future research must focus on providing an improved and definitive design in order to maximize ATEG capabilities. 3D manufacturing and generative design could improve cooling plate geometries and clamping systems. Furthermore, energy storage and its control is another theme that must be studied and optimized in the near future to broaden TATH possibilities.

Bibliography

[1] G. Kalghatgi, Is it really the end of internal combustion engines and petroleum in transport?, Appl. Energy. 225 (2018) 965–974. https://doi.org/10.1016/J.APENERGY.2018.05.076.

[2] Z. Mera, N. Fonseca, J.-M. López, J. Casanova, Analysis of the high instantaneous NOx emissions from Euro 6 diesel passenger cars under real driving conditions, Appl. Energy. 242 (2019) 1074–1089. https://doi.org/10.1016/J.APENERGY.2019.03.120.

[3] K. Ghasemzadeh, S.M.S. Tilebon, A. Basile, Conventional systems for exhaust gas cleaning and carbon capture and sequestration, in: Curr. Trends Futur. Dev. Membr., Elsevier, 2020: pp. 65–96. https://doi.org/10.1016/b978-0-12-817807-2.00004-6.

[4] M.S. Reiter, K.M. Kockelman, The problem of cold starts: A closer look at mobile source emissions levels, Transp. Res. Part D Transp. Environ. 43 (2016) 123–132. https://doi.org/10.1016/j.trd.2015.12.012.

[5] J. Gao, G. Tian, A. Sorniotti, A.E. Karci, R. Di Palo, Review of thermal management of catalytic converters to decrease engine emissions during cold start and warm up, Appl. Therm. Eng. 147 (2019) 177–187. https://doi.org/10.1016/j.applthermaleng.2018.10.037.

[6] J. Zhao, J. Wang, Integrated Model Predictive Control of Hybrid Electric Vehicles Coupled with Aftertreatment Systems, IEEE Trans. Veh. Technol. 65 (2016) 1199–1211. https://doi.org/10.1109/TVT.2015.2405918.

[7] J. Gao, H. Chen, Y. Li, J. Chen, Y. Zhang, K. Dave, Y. Huang, Fuel consumption and exhaust emissions of diesel vehicles in worldwide harmonized light vehicles test cycles and their sensitivities to eco-driving factors, Energy Convers. Manag. 196 (2019) 605–613. https://doi.org/10.1016/J.ENCONMAN.2019.06.038.

[8] H. Chang, J. Li, X. Chen, L. Ma, S. Yang, J.W. Schwank, J. Hao, Effect of Sn on MnO x-CeO 2 catalyst for SCR of NO x by ammonia: Enhancement of activity and remarkable resistance to SO 2, Catal. Commun. 27 (2012) 54–57.

https://doi.org/10.1016/j.catcom.2012.06.022.

[9] Z. Hao, Y. Jiao, Q. Shi, H. Zhang, S. Zhan, Improvement of NH 3 -SCR performance and SO 2 resistance over Sn modified CeMoO x electrospun fibers at low temperature, Catal. Today. 327 (2019) 37–46. https://doi.org/10.1016/j.cattod.2018.07.037.

[10] D. Damma, P.R. Ettireddy, B.M. Reddy, P.G. Smirniotis, A review of low temperature NH 3 -SCR for removal of NO x, Catalysts. 9 (2019). https://doi.org/10.3390/catal9040349.

[11] T.J. Wang, Effects of insulation on exhaust temperature and subsequent SCR efficiency of a heavy-duty diesel engine, J. Mech. Sci. Technol. 33 (2019) 923–929. https://doi.org/10.1007/s12206-019-0149-9.

[12] Y. Okada, H. Hirabayashi, S. Sato, H. Inoue, Study on Improvement of NOx Reduction Performance at Low Temperature Using Urea Reforming Technology in Urea SCR System, in: SAE Tech. Pap., SAE International, 2019. https://doi.org/10.4271/2019-01-0317.

[13] M. Rink, G. Eigenberger, U. Nieken, Heat-integrated exhaust purification for natural gas engines, Chemie-Ingenieur-Technik. 85 (2013) 656–663. https://doi.org/10.1002/cite.201200162.

[14] M. Rink, G. Eigenberger, U. Nieken, Comparison of two different heat-integrated exhaust purification devices for monovalent CNG engines, Top. Catal. 56 (2013) 421–426. https://doi.org/10.1007/s11244-013-9990-8.

[15] C. Sharp, C.C. Webb, S. Yoon, M. Carter, C. Henry, Achieving Ultra Low NOX Emissions Levels with a 2017 Heavy-Duty On-Highway TC Diesel Engine - Comparison of Advanced Technology Approaches, SAE Int. J. Engines. 10 (2017) 1722–1735. https://doi.org/10.4271/2017-01-0956.

[16] D. Culbertson, M. Khair, S. Zhang, J. Tan, J. Spooler, The Study of Exhaust Heating to Improve SCR Cold Start Performance, SAE Int. J. Engines. 8 (2015). https://doi.org/10.4271/2015-01-1027.

[17] A. Massaguer, T. Pujol, M. Comamala, E. Massaguer, Feasibility study on a vehicular thermoelectric generator coupled to an exhaust gas heater to improve aftertreatment's efficiency in cold-starts, Appl. Therm. Eng. (2020).

https://doi.org/10.1016/j.applthermaleng.2019.114702.

[18] F. Posada, H. Badshah, F. Rodriguez, In-Use NOx Emissions and Compliance Evaluation for Modern Heavy-Duty Vehicles in Europe and the United States, ICCT White Pap. (2020).

[19] M. Rink, G. Eigenberger, U. Nieken, U. Tuttlies, Optimization of a heat-integrated exhaust catalyst for CNG engines, in: Catal. Today, 2012: pp. 113–120. https://doi.org/10.1016/j.cattod.2011.10.017.

[20] M. Dinsmore, S. Doshi, V. Sin, C. Matava, Design and evaluation of a novel and sustainable human-powered low-cost 3D printed thermal laryngoscope, J. Med. Syst. 43 (2019) 143. https://doi.org/10.1007/s10916-019-1275-8.

[21] H.W. Coleman, W.G. Steele, M. Buzhuga, Experimentation, Validation, and Uncertainty Analysis for Engineers, Noise Control Eng. J. 58 (2010) 343. https://doi.org/10.3397/1.3383084.

[22] R.J. Moffat, Describing the uncertainties in experimental results, Exp. Therm. Fluid Sci. 1 (1988) 3–17. https://doi.org/10.1016/0894-1777(88)90043-X.

[23] H.W. Coleman, W.G. Steele, Experimentation, validation, and uncertainty analysis for engineers: Fourth edition, Exp. Validation, Uncertain. Anal. Eng. Fourth Ed. (2018) 1–368. https://doi.org/10.1002/9781119417989.

[24] J.Y. Kim, S.H. Ryu, J.S. Ha, Numerical Prediction on the Characteristics of Spray-Induced Mixing and Thermal Decomposition of Urea Solution in SCR System, (2004) 165–170. https://doi.org/10.1115/ICEF2004-0889.

[25] T. Grigoratos, G. Fontaras, B. Giechaskiel, N. Zacharof, Real world emissions performance of heavy-duty Euro VI diesel vehicles, Atmos. Environ. 201 (2019) 348–359. https://doi.org/10.1016/J.ATMOSENV.2018.12.042.

[26] L. He, J. Hu, S. Zhang, Y. Wu, X. Guo, J. Song, L. Zu, X. Bao, Investigating Real-World Emissions of China's Heavy-Duty Diesel Trucks: Can SCR Effectively Mitigate NOx Emissions for Highway Trucks?, Aerosol Air Qual. Res. 17 (2017). https://doi.org/10.4209/aaqr.2016.12.0531.

[27] O. Kröcher, Selective Catalytic Reduction of NOx, Catalysts. 8 (2018) 459.

https://doi.org/10.3390/catal8100459.

[28] W. Brack, B. Heine, F. Birkhold, M. Kruse, O. Deutschmann, Formation of Urea-Based Deposits in an Exhaust System: Numerical Predictions and Experimental Observations on a Hot Gas Test Bench, Emiss. Control Sci. Technol. 2 (2016) 115–123. https://doi.org/10.1007/s40825-016-0042-2.

[29] J. Guo, Y. Ge, L. Hao, J. Tan, Z. Peng, C. Zhang, Comparison of real-world fuel economy and emissions from parallel hybrid and conventional diesel buses fitted with selective catalytic reduction systems, Appl. Energy. 159 (2015) 433–441. https://doi.org/10.1016/J.APENERGY.2015.09.007.

[30] S. Zhang, Y. Wu, J. Hu, R. Huang, Y. Zhou, X. Bao, L. Fu, J. Hao, Can Euro V heavy-duty diesel engines, diesel hybrid and alternative fuel technologies mitigate NOX emissions? New evidence from on-road tests of buses in China, Appl. Energy. 132 (2014) 118–126. https://doi.org/10.1016/J.APENERGY.2014.07.008.

[31] J.M. Luján, A. García, J. Monsalve-Serrano, S. Martínez-Boggio, Effectiveness of hybrid powertrains to reduce the fuel consumption and NOx emissions of a Euro 6d-temp diesel engine under real-life driving conditions, Energy Convers. Manag. 199 (2019) 111987. https://doi.org/10.1016/J.ENCONMAN.2019.111987.

[32] J. Jiang, D. Li, Theoretical analysis and experimental confirmation of exhaust temperature control for diesel vehicle NOx emissions reduction, Appl. Energy. 174 (2016) 232–244. https://doi.org/10.1016/J.APENERGY.2016.04.096.

[33] M.R. Hamedi, O. Doustdar, A. Tsolakis, J. Hartland, Thermal energy storage system for efficient diesel exhaust aftertreatment at low temperatures, Appl. Energy. 235 (2019) 874–887. https://doi.org/10.1016/J.APENERGY.2018.11.008.

[34] E. Massaguer, A. Massaguer, T. Pujol, M. Comamala, L. Montoro, J.R. Gonzalez, Fuel economy analysis under a WLTP cycle on a mid-size vehicle equipped with a thermoelectric energy recovery system, Energy. 179 (2019) 306–314. https://doi.org/10.1016/j.energy.2019.05.004.

[35] A. Massaguer, E. Massaguer, M. Comamala, T. Pujol, L. Montoro, M.D.D. Cardenas, D. Carbonell, A.J.J. Bueno, Transient behavior under a normalized driving cycle of an

automotive thermoelectric generator, Appl. Energy. 206 (2017) 1282–1296. https://doi.org/10.1016/j.apenergy.2017.10.015.

[36] M. Comamala, A. Massaguer, E. Massaguer, T. Pujol, Validation of a fuel economy prediction method based on thermoelectric energy recovery for mid-size vehicles, Appl. Therm. Eng. 153 (2019) 768–778. https://doi.org/10.1016/j.applthermaleng.2019.03.004.

[37] A. Massaguer, E. Massaguer, M. Comamala, T. Pujol, J.R. González, M.D. Cardenas, D. Carbonell, A.J. Bueno, A method to assess the fuel economy of automotive thermoelectric generators, Appl. Energy. (2018). https://doi.org/10.1016/j.apenergy.2018.03.169.

[38] L.S. Hewawasam, A.S. Jayasena, M.M.M. Afnan, R.A.C.P. Ranasinghe, M.A. Wijewardane, Waste heat recovery from thermo-electric generators (TEGs), in: Energy Reports, Elsevier Ltd, 2020: pp. 474–479. https://doi.org/10.1016/j.egyr.2019.11.105.

[39] E. Massaguer, A. Massaguer, L. Montoro, J.R. Gonzalez, Development and validation of a new TRNSYS type for the simulation of thermoelectric generators, Appl. Energy. 134 (2014) 65–74. https://doi.org/10.1016/j.apenergy.2014.08.010.

[40] C. Suter, Z.R. Jovanovic, A. Steinfeld, A 1kWe thermoelectric stack for geothermal power generation - Modeling and geometrical optimization, Appl. Energy. (2012). https://doi.org/10.1016/j.apenergy.2012.05.033.

[41] M. Chrysostomou, N. Christofides, A review on solar thermal waste heat energy recovery using thermoelectric generators, 2016.

[42] E. Massaguer, A. Massaguer, L. Montoro, J.R. Gonzalez, Modeling analysis of longitudinal thermoelectric energy harvester in low temperature waste heat recovery applications, Appl. Energy. 140 (2015) 184–195. https://doi.org/10.1016/j.apenergy.2014.12.005.

[43] E. Massaguer, A. Massaguer, T. Pujol, J.R. Gonzalez, L. Montoro, Modelling and analysis of longitudinal thermoelectric energy harvesters considering series-parallel interconnection effect, Energy. 129 (2017) 59–69. https://doi.org/10.1016/j.energy.2017.04.061.

[44] S. Lan, Z. Yang, R. Stobart, R. Chen, Prediction of the fuel economy potential for a skutterudite thermoelectric generator in light-duty vehicle applications, Appl. Energy. 231 (2018) 68–79. https://doi.org/10.1016/J.APENERGY.2018.09.087.

[45] Z.-G. Shen, L.-L. Tian, X. Liu, Automotive exhaust thermoelectric generators: Current status, challenges and future prospects, Energy Convers. Manag. 195 (2019) 1138–1173. https://doi.org/10.1016/J.ENCONMAN.2019.05.087.

[46] M. Comamala, T. Pujol, I.R. Cózar, E. Massaguer, A. Massaguer, Power and Fuel Economy of a Radial Automotive Thermoelectric Generator: Experimental and Numerical Studies, Energies. 11 (2018). https://doi.org/10.3390/en11102720.

[47] M. Comamala, I.R. Cózar, A. Massaguer, E. Massaguer, T. Pujol, Effects of design parameters on fuel economy and output power in an automotive thermoelectric generator, Energies. 11 (2018). https://doi.org/10.3390/en11123274.

[48] P. Fernández-Yañez, O. Armas, A. Capetillo, S. Martínez-Martínez, Thermal analysis of a thermoelectric generator for light-duty diesel engines, Appl. Energy. 226 (2018) 690–702. https://doi.org/10.1016/J.APENERGY.2018.05.114.

[49] A. Marvão, P.J. Coelho, H.C. Rodrigues, Optimization of a thermoelectric generator for heavy-duty vehicles, Energy Convers. Manag. 179 (2019) 178–191. https://doi.org/10.1016/J.ENCONMAN.2018.10.045.

[50] D. Di Battista, M. Di Bartolomeo, C. Villante, R. Cipollone, On the limiting factors of the waste heat recovery via ORC-based power units for on-the-road transportation sector, Energy Convers. Manag. 155 (2018) 68–77. https://doi.org/10.1016/J.ENCONMAN.2017.10.091.

[51] D. Vittorini, R. Cipollone, R. Carapellucci, Enhanced performances of ORC-based units for low grade waste heat recovery via evaporator layout optimization, Energy Convers. Manag. 197 (2019) 111874. https://doi.org/10.1016/J.ENCONMAN.2019.111874.

[52] M. Villani, L. Tribioli, Comparison of different layouts for the integration of an organic Rankine cycle unit in electrified powertrains of heavy duty Diesel trucks, Energy Convers. Manag. 187 (2019) 248–261. https://doi.org/10.1016/J.ENCONMAN.2019.02.078.

[53] GT-SUITE Overview | Gamma Technologies, (n.d.). https://www.gtisoft.com/gt-suite/gt-suite-overview/ (accessed March 4, 2021).

[54] S. Hasanpour Omam, Exhaust waste energy recovery using Otto-ATEG-Stirling engine combined cycle, Appl. Therm. Eng. 183 (2020) 116210. https://doi.org/10.1016/j.applthermaleng.2020.116210.

[55] I.R. Cózar, T. Pujol, M. Lehocky, Numerical analysis of the effects of electrical and thermal configurations of thermoelectric modules in large-scale thermoelectric generators, Appl. Energy. 229 (2018) 264–280. https://doi.org/10.1016/j.apenergy.2018.07.116.

[56] Q.E. Hussain, D.R. Brigham, C.W. Maranville, Thermoelectric exhaust heat recovery for hybrid vehicles, in: SAE Tech. Pap., 2009. https://doi.org/10.4271/2009-01-1327.

[57] N. Zienna, A Model to Evaluate The Potential Benefits of a Thermoelectric Generator in Reducing CO2 Emisssions, in: Proc. Eur. GT Conf., 2017.

[58] E. Maciá-Barber, Thermoelectric materials: Advances and applications, 2015. https://doi.org/10.4032/9789814463539.

[59] E.J. Sandoz-Rosado, S.J. Weinstein, R.J. Stevens, On the Thomson effect in thermoelectric power devices, Int. J. Therm. Sci. 66 (2013) 1–7. https://doi.org/10.1016/j.ijthermalsci.2012.10.018.

[60] Incropera, DeWitt, Bergman, Lavine, Fundamental of Heat and Mass Transfer Sixth Edition, 2007.

[61] CO2 Emissions from Fuel Combustion 2016, OECD, 2016. https://doi.org/10.1787/co2_fuel-2016-en.

[62] R. Muncrief, B. Sharpe, Overview of the heavy-duty vehicle market and CO2 emissions in the European Union, Int. Counc. Clean Transp. (2015). https://doi.org/10.1007/978-3-319-76451-1_34.

[63] J. Fenger, Air pollution in the last 50 years - From local to global, Atmos. Environ. (2009). https://doi.org/10.1016/j.atmosenv.2008.09.061.

[64] J.B. Heywood, O.Z. Welling, Trends in Performance Characteristics of Modern Automobile SI and Diesel Engines, SAE Int. J. Engines. 2 (2009) 1650–1662.

https://doi.org/10.4271/2009-01-1892.

[65] J. Wu, F. Ge, Y. Li, A vehicle exhaust NO x electrochemical sensor based on Au-Yttria Stabilized Zirconia nanocomposite, Int. J. Electrochem. Sci. (2017). https://doi.org/10.20964/2017.03.52.

[66] J. Sowman, S. Box, A. Wong, M. Grote, D.S. Laila, G. Gillam, A.J. Cruden, J.M. Preston, P. Fussey, In-use emissions testing of diesel-driven buses in Southampton: is selective catalytic reduction as effective as fleet operators think?, IET Intell. Transp. Syst. 12 (2018) 521–526. https://doi.org/10.1049/iet-its.2017.0173.

[67] Z. Hao, Y. Jiao, Q. Shi, H. Zhang, Improvement of NH3-SCR performance and SO2 resistance over Sn modified CeMoOx electrospun fibers at low temperature, Catal. Today. 327 (2019) 37–46. https://doi.org/10.1016/J.CATTOD.2018.07.037.

[68] NOx emissions from heavy-duty and light-duty diesel vehicles in the EU: Comparison of real-world performance and current type-approval requirements | International Council on Clean Transportation, (n.d.).

[69] M.S. Reiter, K.M. Kockelman, The problem of cold starts: A closer look at mobile source emissions levels, Transp. Res. Part D Transp. Environ. (2016). https://doi.org/10.1016/j.trd.2015.12.012.

[70] K. Robinson, S. Ye, Y. Yap, S.T. Kolaczkowski, Application of a methodology to assess the performance of a full-scale diesel oxidation catalyst during cold and hot start NEDC drive cycles, Chem. Eng. Res. Des. (2013). https://doi.org/10.1016/j.cherd.2013.02.022.

[71] B. Guan, R. Zhan, H. Lin, Z. Huang, Review of state of the art technologies of selective catalytic reduction of NOx from diesel engine exhaust, Appl. Therm. Eng. (2014). https://doi.org/10.1016/j.applthermaleng.2014.02.021.

[72] L. Zhu, Z.Y. He, Z. Xu, Z. Gao, A. Li, Z. Huang, Improving cold start, combustion and emission characteristics of a lean burn spark ignition natural gas engine with multi-point hydrogen injection, Appl. Therm. Eng. 121 (2017) 83–89. https://doi.org/10.1016/j.applthermaleng.2017.04.023.

[73] J. Chung, H. Kim, M. Sunwoo, Reduction of transient NOx emissions based on set-point

adaptation of real-time combustion control for light-duty diesel engines, Appl. Therm. Eng. 137 (2018) 729–738. https://doi.org/10.1016/J.APPLTHERMALENG.2018.03.082.

[74] S. Bai, J. Han, M. Liu, S. Qin, G. Wang, G. Li, Experimental investigation of exhaust thermal management on NOx emissions of heavy-duty diesel engine under the world Harmonized transient cycle (WHTC), Appl. Therm. Eng. 142 (2018) 421–432. https://doi.org/10.1016/J.APPLTHERMALENG.2018.07.042.

[75] J. Ximinis, A. Massaguer, T. Pujol, E. Massaguer, Nox emissions reduction analysis in a diesel Euro VI Heavy Duty vehicle using a thermoelectric generator and an exhaust heater, Fuel. 301 (2021) 121029. https://doi.org/https://doi.org/10.1016/j.fuel.2021.121029.

[76] Estimated cost of diesel emissions control technology to meet future Euro VII standards | International Council on Clean Transportation, (n.d.).

[77] ACEA, Principles for potential post-Euro 6 and post-Euro VI emission regulations, 2020.

[78] A. Noble, Next Generation, EURO 7 Updat. Transp. Eng. (2017).

[79] AERIS Europe, EURO 7 IMPACT ASSESSMENT: THE OUTLOOK FOR AIR QUALITY COMPLIANCE IN THE EU AND THE ROLE OF THE ROAD TRANSPORT SECTOR, 2021.

[80] T.& ENVIRONMENT, Road to Zero: the last EU emission standard for cars, vans, buses and trucks, 2020.

[81] Fuel efficiency technology in European heavy-duty vehicles: Baseline and potential for the 2020–2030 timeframe | International Council on Clean Transportation, (n.d.).

[82] M. Coyle, EFFECTS OF PAYLOAD ON THE FUEL CONSUMPTION OF TRUCKS, 2007.

[83] L. Meda, M. Romzek, Y. Zhang, M. Cleary, Development of a 1kW Exhaust Waste Heat Thermoelectric Generator, SAE Int. J. Commer. Veh. 9 (2016) 21–30. https://doi.org/10.4271/2016-01-1273.

[84] A.E. Risseh, H.-P. Nee, O. Erlandsson, K. Brinkfeldt, A. Contet, F.F. lng, G. Gaiser, A. Saramat, T. Skare, S. Nee, J. Dellrud, Design of a Thermoelectric Generator for Waste Heat Recovery Application on a Drivable Heavy Duty Vehicle, SAE Int. J. Commer. Veh. 10 (2017) 26–44. https://doi.org/10.4271/2017-01-9178.

[85] R. Vermeulen, J. Spreen, N. Ligterink, W. Vonk, The Netherlands In-Service Emissions Testing Programme for Heavy-Duty, 2011.

[86] R. Vermeulen, W. Vonk, R. van Gijlswijk, The Netherlands in-service emissions testing programme for heavy-duty vehicles 2015-2016-Annual report, 2016.

[87] G.A. Bishop, B.G. Schuchmann, D.H. Stedman, Heavy-duty truck emissions in the south coast air basin of California, Environ. Sci. Technol. 47 (2013) 9523–9529. https://doi.org/10.1021/es401487b.

[88] M. Vojtisek-Lom, A.F. Arul Raj, P. Jindra, D. Macoun, M. Pechout, On-road detection of trucks with high NOx emissions from a patrol vehicle with on-board FTIR analyzer, Sci. Total Environ. 738 (2020) 139753. https://doi.org/10.1016/j.scitotenv.2020.139753.

[89] A.J. Kotz, D.B. Kittelson, W.F. Northrop, Lagrangian Hotspots of In-Use NOX Emissions from Transit Buses, Environ. Sci. Technol. 50 (2016) 5750–5756. https://doi.org/10.1021/acs.est.6b00550.

[90] Y. Tan, P. Henderick, S. Yoon, J. Herner, T. Montes, K. Boriboonsomsin, K. Johnson, G. Scora, D. Sandez, T.D. Durbin, On-Board Sensor-Based NOx Emissions from Heavy-Duty Diesel Vehicles, Environ. Sci. Technol. 53 (2019) 5504–5511. https://doi.org/10.1021/acs.est.8b07048.

[91] S. Ko, J. Park, H. Kim, G. Kang, J. Lee, J. Kim, J. Lee, NOx emissions from Euro 5 and Euro 6 heavy-duty diesel vehicles under real driving conditions, Energies. 13 (2020). https://doi.org/10.3390/en13010218.

[92] G. Karavalakis, M. Hajbabaei, T.D. Durbin, K.C. Johnson, Z. Zheng, W.J. Miller, The effect of natural gas composition on the regulated emissions, gaseous toxic pollutants, and ultrafine particle number emissions from a refuse hauler vehicle, Energy. 50 (2013) 280–291. https://doi.org/10.1016/j.energy.2012.10.044.

[93] J. Han, J. Lee, Y. Oh, G. Cho, H. Kim, Effect of UWS injection at low exhaust gas temperature on NOx removal efficiency of diesel engine, Int. J. Automot. Technol. 18 (2017) 951–957. https://doi.org/10.1007/s12239-017-0093-6.

[94] Z. Mera, C. Matzer, S. Hausberger, N. Fonseca, Performance of selective catalytic

reduction (SCR) system in a diesel passenger car under real-world conditions, Appl. Therm. Eng. 181 (2020) 115983. https://doi.org/10.1016/j.applthermaleng.2020.115983.

[95] E. Massaguer, A. Massaguer, E. Balló, I.R. Cózar, T. Pujol, L. Montoro, M. Comamala, Electrical generation of a ground-level solar thermoelectric generator: Experimental tests and one-year cycle simulation, Energies. 13 (2020). https://doi.org/10.3390/en13133407.

[96] L.C.M. Sales, E.P. Pacheco, L.G.C. Monteiro, L.G. Souza, M.S. Mota, Evaluation of the Influence of an Alternator with Mechanical Decoupling on Energy Consumption and CO_2 Emission in a Flex Fuel Vehicle, SAE Tech. Pap. 2017-Novem (2017). https://doi.org/10.4271/2017-36-0116.